UNIVERSITY OF CALIFORNIA
SANTA CRUZ

GIVING THE VOID ITS COLORS: META-STATISTICS OF THE ETERNAL INFLATION SCENARIO

A dissertation submitted in partial satisfaction of the
requirements for the degree of

DOCTOR OF PHILOSOPHY

in

PHYSICS

by

Ross Norman Greenwood

December 2019

The Dissertation of Ross Norman Greenwood
is approved:

Professor Anthony Aguirre, Chair

Professor Michael Dine

Professor Stefano Profumo

Quentin Williams
Acting Vice Provost and Dean of Graduate Studies

Table of Contents

List of Figures

Abstract

Giving the Void Its Colors:

Meta-statistics of the Eternal Inflation Scenario

by

Ross Norman Greenwood

The possibility of everlasting cosmological inflation – and the resulting unbounded number of causally disconnected post-inflationary regions – has gained more far-reaching implications since it was uncovered early in the history of inflation theory. This is owing to the growth in acceptance of theory landscapes and anthropic arguments weighing on the origins of cosmological parameters and low-energy particle physics. To what extent does inflation *generically* produce an eternal "multiverse," without apparent fine-tuning with respect to probability measures over the space of inflationary cosmologies driven by a single, minimally coupled scalar field? We address this and related questions with numerical simulations of inflationary dynamics across populations of randomly generated inflation models, instantiating a few particular simply-defined measures. We go on to explore the toy landscapes sampled from these measures, correlating eternal inflation with observables and characterizing fractal dimension of inflating topological defects.

To my parents.

"Performing these two tasks simultaneously, negating on the one hand and magnifying on the other, is the way open to the absurd creator. He must give the void its colors."

– A. Camus

"What really interests me is whether God had any choice in the creation of the World."

– A. Einstein

Acknowledgments

I would like to recognize to all those in my professional and personal lives who made this achievement possible and immeasurably fulfilling, but must limit myself in this space to mentioning a very select few. I would first like to acknowledge my research adviser, Anthony Aguirre, for his support, guidance, and countless hours of thought-provoking discussions. I offer my sincere gratitude to Anthony, as well as the other members of my advancement and reading committees: Michael Dine, Stefano Profumo, and George Blumenthal. Thanks to the members of our research group – Joe Schindler, Amita Kuttner, Dominik Safranek, and Dana Faiez – for fostering a stimulating environment in which to explore a wonderful subject. Shout out to the administrative staff in the UCSC physics department and SCIPP, who keep this whole ship afloat: Amy, Ben, Cathy, Vicki, and Maria.

Thank you Mom and Marken for your love and support during this process, and always. Thank you Dad for your love and your example. I strive to continue making you all proud.

Thank you Afshin and Ryan for helping me prepare the dissertation and coaching me on my defense talk, and Emily for moral support in the last days. I'm so grateful to all of the wonderful friends I've made during graduate school; your company has brightened my time in Santa Cruz and kept me sane. Kyle and Elan, John, Ashley: thank you for long and beautiful friendships.

Chapter 1

Introduction

1.1 Precedence for Naturalness in Cosmology

As the community comprising a field of natural science approaches consensus with respect to modeling the bulk of available data, aesthetically- and philosophically-motivated problems of *naturalness* come out of the woodwork of the emerging theoretic edifice. Naturalness problems address a clash between assumptions that must be taken on *post hoc* for a model to continue to account for observations (upon reflection or new data) and arguments that supported the model's original adoption. They often pertain to model parameters or setup assumptions that require a seemingly unwarranted degree of *fine-tuning*, or to a glut of valid predictions among which none matching the data are unambiguously preferred.

Naturalness plays an inflated role in cosmology because we only have a sample size of One (and much curious energy to expend on that one sample). The Inflationary Universe scenario was proposed as a solution to the perceived *un*naturalness of a highly correlated configuration spanning cosmological distance scales without a mechanism for past causal connection, and the high degree of fine-tuning of primordial densities in the hot Big Bang model needed to achieve the present-day small value of the asymptotic spatial curvature. Both could have been accepted as uncanny but ultimately unproblematic features of the universe; yet at a human level, they begged for an origin story grounded in some physical mechanism. The resolution of both problems stems from a reduction of the Friedmann equations

$$H^2 \equiv \left(\frac{\mathrm{d}(\ln a)}{\mathrm{d}t}\right)^2 = \frac{8\pi G}{3}\rho - \frac{kc^2}{a^2} \qquad \frac{\mathrm{d}H}{\mathrm{d}t} + H^2 = -\frac{4\pi G}{3}\left(\rho + \frac{3p}{c^2}\right) \tag{1.1}$$

governing the evolution of a Friedmann-Lamaître-Robertson-Walker (FLRW) spacetime

$$\mathrm{d}s^2 = \mathrm{d}t^2 - a(t)^2\left(\frac{\mathrm{d}r^2}{1-kr^2} + r^2\,\mathrm{d}\Omega\right) \tag{1.2}$$

under particular conditions on the energy density ρ and pressure p to simply $\dot{H} \equiv \ddot{a} - (\dot{a}/a)^2 = 0$ – describing a sustained exponential growth of the scale factor $a(t)$. No longer settling for an extraordinary degree of homogeneity and flatness as a given, we invoke an early bout of incredibly rapid expansion – *cosmological inflation* – to connect present-day distant regions in the past and dilute away any

initial spatial curvature.

1.2 New Problems of Naturalness

With the standard model of cosmology firmly established and inflation widely accepted as a core component of that model, we have come to a peculiar place. After addressing the Flatness and Horizon Problems following from past iterations of the hot Big Bang picture, inflation leaves open questions of naturalness pertaining to the initial conditions and theoretic superstructure needed to give rise to it [1]. Some examples include: How do the scalar field(s) that may drive inflation fit into our fundamental theories? Do we need to introduce new sectors to the Standard Model in an *ad hoc* fashion? What is the origin of the potential governing the field(s)? Is it anthropic? How finely must we tune the initial conditions? What does that mean?

Measurements from ESA's *Planck* survey mission broadly favor minimally coupled single-field models of inflation, but disfavor the simplest among them that may have the firmest foundations from the standpoint of particle physics [2]. For example, adopting a free massive scalar field as the inflaton generates too much power in tensor perturbations of the metric, beyond the upper bound on the tensor-to-scalar ratio from *Planck 2018* [3]. The most favored models are single-field with plateau-like potentials initialized atop the plateau, which come across

as highly fine-tuned to give inflation with precisely the features needed to account for observation. Meanwhile, various conceptions of a *landscape* of realizable low-energy effective theories have taken hold in the academy as well as the popular press (as a "multiverse" or "theory of anything"), motivated primarily by developments in string theory [4, 5, 6]. The landscape calls into question the necessity and uniqueness of the conditions that manifest in our observable universe, opening the door to *anthropic* reasoning[1] at a grander scale than had been admitted previously [7].

Coincident with this line of reasoning is the early discovery that inflation can be *eternal* or *everlasting* [8, 9, 10]. This means that there is a coordinate system in which the 3-volume of the Universe increases quasi-exponentially forever, there are future-directed worldlines of infinite proper time threading inflating regions, and there are an unbounded number of thermalized post-inflationary regions – potentially with different cosmological properties (see, e.g. [11] for a review). *Eternal inflation* thus adds another population layer for anthropic selection, in the form of infinite variable histories leading up to the end of inflation as well as conditions for subsequent cosmological evolution.

While it is sufficient for progress of a historical science that a prevailing model merely accounts for the available data, one aspires to a model that is both ex-

[1] Anthropic arguments infer large unobserved populations subject to selection effects in order to explain apparent fine-tuning of an observed state-of-affairs.

planatory and *prescriptive*. By this we mean yielding a set of retrodictions in which the actual state of the world is well represented, using much less information than is entailed by just knowing all of the data. Eternal inflation and the landscape appear to undermine a pursuit of a prescriptive cosmological model, and reflect a modern trend in some areas of theoretical physics that welcomes anthropic selection and emergent structure "all the way down."

1.3 Aims and Structure of this Study

Many of inflation's architects hold [12, 13, 14] that a *generic* consequence of inflation is that it is eternal in the meaning outlined above, and via the mechanisms discussed in Chapter 2. If interminable proliferation really were a difficult-to-avoid consequence of inflation, then this would make the "multiverse"[2] the *de facto* standard cosmology, ushering in a host of difficulties [15, 16] (or opportunities, to those so inclined [17, 18, 19]) in the interpretation of cosmological predictions.

Let us suppose that in a past Hubble volume coincident with our observable universe, a single minimally coupled scalar field is responsible for driving inflation and governed by an effective potential. Further suppose that we are ignorant of the process determining the form of that potential.[3] Subject to conceivable

[2]Our use of "multiverse" here and henceforth refers to the Level II multiverse in Tegmark's classification scheme – causally-disconnected regions situated within the same base manifold.

[3]The author takes this to be an uncontroversial position given the present state of the field.

probability measures over the shape and scales of the effective potential, it would be worthwhile to discover how "often" this setup leads to eternal inflation, and how eternal behavior correlates with observables. With few firm constraints from theory on the shape the effective potential can take, such measures would admit variability that need not be so simple as to be encapsulated in just a few model parameters. Furthermore, one can reasonably argue for different priors on initial conditions in such models – the field configuration, its derivatives, and metric perturbations in an initial volume – which can dramatically affect both the likelihood of successful inflation and of inflation being eternal.

Any conclusive statements on the likelihood of eternal inflation conditioned on observations of the Cosmic Microwave Background (CMB) and large-scale structure (or even inconclusive ones derived from a more rigorous analysis than has yet been brought to bear) would inform the credibility of the multiverse picture and anthropic reasoning at a cosmic scale. The present dissertation investigates the degree to which eternality should be considered a generic or finely-tuned consequence of inflation, with respect to various measures one might adopt over the combined space of model parameters and "initial conditions" for the Universe. Our primary research questions include:

- Is eternal inflation a generic consequence of inflation conditioned on observations?

- By what mechanisms and to what extent is it generic?
- How is genericity to be defined? On what can we base our prior beliefs regarding the structure of an inflation model and its initial state, from which to construct a measure?
- How much freedom do we have, in specifying the measure, to affect whether and to what extent eternal inflation is generic?

This dissertation is organized as follows: In Chapters 2-3, we review theoretic treatments and establish criteria for the three modes of eternal inflation – *stochastic*, *false-vacuum*, and *topological* – and present analytical arguments as to whether eternal behavior might or might not be generic. We then outline the structure of measures over single-field inflation models, and how one would term certain properties generic or fine-tuned. In Chapters 4-5, we employ Monte Carlo simulations to assess the typicality of eternal inflation, computing inflationary dynamics across an ensemble of randomly generated potential functions, in the tradition of Tegmark's "What does inflation really predict?" [20]. We adopt several simple, more-or-less physically justifiable measures defined by a sampling procedure that lends itself to computational efficiency. We apply statistics to the simulated data to inform rates of incidence of eternal inflation, in its various instantiations, in partitions of the space of observables and scales of the potential. In Chapter 6, we discuss our findings from the Monte Carlo analyses in terms to the research

questions listed above, as well as implications for interpretation of eternal inflation in the landscape and avenues for further research on this topic. Chapter 7 summarizes our conclusions and reflects on themes discussed in this introduction. Appendix A presents a further exploration of the simulated data output by the sampling scheme established in Chapter 4 (a "toy landscape") for insights that do not directly relate to the questions listed above, including inference of eternal behavior from the scalar perturbation spectrum, and the self-reproducing fractal dimension of inflating domain walls.

Chapter 2

Three Roads to Eternal Inflation

We restrict our attention to models in which inflation is driven by a scalar field φ that is subject to an effective potential $V(\varphi)$ and minimally coupled to the metric, with a standard kinetic term. The general form of the action is then

$$S[\varphi, g_{\mu\nu}] = \int \mathrm{d}^4x \sqrt{-g} \left[\tfrac{1}{2} g^{\mu\nu} \partial_\mu \varphi \partial_\nu \varphi - V(\varphi) + \frac{M_{\rm P}^2}{2} R(g_{\mu\nu}) \right]$$

where $M_P \equiv \sqrt{\hbar c/8\pi G}$ is the reduced Planck mass. (We generally assume natural units in which $\hbar = c = G \equiv 1$.) For those models characterized by a suitable effective potential and initialized such that inflation can end (after at least 70 e-folds to be observationally viable), is the inflating physical 3-volume on space-like hypersurfaces in the future of a finite initial volume bounded in every coordinate system? If not, then inflation is "eternal."

Accounting for quantum and thermal effects, this statement must be inter-

pretted probabilistically, concerning the 4-volume coincident with a suitably large population of initial Hubble volumes tracked over many elapsed Hubble times.[1] In place of global statements pertaining to inflating 3-volume and number of causally disconnected themalized regions, one substitutes probabilistic criteria that can be evaluated from the potential, related to three well-established mechanisms by which eternal inflation might come about. The corresponding modes are termed *stochastic*, *false-vacuum*, and *topological* eternal inflation. More than one of these modes may manifest in a given model, but only one of the associated sets of criteria and setup assumptions need be satisfied to all but ensure ever-lasting inflation.

2.1 Stochastic Inflation

Departing from Guth's inflationary universe [21] in which semi-classical phase transitions played a central role, the "slow roll" scenario that gained preeminence after its 1982 proposal [22, 23] does not explicitly rely on quantum effects in order to solve the Horizon and Flatness Problems. But because Hubble-sized regions during inflation are of a size at which quantum effects are important, and one should expect phenomena at those scales to be manifest at cosmological distance scales after inflation, one must treat perturbations to the slowly-rolling inflaton

[1] As inflation proceeds, the sample size of Hubble volumes descending from any initial volume grows exponentially – bringing statistical and deterministic statements into arbitrarily good agreement.

expectation value quantum mechanically if one hopes to validate the model against observations. Doing so provides an excellent account of the statistics of temperature fluctuations in the CMB [24], but opens the door to more than was bargained for: an unbounded, self-reproducing inflationary Universe.

In this section, we briefly review treatment of coupled perturbations to a single scalar field and linearized metric perturbations atop a Friedmann-Lamaître-Robertson-Walker background, discuss treatment of the quantum-to-classical transition and freeze-out for perturbation modes blown up to larger than the Hubble scale, and establish criteria for self-reproducing configurations during slow roll.

2.1.1 Scalar Perturbations During Inflation

It is expedient to decompose the inflaton into a homogeneous background expectation value and a perturbation atop that value: $\varphi(\tau, \mathbf{x}) \equiv \varphi_0(\tau) + \delta\varphi(\tau, \mathbf{x})$. Employing a semi-classical coupling to gravity (taking the Einstein field equations to uniquely determine the background geometry in terms of φ) results in correlated perturbations to the metric $g_{\mu\nu}$. To the coupled perturbation at each point is assigned a Hermitian operator acting on the quantum state space. Atop a curved de Sitter background, we derive an equation of motion for the Fourier components of the coupled perturbations, which is then quantized in a similar manner to the harmonic oscillator analogue in Minkowski space. Adopting the conformal time

coordinate $\mathrm{d}\tau = a(t)^{-1}\mathrm{d}t$ and comoving spatial coordinates $\mathrm{d}x^i$, we parameterize the perturbed FLRW line element as

$$g_{\mu\nu}\mathrm{d}x^\mu\mathrm{d}x^\nu = a^2\left[(1+2A)\,\mathrm{d}\tau^2 - 2\partial_i B\,\mathrm{d}\tau\,\mathrm{d}x^i - ((1-2\psi)\delta_{ij} + 2\partial_i\partial_j E)\,\mathrm{d}x^i\mathrm{d}x^j\right]$$

where we have omitted vector and tensor perturbative degrees of freedom.

The Mukhanov-Sasaki variable $v(\tau,\mathbf{x}) \equiv a\,\delta\varphi + z\,\psi$, with $z \equiv a\varphi_0' H^{-1}$, is a parameterization of the coupled perturbations of the inflaton and metric that is invariant to first order under arbitrary coordinate transformations. Here a prime denotes a derivative with respect to conformal time, and ψ is the comoving curvature perturbation. The equation of motion for the co-scaled perturbation field $v(\tau,\mathbf{x})$ is then

$$\frac{1}{a^2\epsilon}\frac{\partial}{\partial\tau}\left(a^2\epsilon\frac{\partial(z^{-1}v)}{\partial\tau}\right) - \nabla^2(z^{-1}v) = 0;$$

in terms of the Fourier coefficients v_k parameterizing $v(\tau,x)$, this becomes

$$0 = v_k'' + \left(k^2 - \tfrac{z''}{z}\right)v_k \approx v_k'' + (k^2 - 2\tau^{-2}(1+\mathcal{O}(\epsilon)+\mathcal{O}(\eta)))\,v_k \tag{2.1}$$

where

$$\epsilon \equiv -\frac{\dot{H}}{H^2} \quad \text{and} \quad \eta \equiv \epsilon - \frac{\ddot{\varphi}}{H\dot{\varphi}} \tag{2.2}$$

are the first and second slow roll parameters, respectively, taken to be much less than unity during inflation. Adopting the Bunch-Davies solution corresponding to the assumption of no particles at $\tau \to -\infty$, and taking $k\tau \ll 1$ for fluctuations

larger than Hubble scale, we have to zeroth order in ϵ,η for $\tau = -(aH)^{-1}(1-\epsilon+\mathcal{O}(\epsilon^2))$

$$v_k \approx \sqrt{\frac{1}{2k}}\left(1+\frac{i}{k\tau}\right)e^{ik\tau}, \quad |v_k| \to \sqrt{\frac{1}{2k}}\frac{aH}{k} \tag{2.3}$$

We then promote the scalar field $v(\tau,\mathbf{x})$ to a bosonic field operator $\hat{v}(\tau,\mathbf{x})$. From the equal-time two-point correlation function, we identify the dimensionless power spectrum $\mathcal{P}_v(k)$ for gauge invariant perturbations

$$\langle\Omega_{\rm BD}|\,\hat{v}(\tau,x_1)\hat{v}(\tau,x_2)\,|\Omega_{\rm BD}\rangle \equiv \int \mathrm{d}^3k\,\frac{\mathcal{P}_v(k)}{4\pi k^3}\,e^{ik(x_1-x_2)}$$

and find that is scale-invariant[2] for $k\tau \ll 1$

$$\mathcal{P}_v(k) = \frac{k^3\,|v_k|^2}{2\pi^2} = a^2\left(\frac{H}{2\pi}\right)^2 \tag{2.4}$$

In applying a statistical treatment to the distribution of *colored* volume (labeled with particular characterisitics, e.g. eternally vs. terminally inflating) during inflation, it is useful to treat worldlines undergoing a consistent rate of volumetric expansion as future-directed. For this, we work in a gauge in which the volumetric expansion rate is homogeneous on spatial hypersurfaces (at least within a region

[2]The true spectrum is nearly so; we have neglected the contributions of ϵ and η to the spectral index in the interest of quickly finding the amplitude. Accounting for them, we can express (2.1) as a Bessel's equation for the rescaled quantity $\sqrt{-\tau}v$, keep terms up to first order in ϵ,η, and find the dimensionless power spectrum to be

$$\mathcal{P}_v(k) = a^2\left(\frac{H}{2\pi}\right)^2\left[(1-\epsilon)\frac{\Gamma(\nu)}{\Gamma(3/2)}\,(2(1-\epsilon))^{\nu-3/2}\right]^2(k\tau)^{3-2\nu}$$

where $\nu \equiv 3/2+3\epsilon-\eta$. For Hubble-scale modes with $k=aH$, the amplitude therefore is only affected when ϵ and η are non-zero up to the factor in square brackets. The author expresses gratitude to [25] for clear pedagogic presentation of this material.

of a few Hubble volumes). Departure from this condition is captured by the perturbation to the number of elapsed e-folds $\mathcal{N}_e \equiv \ln(a/a_0)$ along a congruence of future-directed worldlines, which takes the form [26]

$$\delta\mathcal{N}_e = -\psi + \tfrac{1}{3}\nabla^2(E' - B)$$

Adopting the uniform-$\mathcal{N}_e$ gauge, in which $\delta\mathcal{N}_e = 0$, is equivalent to asserting $\psi = \frac{1}{2}\nabla^2 E$ when $B = 0$; spatial hypersurfaces will only be flat to the extent that $\nabla^2 E$ vanishes, as it does over large regions during slow roll. So taking $\psi \approx 0$ and therefore $v \approx a\,\delta\varphi$ is a reasonable approximation to the uniform-$\mathcal{N}_e$ gauge. With this approximation we find from (2.4) that the amplitude of perturbations to the inflaton at the Hubble scale is

$$\delta\varphi_q \equiv \left\langle \delta\varphi^2 \right\rangle^{1/2} \approx H/2\pi \tag{2.5}$$

From considerations of the ladder operator algebra for the single field, it is clear that the third moment $\langle 0|\, \hat{\delta\varphi}(\tau, x_1)\hat{\delta\varphi}(\tau, x_2)\hat{\delta\varphi}(\tau, x_3)\,|0\rangle$ vanishes, the fourth is equal to $3\langle\delta\varphi^2\rangle^2$, and so on – consistent with the amplitude of Hubble-scale modes behaving as Gaussian distributed with standard deviation $\delta\varphi_q$.[3] The first moment is of course the expectation value φ_0, which evolves according to the unperturbed

[3]Non-Gaussianities in the density perturbations can arise in models with multiple interacting fields.

classical equation of motion.

$$\nabla_t \dot{\varphi} + \frac{\mathrm{d}V}{\mathrm{d}\varphi} = \ddot{\varphi}_0 + 3H\dot{\varphi}_0 + \frac{\mathrm{d}V}{\mathrm{d}\varphi} = 0 \tag{2.6}$$

Quantum-to-Classical Transition We demonstrated above that the Fourier coefficients of field perturbations of wavelength on the order of the Hubble scale H^{-1} undergo Gaussian fluctuations of width $H/2\pi$ about a classical background trajectory that satisfies (2.6). From (2.3), the time evolution of Fourier components of the field perturbations goes like

$$a(\dot{a}\delta\varphi_k + a\dot{\delta\varphi_k}) \approx \sqrt{\frac{1}{2k}}\left(ik - \tau^{-1} - \frac{i}{k\tau^2}\right)e^{ik\tau} \implies \dot{\delta\varphi_k} \approx \left(\frac{k^2}{a^3H^2} - 2\right)H\,\delta\varphi_k \tag{2.7}$$

implying that new perturbations are not introduced for $k \ll aH$ (where the equation of motion for the mode coefficients corresponds to exponential decay). The only contributions at those scales are the originally sub-Hubble and Hubble-scale modes that have since expanded to much larger than the physical Hubble radius, thereafter "frozen out" until after the end of inflation. A similar statement applies to curvature perturbations, and conveniently lets us identify the distribution produced during inflation with the distribution as modes re-enter the Hubble horizon during a radiation dominated epoch to affect the last scattering surface for the CMB.

However, freeze-out alone does not account for how the quantum superposition

becomes a classical distribution over field configurations; one hopes for a consistent account of what constitutes a "measurement" in this system. The hand-wavy account of the quantum-to-classical "transition" invokes causal disconnectedness of separated regions in de Sitter space. Because the coordinate system with respect to which v_k is defined contains a horizon, it cannot be claimed that the Fourier coefficients pertain to coherent field perturbations spanning a scale larger than the Hubble radius. The amplitude v_k describes modes varying with spatial frequency k *locally*; modes in a Hubble volume far away must be described by different quantum variables. We must do a partial trace over the degrees of freedom that are not measureable in principle; this yields a mixed state, and from the standpoint of observers in any given Hubble volume constitutes a measurement on the Hubble-sized fluctuations. Alternative approaches carried out with more mathematical rigor come to the same conclusion – that the "Separate Universes" picture is most sensible.[4]

[4] One can also imagine the Hubble horizon producing a thermal bath of particles with the de Sitter temperature, and interaction of long wavelength modes with that bath constituting a measurement. Following from (2.7), the conjugate momentum to the generalized coordinate $\delta\varphi_k$ tends to be constant, and the quantum state must reflect an ever shrinking probability of momentum values away from zero [27]. The field perturbation is therefore described by a highly squeezed state during inflation [27]. In [28], it is suggested that no need to trace over the degrees of freedom of an environment to get decoherence of super-Hubble scale modes; but their method also involves taking an $\hbar \to 0$ limit, which seems contradictory.

2.1.2 Self-reproducing Inflation

Stochastic eternal or self-reproducing inflation occurs when quantum fluctuations of the inflaton field – in conjunction with a quantum-to-classical transition yielding a stochastic distribution over Hubble-sized field configurations – dominate over its classical evolution according to the slow roll equation of motion (2.6), delaying the end of inflation indefinitely in a non-decreasing physical 3-volume. Under conditions when fluctuations are significant, the inflaton's evolution is governed by a Langevin equation from the perspective of individual Hubble volumes, or by a Fokker-Planck equation giving a time-dependent probability distribution over field values, from which the conditions in population members in the Separate Universes approach are sampled.

Langevin Picture Inflation accounting for stochastic fluctuations of the long-wavelength modes discussed in Section 2.1.1 is equivalent to a system undergoing Brownian motion, in which the number of elapsed e-folds takes the place of the time or step parameter. The corresponding Langevin equations for the long-wavelength field φ and its conjugate momentum π in the uniform-$\mathcal{N}_e$ gauge are

$$\frac{\mathrm{d}\hat{\varphi}}{\mathrm{d}\mathcal{N}_e} = \hat{\pi} + \frac{H}{2\pi}\,\hat{\xi}_\varphi(\mathcal{N}_e) \qquad \frac{\mathrm{d}\bar{\pi}}{\mathrm{d}\mathcal{N}_e} = -(3-\epsilon)\bar{\pi} - \frac{V_{,\varphi}(\bar{\varphi})}{H^2} + \bar{\xi}_\pi(\mathcal{N}_e) \tag{2.8}$$

where a bar indicates that a variable is stochastic, and $\bar{\xi}_\varphi$ and $\bar{\xi}_\pi$ are Gaussian distributed noise contributions [26]. During slow roll ($\epsilon \ll 1$), dynamics are domi-

nated by Hubble friction, with deviations of the field velocity from $\dot{\varphi}_{\rm sr} = -V_{,\varphi}/3H$ quickly dying out (a consequence of the attractor behavior of the full equations of motion [29]). So Brownian fluctuations of the field momentum do not "stick"; $\bar{\pi}$ is effectively a function of the field value $\bar{\varphi}$. and (2.8) reduces to a single Langevin equation

$$\frac{\mathrm{d}\bar{\varphi}}{\mathrm{d}\mathcal{N}_e} = -\frac{V_{,\varphi}(\bar{\varphi})}{3H^2} + \frac{H}{2\pi}\,\bar{\xi}_{\varphi}(\mathcal{N}_e) \tag{2.9}$$

Over the passage of a Hubble time H^{-1}, the field's expectation value changes by an amount $\Delta\varphi = |\dot{\varphi}|H^{-1} = V_{,\varphi}/3H^2$ as it slowly rolls. During the same time interval, quantum fluctuations with wavelength H^{-1} and amplitude drawn from a Gaussian distribution of width $H/2\pi$ may drive the field in a given Hubble volume up or down the potential slope relative to its classical trajectory. If in that time, the probability for the field to move higher up the slope is greater than the ratio of initial to final physical volumes ($1/e^3$), then at least one Hubble volume is likely to continue inflating.

The probability that after a time Δt the slowly rolling field sampled from its stochastic Gaussian distribution is found to be higher on the slope is expressed

as[5]

$$P(\varphi(t+\Delta t) > \varphi(t)) = \frac{1}{\sqrt{2\pi\delta\varphi_q^2}} \int_{\varphi_-}^{0} \exp\left[-\frac{(\varphi - |V'(\varphi)|\,\Delta t/(3H))^2}{2\delta\varphi_q^2}\right] \tag{2.10}$$

where we assume that the potential gradient is negative, and φ_- is the location of the nearest local maximum in the uphill direction. In terms of this probability, the stochastic eternal inflation criterion is

$$P(\varphi(t+\Delta t) > \varphi(t)) > e^{-3H\Delta t}$$

Taking Δt to be the natural time-scale for the problem H^{-1} and φ_- as effectively $-\infty$ at $\gtrsim 4\sigma$ fluctuations away from the maximum, this amounts to the constraint

$$V'(\varphi)/(3H^2) \lesssim (H/2\pi)\,\sqrt{2}\,\mathrm{erfc}^{-1}(2e^{-3})$$

In terms of the potential and its derivative, this becomes

$$V(\varphi)^{3/2} \gtrsim 6.6\ |V'(\varphi)|\, M_{\rm P}^3 \tag{2.11}$$

[5] If the slow roll conditions $\epsilon, \eta \ll 1$ are met but classical evolution is dominated by the second derivative term in the equation of motion $\ddot{\varphi} \sim V_{,\varphi} \gg H\dot{\varphi}$ (as is the case when initializing with a small field velocity at an inflating local maximum), then the field excursion becomes

$$\Delta\varphi^{(2)} \approx \tfrac{1}{2}\ddot{\varphi}\Delta t^2 \approx -\,|V_{,\varphi}|\,/H^2 = 3\Delta\varphi^{(1)}$$

In that case, the argument of the exponential in the integrand of (2.10) becomes

$$\frac{(\varphi - |V'(\varphi)|\,/H^2)^2}{2(H/2\pi)^2}$$

When $\dot{\varphi} \gg \ddot{\varphi}/3H$, the first-derivative form of the field excursion takes over.

Fokker-Planck Picture Stochastic inflation may also be described by a Fokker-Planck equation for the time-varying distribution $\rho(\varphi, t)$, describing the probability density per comoving volume at time t for measuring the field value φ.

$$\frac{\partial}{\partial t}\rho(\varphi,t) = \frac{H^3}{8\pi}\frac{\partial^2\rho}{\partial\varphi^2} + \frac{1}{3H}\frac{\partial}{\partial\varphi}\left(\rho\frac{\mathrm{d}V}{\mathrm{d}\varphi}\right) \tag{2.12}$$

This approach allows one to follow a population from some initial distribution over field values, enforce boundary conditions, and characterize a subpopulation of inflating Hubble volumes. For the example of an inverted quadratic potential $V(\varphi) = V_0 - \frac{1}{2}M^2\varphi^2$ with the field initially localized at the peak, $\rho(\varphi, 0) = \delta(\varphi)$, the solution to (2.12) is a Gaussian distribution with a time-varying variance.

$$\rho(\varphi,t) = \frac{1}{\sqrt{\pi\sigma(t)^2}}\exp\left(-\frac{\varphi^2}{2\sigma(t)^2}\right)$$

$$\sigma(t)^2 \equiv \frac{3H^4}{4\pi^2M^2}\left[\exp\left(\frac{2M^2t}{3H^2}\right) - 1\right]$$

Equation (2.12) does not account for the expansion of inflating regions. In the late-time limit, the criterion (2.10) for self-reproducing inflation takes the form

$$\int_{\mathrm{inf}} \mathrm{d}\varphi\, \rho(\varphi, t+\Delta t) \gtrsim e^{-3H\Delta t}\int_{\mathrm{inf}} \mathrm{d}\varphi\, \rho(\varphi, t) \tag{2.13}$$

where the integral is taken over the interval of field space in which inflation occurs.

2.2 Long-lived Meta-stable de Sitter Vacua

A general effective potential can feature multiple local minima. In the false-vacuum eternal inflation scenario, the inflaton comes to occupy a local minimum with a positive vacuum energy – the same initial setup as Guth's original inflation scenario [21]. As long as the field remains in that vacuum, spacetime is de Sitter with Hubble parameter $H_{\rm F} = (V(\varphi_{\rm F})/3M_{\rm P}^2)^{1/2}$. Either by non-perturbative quantum effects (tunneling through the barrier to a new field configuration and geometry) or by ascending the barrier wall by a sequence of perturbative quantum and/or thermal fluctuations, the field may "escape" to continue its descent toward a lower minimum. If the transition rate is small, then the volume of space that exits the false vacuum in these ways is recouped by the expansion of neighboring regions that do not.

Consider worldlines that pass through a flat hypersurface of the false-vacuum de Sitter space characterized by Hubble parameter $H_{\rm F}$ at an initial time t_0. The fraction of those worldlines that pass through a locally still-inflating patch of a similarly defined hypersurface at time $t > t_0$ is

$$f_{\rm inf} = \exp\left[-\frac{4\pi}{3}\frac{\lambda(t-t_0)}{H_{\rm F}^3}\right] \tag{2.14}$$

where λ is the nucleation rate per 4-volume. The physical inflating volume goes

like $v_{\rm inf} \propto f_{\rm inf}\, e^{3H_{\rm F}t}$, so a transition rate

$$\lambda < 9H_{\rm F}^4/4\pi \tag{2.15}$$

ensures that the 3-volume of inflating space never decreases in the 4-volume coincident with a statistically large population of initial Hubble volumes [11]. The transition rate is determined by the type of transition and the shape of the potential, as discussed in the following sections. If a transition is followed by enough slow roll inflation to hide any otherwise observable relics of bubble nucleation and solve the horizon problem, then it may have occurred in the past of our own observable universe.

The case of tunneling through the barrier is treated by the Coleman-de Luccia (CDL) formalism; the single-field case is reviewed below. The case of stochastic fluctuation of Hubble volumes up the barrier wall (or equivalently, thermal fluctuation with a characteristic de Sitter temperature) was first explored by Hawking and Moss as the limiting case of a CDL instanton in which both termini are identified with the top of the barrier; we outline this important case in § 2.2.2.

2.2.1 Coleman-de Luccia Instanton

By treating a single scalar field governed by a one-dimensional potential with two local minima as analogous to a particle in a double potential well, we can

compute instanton solutions in the absence of gravity using the imaginary time formalism. Coleman and de Luccia [30] took this a step further to account for the effects of gravity in the transitions between de Sitter or Minkowski minima.

The geometry of de Sitter space can be represented as that of a 4D hyperboloid embedded in a 5D Minkowski space, with the metric carried over from the embedding space. After Wick rotation, the time coordinate becomes imaginary, and the hyperbolic geometry becomes a compact spherical geometry. The squared line element $\mathrm{d}s^2$ on that 4-sphere is $\mathrm{d}\xi^2 + \rho(\xi)^2\mathrm{d}\Omega_3$, where ξ is a radial coordinate measured along the surface with respect to an arbitrary point therein (the 4-origin) and $\rho(\xi)$ is the cylindrical radius (measured through the embedding space) of the 3-sphere made up of all points at a given sphere-distance ξ from the 4-origin. At the 4-origin, the Euclidean radius $\rho(0) = 0$ by definition. On the 4-sphere, $\rho(\xi) = w^{-1}\sin(w\xi)$, where w is the inverse Hubble radius. For Hubble-sized regions that depart from de Sitter (like the bubble solutions we consider), the Wick-rotated Euclidean space is not a 4-sphere, but the action-minimizing solutions we consider are still symmetric under $O(3,1)$ rotations of the embedding space that preserve ξ, so we can use the same metric to describe it.

The Euclidean analogue to the Einstein-Hilbert action in this $O(3,1)$-symmetric space is

$$S_\mathrm{E} = 2\pi^2 \int \mathrm{d}\xi \left[\rho^3 \left(\tfrac{1}{2}\varphi'^2 + V(\varphi)\right) + \frac{3}{\kappa}\left(\rho^2\rho'' + \rho\rho'^2 - \rho\right)\right] \tag{2.16}$$

The second derivative term can be eliminated with integration by parts[6], which also changes the sign of the $\rho\rho'^2$ term. We assume that classical general relativity specifies $\rho(\xi)$ in terms of $\varphi(\xi)$ (no quantum gravity here), and substitute the Einstein field equations (EFE). The $\xi\xi$ component of the EFE give an expression for ρ'^2, which rearranges to

$$\frac{3}{\kappa}\rho\rho'^2 = \frac{3}{\kappa}\rho + \rho^3\left(\frac{1}{2}\varphi'^2 - V(\varphi)\right) \implies \mathrm{d}S_{\mathrm{E}} = 2\pi^2\rho^3\,\mathrm{d}\xi\left(2V(\varphi) - \frac{6}{\kappa\rho^2}\right)$$

Instanton solutions extremize the Euclidean action with respect variation in $\varphi(\xi)$ and $\rho(\xi)$; they are solutions to the Euclidean equations of motion

$$\varphi'' + \frac{3\rho'}{\rho}\varphi' = \frac{\mathrm{d}V}{\mathrm{d}\varphi} \qquad \rho'' = -\frac{8\pi}{3M_{Pl}^2}\left(\varphi'^2 + V(\varphi)\right) \tag{2.17}$$

with the condition that $\varphi'(\xi)$ and $\rho(\xi)$ vanish at the poles of the compact sphere. Generally, instanton solutions with gravity do not interpolate between the false vacuum and the true vacuum, but rather terminate on the walls of the barrier in the two basins. In the "thin wall" limit, the instanton terminates very close to the minima, with a well localized bubble radius that is much smaller than the Hubble scale.

Semi-classical Thin-wall Case In the thin wall limit, the bubble history is for all intents completely defined by its initial radius R_0, surface tension σ, and

[6]We assume that the instanton solution and the indefinitely metastable solution have the same geometry at the boundary, so that the surface term vanishes.

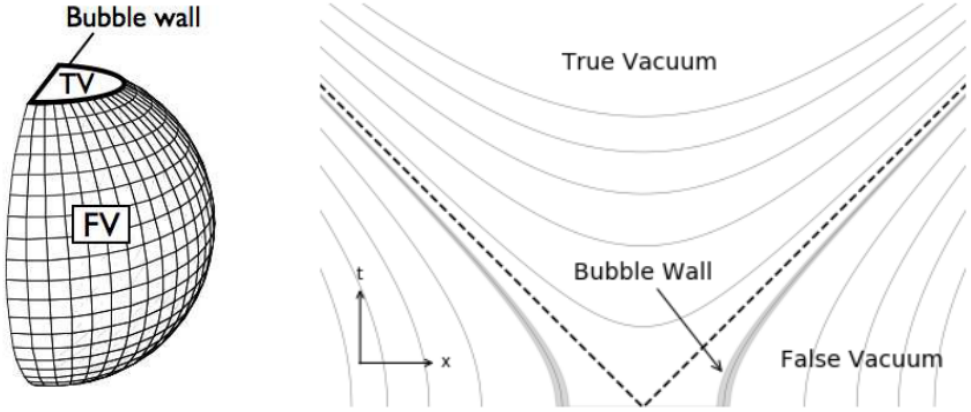

Figure 2.1: (Left) Illustration of the Euclidean geometry of a de Sitter-Minkowski bubble in a higher dimensional embedding space (image source: [31]). (Right) Space-time diagram depicting nucleation and evolution of an $O(3,1)$-symmetric thin-wall bubble. We can define n spatially open coordinate system in the light cone enclosed by the dashed lines, entirely within the bubble interior.

energy density ΔV of the interior relative to the surrounding space. The action then consists of surface and volume contributions

$$\bar{S}_{\mathrm{E}} = \mathcal{S}_3(R_0)\sigma - \mathcal{V}_3(R_0)\Delta V = 2\pi^2 H^{-3}\sin^3\theta_0\,\sigma - \frac{8\pi^2}{3}H^{-4}(2+\cos\theta_0)\sin^4\tfrac{\theta_0}{2}\,\Delta V$$

where the bubble wall tension is computed as $\mathrm{d}\sigma = \mathrm{d}\phi\,(V_F - V(\phi))$. Minimizing this Euclidean action with respect to geometric parameters for constant σ, H, and ΔV yields the semi-classical bubble radius

$$R_0 = H^{-1}\sin\theta_0 = 3\sigma(9H^2\sigma^2 + (\Delta V)^2)^{-1/2}$$

With θ_0 determined we obtain the leading order contribution to the transition rate

$$\exp(-S_{\rm E}) = \exp\left[-\frac{2\pi^2}{3H^4}\left[\frac{9H^2\sigma^2 + 2(\Delta V)^2}{(9H^2\sigma^2 + (\Delta V)^2)^{1/2}} - 2\Delta V\right]\right]$$

To obtain the full transition rate, we must account for perturbations to that trajectory that add next to leading order contributions, appending a *pre-factor* A to the rate exponentially suppressed by the Euclidean action: $\Gamma = Ae^{-S_{\rm E}}$.

We can consider these to be perturbations to the shape of the bubble in a 5D Euclidean embedding space, parameterized by a scalar field ϕ with support on the 4D bubble wall history, taken to obey the equation of motion $\hat{\mathcal{O}}\phi = 0$ for

$$\hat{\mathcal{O}} = R_0^2(-\Delta + M^2), \quad M^2 = -3R_0^2$$

Expanding ϕ in terms of spherical harmonics with coefficients C_{LJ}, the partition function for a single bounce is

$$Z_1 \equiv \int e^{-S_E^{(2)}[\phi]}\, D\phi = e^{-\bar{S}_{\rm E}} \int \exp\left(-\frac{1}{2}\sum_{LJ}\frac{(\mu C_{LJ})^2}{\mu^2(M^2 - \lambda_L)^{-1}}\right) \prod_{LJ} \mu \frac{{\rm d}C_{LJ}}{(2\pi)^{1/2}}$$

where μ is a mass scale for the field. Treating the bubble as a thermodynamic system with characteristic parameter $\beta \equiv 1/k_B T$, we then express the equilibrium number of bubbles $\bar{\mathcal{N}}$ in terms of the Euclidean partition function Z constructed by integrating over small perturbations to the bubble shape, as

$$\mathcal{N} = \beta^{-1}\partial_{\tilde{\mu}} \ln Z\big|_V = e^{\tilde{\mu}\beta} Z_1$$

where $Z = \exp(e^{\tilde{\mu}\beta} Z_1)$ is the partition function accounting for any number of bounces, and $\tilde{\mu}$ is a fictitious chemical potential. Since no strictly per-bubble energy cost is actually incurred, we may set $\tilde{\mu}$ to zero, and obtain

$$\mathrm{d}\mathcal{N} = \mathrm{d}Z_1 = \left[\det{}' \left[(\mu R_0)^{-2}\hat{O}\right]\right]^{-1/2} \left(\tfrac{\sigma S_3(R_0)}{8\pi}\right)^2 e^{-\bar{S}_\mathrm{E}}\, \mathrm{d}t_E\, \mathrm{d}V$$

The first factor is the closed form Gaussian integral giving quantum corrections to second order in ϕ. (The prime indicates that the zero eigenvalues for the $L = 1$ spherical harmonic coefficients are excluded from the determinant – since the integral over the $L = 1$ coefficients remains as an integral over $\mathrm{d}t_E\, \mathrm{d}V$.) The second factor is the Jacobian associated with converting from spherical harmonic coefficients C_{1J} of the wall perturbation field ϕ to Minkowski coordinates as the variables of integration. These two terms make up the prefactor. Evaluating the determinant with zeta function regularization, we have

$$\det{}'[(\mu R_0)^{-2}\hat{O}] = \frac{(\mu R_0)^{-2\zeta_\mathcal{O}(0)} e^{-\zeta'_\mathcal{O}(0)}}{(M^2 + N^2 R_0^2)^4}$$

where $\zeta_\mathcal{O}(z)$ is a generalized zeta function customized for $\hat{O}$

$$\zeta_{\hat{O}}(z) \equiv \textstyle\sum_L g_L \Lambda_L^{-z} = \sum_L g_L \left[-R_0^2(\lambda_L + 3R_0^2)\right]^z$$

g_L is the degeneracy of spherical harmonics with a given L, and $\zeta'(z) \equiv \mathrm{d}\zeta/\mathrm{d}z$. Despite $g_L > 0\ \forall\, L$, the regularized $\zeta_\mathcal{O}(0)$ evaluates to zero.

For bubble nucleation in 3+1 dimensions, $\zeta(0) = 0$, and we can express $\zeta'(z)$

in terms of the derivative of the Riemann zeta function $\zeta_R(z)$ and constants.

$$\left|\det{}' \left[(\mu R_0)^{-2}\mathcal{O}\right]\right|^{1/2} = 4i(\pi R_0^2)^{-2}\, e^{\zeta_R'(-2)}$$

Substituting $S_3(R_0) = 2\pi^2 R_0^3$ and $e^{\zeta_R'(-2)} = 0.9700$, this becomes

$$\frac{\mathrm{d}\mathcal{N}}{\mathrm{d}t\,\mathrm{d}V} = \frac{\Gamma}{V} = \left(\frac{\sigma\pi R_0^3}{4}\right)^2 \frac{4R_0^{-4}}{\pi^2} \times 0.97 \times e^{-\bar{S}_{\mathrm{E}}} \approx (\tfrac{1}{2}\sigma R_0)^2\, e^{-\bar{S}_{\mathrm{E}}} \tag{2.18}$$

In a de Sitter background, this gives the transition rate per physical four-volume. A more complete treatment of the pre-factor calculation for membrane nucleation in curved spacetime may be found in [32].

Viability Old bubbly inflation does not work [8] because the rate of bubble nucleation is generically too slow; even as differential pressure pushes the bubble walls to expand at a speed approaching c, bubbles cannot coalesce within the inflating background to form large homogeneous post-inflationary regions in the true vacuum.

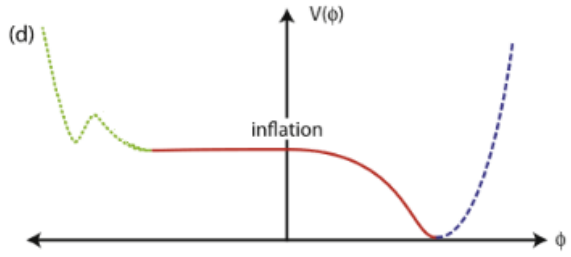

Figure 2.2: An example of a "designer" potential in which a Coleman-de Luccia transition could precede slow roll inflation and avoid the slow bubble nucleation problem in false vacuum eternal inflation. Original image source: [2]

A Coleman de Luccia transition must be followed by a period of slow roll to produce an observationally viable cosmology. This tends to require "designer" potentials that feature both a sharp barrier with a large second derivative and a flat region in which slow roll can take place, in adjacent intervals in field space. See [33] for an overview of open universes from bubble nucleation during inflation.

2.2.2 Hawking-Moss Instanton

As seen with Coleman de Luccia, when gravity is included the instanton terminates on the *walls* of the true and false vacuum basins, rather than at the minima. As we widen the barrier, the starting point on the true-vacuum side and the ending point where $\rho = 0$, $\dot{\varphi} = 0$ on the false-vacuum side both approach the maximum.

If the peak is too broad, then the Hubble friction acting during a long excursion near the maximum of the potential pulls too much kinetic energy out of the field, preventing it from closing the compact geometry with non-singular boundary conditions [34]. Or equivalently, if we evolve the equations of motion backward from the true-vacuum side, the Hubble friction acts in reverse, adding to $\dot{\varphi}$ the more time is spent in the region around the maximum. The integration always overshoots the false vacuum; at some point a minimum of $\dot{\varphi}$ evaluated when the field obtains $\varphi_{\rm F}$ is reached, and bringing the final condition closer to the maximum

on the true-vacuum side translates to a higher $\dot{\varphi}$ at the false vacuum. Taken to the extreme of a nearly flat barrier $V''(\varphi) \gtrsim M_{\rm P}^2$, the only non-singular solution to the Euclidean equations of motion is one in which the Euclidean geometry is spherical (de Sitter) and the field sits atop the barrier everywhere. This *Hawking-Moss instanton* [35] can be seen as the limit opposite to the thin-wall limit, in which the "thickness" of the "bubble" exceeds the Hubble scale.

Since the CDL and HM solutions make contact with neither the true nor false vacua, in what sense can it be considered a transition between de Sitter minima? If perturbative quantum or thermal fluctuations in the false vacuum basin produce a distribution of field values that reaches to the instanton's terminating point in that basin, then instanton-mediated tunneling between the two basins can proceed. In the Hawking-Moss case, the terminating points of the instanton are both at the top of the barrier, so the burden falls entirely on thermal or quantum diffusion to carry the field – initially well localized at the minimum – to the top of the barrier.

In the late-time limit, the diffusion equation (2.12) leads to a nearly time-independent distribution for field values around an inflating false minimum, and the probability of a field value sampled from that distribution being found at the peak matches the semi-classical Hawking-Moss calculation, with the tunneling rate exponentially suppressed by the difference between Euclidean actions for the two configurations. Because the Wick rotation of de Sitter space is compact

and periodic in imaginary time, we can think of it as having a temperature with thermodynamic-β proportional to H. A Hawking-Moss instanton is best conceptualized as a thermal fluctuation to the top of the barrier, which happens to coincide with the rate computed from the zero-temperature quantum calculation.

2.3 Inflating Topological Defects

A third mechanism for eternal inflation operates even in a classical setting: what if conditions for inflation *cannot* end everywhere, due to topological considerations? Take a potential with two vacua, separated by a local maximum at $\varphi = 0$

$$V(\varphi) = \frac{\lambda}{4}\left(\varphi^2 - \frac{m^2}{\lambda}\right)^2 \tag{2.19}$$

as illustrated in Figure 2.3. If in different regions of space the field has settled into different vacua at $\varphi = \pm\eta$, with $\eta \equiv m/\sqrt{\lambda}$, then by continuity the field must obtain the local maximum of the potential somewhere in between – forming a *domain wall* with a possibly large positive energy density. Such a configuration cannot classically evolve into a true vacuum solution with the field everywhere sitting at one or the other minimum, as that would require the energy to increase as the field in one region traverses the central maximum.

The next best move is for the domain wall to minimize the potential energy of the configuration by collapsing; however, doing so increases the gradient energy.

In three spatial dimensions, for the above potential there exist static solitons in which the gradient and potential energies are balanced. Neglecting gravitational effects, the static solution is

$$\varphi(t, \mathbf{x}) = \eta \tanh\left(\sqrt{\tfrac{\lambda}{2}}\,\eta\, x\right)$$

When the characteristic width of domain walls is comparable to the Planck scale, gravitational effects become important, and can lead to *topological eternal inflation.*

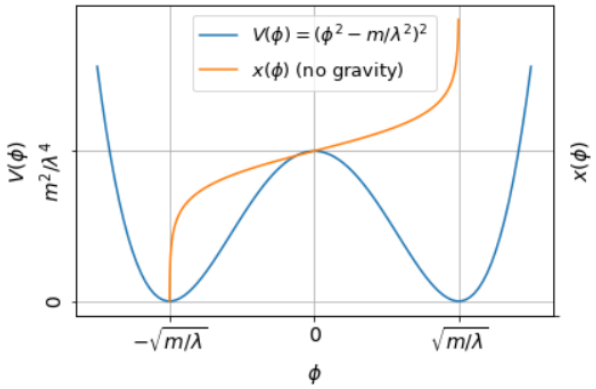

Figure 2.3: Representative potential in which topological defects can form for single field models; studied in [36]. Also shown is the static domain wall solution when gravitational effects are neglected in the limit $\eta \ll M_{\rm P}$.

Let Regions I and III occupy different vacua of (2.19), with a Region II interpolating between $\pm\eta$. The Hubble scale at the top of the potential barrier is

$$H = \sqrt{\frac{2\pi\lambda}{3}}\,\frac{\eta^2}{M_{\rm P}}$$

If the displacement of the minima in field space η is comparable to the Planck mass, or if the physical width of the domain wall is larger than the Hubble scale, then even a large thermal fluctuation of Region III into Region I's vacuum could not propagate to bring down the wall. If the space occupying the middle ground is inflating at a rate sufficient to compensate for the inward collapse of its boundaries in comoving coordinates, then it will undergo topological eternal inflation. These results are generic for distortions of the barrier (2.19) and for defects with other co-dimensions (monopoles, strings).

Topological inflation can occur only when φ obtains a spatially inhomogeneous configuration around a local maximum. Per the setup assumptions we have adopted, we consider one Hubble volume initialized with a homogeneous field expectation value. Inhomogenity then originates with quantum fluctuations, which are assumed to behave classically after being stretched to scales much larger than H^{-1}; so initially the field has not obtained a time-independent classical background solution. If the scale at which $V(\varphi)$ varies near the maximum is much less than $m_{\rm P}$, then domain walls are more or less unchanged by including gravity, and approximately static solutions exist. The question is then whether an initial configuration with $\varphi(t, x)$ having a large wavelength around the peak quickly collapses into that static solution, *before* inflation produces many Hubble volumes with field values at the peak.

Initially Homogeneous atop the Barrier Suppose a nearly static domain wall (necessarily of a thickness much less than the Hubble radius associated with the potential energy at the peak) is a solution of a given double well potential. Given an initial Hubble volume not containing a domain wall, but in which φ is nearly homogeneous around the top of the barrier, it is of interest to determine under what conditions the domain wall that forms as a consequence of the field's classical descent from the peak is nearly static and sub-Hubble in scale. An alternative might be that despite the existence of such a solution, the nearly homogeneous initial configuration results in inflation of what will become the domain wall core, and a localized solution is precluded by the ensuing expansion.

A necessary but insufficient condition for a sub-Hubble defect to form is that the gradient of the field configuration around the top of a potential barrier is initially increasing in physical coordinates. Assume that $\varphi(t, x)$ is initially linear in its spatial dependence in a small region around which it obtains the peak value, with a small proportionality factor $k(t)$, defined with respect to the physical distance $xe^{H_0 t}$:

$$\varphi(t, x) \approx k(t)a(t)xH_0$$

where H_0 is the Hubble parameter at the peak (a convenient mass scale), x is a comoving coordinate, and $a(t) \approx e^{H_0 t}$. In the vicinity of the maximum we take the potential to be approximately quadratic: $V(\varphi) \approx V_0 - \frac{1}{2}\mu^2\varphi^2$. The equation

of motion for $k(t)$ is then

$$\ddot{k} + 5H\dot{k} + (4H^2 + \dot{H} - \mu^2)k = 0$$

If the expression in parentheses is positive, then $k(t)$ behaves like an overdamped harmonic oscillator, and the domain wall grows (k(t) vanishes at late times) even if a nearly static sub-Hubble-scale domain wall solution exists. Using the Friedmann equations (1.1) sourced by the scalar φ, this occurs when

$$V''(\varphi_{\text{peak}}) \lesssim \frac{1}{M_P^2}(\tfrac{1}{2}\dot{\varphi}^2 + V(\varphi_{\text{peak}})) - \frac{1}{3M_P^2}(\tfrac{1}{2}\dot{\varphi}^2 - V(\varphi_{\text{peak}}))$$

So if the potential is sufficiently flat near the maximum

$$\frac{1}{\kappa V_0}\left|\frac{\mathrm{d}^2 V}{\mathrm{d}\varphi^2}\right|_{\varphi=0} < \frac{4-\epsilon}{3} \tag{2.20}$$

where ϵ is the first slow roll parameter from (2.2), then the domain wall grows even if a nearly static sub-Hubble-scale domain wall solution were possible. Otherwise, $k(t)$ grows monotonically within the validity of this approximation, leading potentially to a collapse.[7]

When considering $\varphi(x)$ centered at the maximum and neglecting metric fluctuations, $\epsilon = 0$ and this criterion is weaker version of the second potential slow roll condition ($\eta_V \ll 1$). Though not required for some quasi-exponential expansion to occur, the latter is almost always needed to solve the horizon problem. Thus,

[7] A full collapse can be thwarted by Hubble friction lower on the potential.

any instance of inflation starting at a maximum leads to topological inflation. If φ is dropped only *near* the maximum and the stochastic inflation criterion is *not* met, then it is not guaranteed that φ will end up straddling the potential peak, and topological inflation may be avoided. Even if φ does not initially interpolate between the two basins of attraction, if it inflates from its initial configuration, then stochastic fluctuations in the population of Hubble volumes produced near the peak may be enough to drive the field in some regions over the hilltop – a less pronounced version of Hawking-Moss transition – creating a topological defect.

Chapter 3

How Generic is Eternality?

A widespread belief in the inflation community is that an eternal "multiverse" is a generic prediction of inflation [13, 37] – a free side effect arising without a need for additional fine-tuning of model parameters or initial conditions (beyond that which might be required for viable inflation). However, the basis for that belief as it is commonly held is to a large extent qualitative – justified in terms of an informal, heuristic sampling of named classes of inflation models with substantial representation in the literature, and not the conclusions of a direct, comprehensive analysis. As inflation continues to gain empirical support as an explanatory account of our cosmic history, it remains an open question whether eternal inflation should be considered generic or fine-tuned among candidate models consistent with observation.

In Sections 3.1 and 3.2, we discuss the implications of eternal inflation that motivate its intrigue, and survey arguments as to whether eternal behavior might or might not be generic. In § 3.3, we outline the structure of measures over single-field inflation models, argue how one would term certain properties generic or fine-tuned, and discuss merits and shortcomings of a few candidate measures over the space of inflationary cosmologies.

3.1 The Case for *Generic*

To emphasize the strength of consensus around the characterization of inflation as generically eternal: the first sentence of [15] reads "Inflation is generically eternal." It is in good company among similar statements in the opening paragraphs of many articles on the topic. Surely this assertion is well motivated, but what precisely is the basis for it?

By inspection of Eq. (2.11), stochastic fluctuations outpace slow roll in models in which the inflaton is initialized near an inflating local maximum or saddle point where $V'(\varphi)$ vanishes and for those in which the potential is unbounded from above with a wide dispersion of initial field values (e.g. inflation in a quadratic potential with mass parameter m and field excursion $\Delta\phi \gtrsim 4(M_P^3/m)^{1/2}$). Slow roll already requires a very flat potential, and stochastic inflation requires only somewhat flatter or more energetic sites of inflation. Plausible extensions to the

standard treatment of fluctuations, like warm inflation [38] with its account of thermal effects, increase the amplitude of fluctuations of the inflaton – shrinking the gap between sufficient conditions for successful inflation and eternal behavior. If we are assumed to occupy a region of model space in which inflation is generic, it seems to follow from the above considerations that eternal inflation should not be much less difficult to avoid. And generally, if the end of inflation is a stochastic process with a large dispersion in the prior distribution on the rate at which that process proceeds, for inflation to end everywhere "all at once" comes across as rather implausible.

The topological inflation criterion given by Eq. (2.20) is always satisfied for a single inflaton initialized at a maximum where the second potential slow roll condition $\eta_V \ll 1$ is met. The latter condition – though not required for some quasi-exponential expansion to occur – is almost always needed to solve the horizon problem[1]. Quantum fluctuations dominate the slow evolution of $\langle\varphi\rangle$ near the peak, resulting in an inhomogeneous field configuration with $\langle\varphi\rangle$ descending toward the minima of both conjoining half-basins in Separate Universes, separated in space by an inflating topological defect that can never be excised. Even if φ is initialized only near the maximum, stochastic inflation always occurs within a neighborhood of the potential peak, and fluctuations can drive some regions over

[1]This is relevant even when initializing at a maximum, as quantum or thermal fluctuations render finite the expected time and e-folds elapsed in the vicinity of the peak.

the top of the peak to descend toward the adjacent minimum, producing a topological defect. This can occur by chance even if the formal stochastic inflation criterion is not met at the initial field value.

If we take the setting of inflation to be a vast landscape potential and populate the presumably large number of false vacua therein, then we get eternal inflation no matter what. The difficulty lies in connecting eternal inflation occurring in these false vacua with the last 60 e-folds that must explain our data. Given an infinite elapsed time to wait in the false vacuum, we are guaranteed to see transitions from one metastable de Sitter minimum to another; but to produce large homogeneous regions in the true vacuum basin, a transition must be followed by a period of slow roll inflation.

If the barrier is broad ($V'' \ll V/m_{\rm P}^2$), then the largest contribution to the transition comes from the Hawking-Moss (HM) instanton – a naive interpretation of which paints a picture of the entire history of the field configuration in the "final" state sitting on top of the barrier, with the background geometry fixed for all time. Rather, we adopt the interpretation the HM calculation [35] as yielding the rate at which Hubble volumes occupying the false vacuum basin thermally fluctuate into the true vacuum basin (essentially a consequence of stochastic inflation), with energy comparable to the height of the barrier [39]. Since this picture of the HM instanton invokes stochastic inflation as a necessary ingredient, all models with a

Hawking-Moss transition are necessrily eternal.

3.2 The Dissent

Two schools of criticism of eternal inflation are represented in the literature: one accepts the established treatments outlined in § 2 but questions the predominance of the associated criteria in conceivably representative measures on model-space (which we address); and another attacks the foundational assumptions on which those established treatments are based. Of the three instantiations, stochastic eternal inflation is most susceptible to the latter, as the topological and false vacuum varieties appear quite unassailable once the setup assumptions are granted (or at least avenues for departure from the usual treatment are much less evident). We begin by noting some of the claims made by the latter school.

Adjudicating on the status of stochastic eternal inflation requires careful consideration of the back-reaction of quantum fluctuations on the metric. In § 2.1.1, we quantized a gauge-invariant small perturbation to the field and the metric in a fixed background; the fully rigorous treatment would account for both field and metric perturbations separately in the full nonlinear theory, in which the perturbations can substantially change the background metric. It is unsettled as to whether the calculations presented in the literature paint an accurate picture of this interaction.

For example, [40] argues that back-reaction becomes important well before the stochastic regime in chaotic inflation and similar models, so that the latter is not well characterized by assuming small perturbations to a background metric fixed at the scale of a Hubble volume or more. In [41], it is argued that applying the appropriate adiabatic regularization procedure in calculating the amplitude of quantum fluctuations of the inflaton (presented in [42]) dramatically reduces that amplitude[2] relative to the commonly cited result of $H/2\pi$, and in so doing increases the energy scale needed to achieve stochastic eternal inflation. Other modifications to the story of how the quantum-to-classical transition comes about could alter the probability of eternal inflation.[3]

Even taking the established treatment as given, several factors make eternal inflation potentially less likely to be well represented in the measure over models and initial conditions producing observationally viable cosmologies.

Scale Discrepancies The primordial perturbation spectrum inferred from measurements of the CMB implies a significant scale discrepancy between a regime of stochastic inflation, in which curvature perturbations $\delta\mathcal{R}/\mathcal{R}$ are of order unity,

[2]The proposed amplitude is given by $\delta\varphi^2 \cong 0.01V''(\varphi)$.

[3]For example, [43] presents a calculation of explicit decoherence of modes for inflaton fluctuations via interaction with metric perturbations suggests that Hubble-scale modes do not decohere until $\mathcal{O}(10)$ Hubble times after they have left the horizon, in tension with the widely accepted $\mathcal{O}(1)$ figure; in [44], it is demonstrated that taking this delay into consideration alters the criterion for stochastic eternal inflation. However, if we do not alter the rate at which we "update" the branching distribution, but only a change in the size of fluctuations relative to the classical field excursion (both of which change slowly during inflation), then it does not greatly affect the probability of eternal inflation.

and horizon exit of modes of observational interest. Suppose we parameterize the inflaton potential in terms of the vertical and horizontal mass coefficients m_v and m_h, along with a dimensionless function $f(x)$ of order unity defining its shape:

$$V(\varphi) \equiv (m_v m_{\rm P})^4 f(\varphi/(m_h m_{\rm P}))$$

Here $m_{\rm P}$ is the Planck mass. With $Q_s \sim \mathcal{O}(10^{-5})$, the quantity $f(x)^{3/2} f'(x)^{-1}$ appearing in both the expression for Q_s and Eq (2.11) must shrink by a factor $\mathcal{O}(10^{-3})$ between a scale of stochastic eternal inflation and the horizon exit scale. In this sense the sufficient conditions for inflation consistent with the data do not strongly constrain the part of the potential relevant for stochastic inflation.

In [45], this scale discrepancy is cast as a negative upper bound on the running of the spectral index as a sufficient condition for non-eternal inflation, assuming higher order runnings-of-the-running can be neglected. The criterion Eq. (2.11) may be expressed in terms of the power in curvature perturbations for modes crossing the horizon:

$$1 \lesssim \frac{\delta\varphi}{\Delta\varphi} = \frac{H^2}{2\pi\dot{\varphi}} = \mathcal{P}_{\mathcal{R}}(k)\Big|_{k=aH} \tag{3.1}$$

Neglecting $\mathrm{d}^n(\ln \mathcal{P}_{\mathcal{R}})/\mathrm{d}(\ln k)^n$ for $n > 2$, we may use this relation to compute a lower bound on the running α (evaluated at horizon exit) for which Eq. (2.11) is satisfied, or an upper bound for non-eternal inflation. The negation of constraint

(3.1) expressed in terms of $\ln \mathcal{P}_{\mathcal{R}}$ may be written as follows:

$$\ln \mathcal{P}_{\mathcal{R}}(k) = \ln \mathcal{P}_{\mathcal{R},\star} + \left[n_s - 1 + \frac{1}{2}\alpha \ln \frac{k}{k_\star} + \cdots \right] \ln \frac{k}{k_\star} < 0$$

where $\mathcal{P}_{\mathcal{R},\star}$ and $k_\star$ are evaluated at horizon exit. Plugging in the value $k_{\max}$ that maximizes $\ln \mathcal{P}_{\mathcal{R}}$, one obtains

$$\ln \mathcal{P}_{\mathcal{R}}(k_{\max}) = \ln \mathcal{P}_{\mathcal{R},\star} - \frac{(1-n_s)^2}{4\alpha} < 0$$

Accepting this as a bound on $\ln \mathcal{P}_{\mathcal{R}}$ yields an upper bound on the running; Kinney and Freese found this bound to be negative but quite small in magnitude relative to current observational bounds on the running:

$$\alpha < \frac{(1-n_s)^2}{4 \ln \mathcal{P}_{\mathcal{R},\star}} \approx -4 \times 10^{-5} \tag{3.2}$$

We will investigate the relation between the running of the scalar spectral index and presence of stochastic eternal inflation in Appendix A – whether (3.2) is in "practice" a useful bound and to what extent α is an informative detection statistic for stochastic inflation. Here we merely note that if the field history does not traverse intervals on the potential with vastly different characteristics before the end of inflation, then there are large portions of parameter space consistent with observation that preclude stochastic eternal inflation.

Run Aground in the Swampland The de Sitter Swampland Conjecture [46, 47] is a proposal that a large proportion of consistent-looking low-energy scalar effective field theories presenting in the string landscape are in fact inadmissible, owing to incompatibility with UV completion to an (as-yet unformulated) theory of quantum gravity. The criteria for the remaining admissible low-energy theories is that the field excursion $\Delta\varphi$ and potential must satisfy

$$\Delta\varphi \gtrsim \Delta \quad \text{and} \quad |V'| > cM_{\rm P}^{-1}V \tag{3.3}$$

or possibly

$$V'' > -\bar{c}M_{\rm P}^{-2}V \tag{3.4}$$

for constants $0 < \{\Delta, c, \bar{c}\} \lesssim \mathcal{O}(1)$. Numerous authors have worked out the implications for inflation, and indicate that the conjecture and its variants rule out sites of stochastic inflation [48, 49, 50, 51], or not [52]. If the proposal is found to withstand scrutiny, then some loophole or exception must be indentified to allow for ordinary inflation. Since stochastic inflation tends to violate the first-derivative criterion in (3.3) more severely than ordinary inflation, it is plausible that any such scheme for selecting viable inflation models would penalize those with stochastic inflation.

Extremely Steep and Incredibly Flat The scenario proposed in 1981 had inflation take place in a false vacuum, invoking a phase transition with bubbles

nucleating near the true vacuum and coalescing to form large post-inflationary regions. But bubbles could not coalesce fast enough in the inflating background; to be consistent with observation; a transition must be followed by a period of slow roll inflation.

If the barrier turns over sharply, the largest contribution to the transition is a Coleman-de Luccia instanton, which tends to terminate very close to the true minimum with a thin-walled bubble. While instanton transition rates are generically much smaller than the upper bound in (2.15), one would need an instanton that terminates atypically high on the slope of a nearly-Minkowski half-basin, separated from the minimum by an interval of field space in which the potential is remarkably flat by the standards of the potential barrier (for example, a potential like that shown in Figure 2.2). However, the rarity of coincidence of such features in a measure over potential shapes may be balanced by conditioning on inflation producing enough e-folds to begin with. Even if the inflaton is initialized in a false vacuum, our prior on the number of e-folds is already high, and the fact that successful inflation following a CDL transition is rare is for the most part counterfactual.

Before conditioning on a small final vacuum energy, one might suspect models with successful inflation following a Hawkiing-Moss transition of being unnatural, as the potential featuring a broad barrier must also vary quickly before the mini-

mum in order to give a clean exit from inflation. This is alleviated only somewhat if we fix the energy of the true vacuum to be very small, so that inflation always ends close to the minimum where $\epsilon_V \sim 1$. This puts a Hawking-Moss transition among field histories yielding sufficient inflation with a viable scalar amplitude and spectral index, but typically too high of a tensor-to-scalar ratio.

Nonvanishing Spatial Curvature A positive spatial curvature is difficult to achieve with eternal inflation [53, 54]. Inflation naturally leads to a reduction in spatial curvature over time, bringing the density Ω_k asymptotically close to its critical value for a flat universe. Cosmological histories that prescribe much more inflationary expansion than the minimum needed to account for the CMB greatly disfavor departures from flatness. With the new results from *Planck 2018 Legacy* suggesting a small but measurable positive curvature with high confidence level [55], eternal inflation may be in trouble.

3.3 Making of a Measure

What would it *mean* for eternal inflation to be generic? As a matter of history, it has meant that of the inflation models that have been devised, many appear to be eternal in most regions of the space of model parameters and initial conditions that have warranted scrutiny. More properly, it should mean that given

some representative *measure* (or class of measures) over inflation models and initial conditions, those combinations resulting in eternal inflation comprise a large fraction of the measure, or perhaps of the measure over combinations that lead to observationally viable cosmologies.

A measure is a recipe we adopt for assigning probabilistic weight to partitions of a space of inputs. The measure over potential functions and initial conditions *should* be informed by details of the process by which the form of those models is determined, stemming from e.g a theory valid at higher energies. It might account for selection effects based on future boundary conditions relating to the existence and properties of reference objects (e.g. protons, galaxies, observers), and ordering effects related to how one defines a population of equivalent reference objects on which to base that selection. (See [20, 56] for in-depth discussions of these issues confronting all would-be measure bearers.) The first is rather open-ended in the absence of a prescriptive theory of the origin of the inflaton potential. The latter two overlap with the notorious Measure Problem in eternal inflation – pertaining to the absence of a physically preferred scheme for identifying a population of equivalent reference objects in an infinite multiverse.

One might make the argument that even if eternal inflation does not dominate the measure over model-space, those models with eternal inflation produce vastly more thermalized regions than those without, and so an observer is warranted in

assuming that the conditions for eternal inflation are in their region's past. This volume weighting stance is sensible only if one grants that a population of models (or of initial conditions on a vast potential with both eternal and non-eternal inflation) is in fact realized, so that they are in effect competing with one another dynamically for representation in a final ensemble.

As the focus of this study, we rather assume that one potential is actually realized, and ask about the likelihood that a Hubble volume sampled with particular initial conditions leads to eternal inflation. To distinguish this from the Measure Problem of Eternal Inflation, let us denote this separate-but-related issue as the Measure Question of Model Selection and Initial Conditions. The two difficulties in working with measures in cosmology interact when it comes to making predictions, as once the model is given, assuming eternal inflation is possible one still must make choices regarding the measure on observable outcomes in that space. The furthest we go in meddling with observer selection effects is to discard models for which observables from inflation do not match the data.

Defining Genericity *Genericity* might refer to a posterior distribution over a collection of parameters $\mathbf{p}_{\text{eternal}}$ characterizing eternal inflation, given priors on those parameters, observational data $\mathbf{d}$, and a dictionary of correlations between the parameters modeling the data and the necessarily hidden parameters in $\mathbf{p}_{\text{eternal}}$ (we only have access to our one observable universe). Let the full vector of pa-

rameters be denoted by

$$\mathbf{p} = (\mathbf{p}_{\text{eternal}}, \mathbf{p}_{\text{obs}}) \tag{3.5}$$

where $\mathbf{p}_{\text{obs}}$ includes those parameters modeling observables from any successful inflation model that are accessible to our instruments:[4]

$$\mathbf{p}_{\text{obs}} = (Q, r, n_s, \alpha, n_t, \delta\rho/\rho, \log|\Omega_{\text{tot}} - 1|, \rho_\Lambda) \tag{3.6}$$

Since our model of the data only connects $\mathbf{d}$ to $\mathbf{p}_{\text{obs}}$, the posterior distribution over the hidden parameters in $\mathbf{p}_{\text{eternal}}$ is determined entirely by how they correlate with those in $\mathbf{p}_{\text{obs}}$; this in turn depends on the choice of a measure.

For each measure m, there is a distribution $f_m(\mathbf{p} \mid \mathbf{p}_{\text{obs}})$ connecting the hidden eternal sector to parameters that make contact with the data. The probability associated with the full parameter vector $\mathbf{p}$ is then

$$p_m(\mathbf{p} \mid \mathbf{d}) = \int f_m(\mathbf{p} \mid \mathbf{p}_{\text{obs}})\, \ell(\mathbf{p}_{\text{obs}} \mid \mathbf{d})\, \mathrm{d}\mathbf{p}_{\text{obs}} \tag{3.7}$$

To estimate $p_m(\mathbf{p} \mid \mathbf{d})$, one could generate a population of simulated models reflecting the measure, and from that population bootstrap a number of subpopulations for which the distribution over $\mathbf{p}_{\text{obs}}$ is consistent with the likelihood $\ell(\mathbf{p}_{\text{obs}} \mid \mathbf{d})$. (Since $\ell(\mathbf{p}_{\text{obs}} \mid \mathbf{d})$ is the primary deliverable in observational cosmology, we take it to be well modeled.) From those samples $\mathbf{p}_i$, we estimate

[4] Q_s and n_s are the scalar amplitude and spectral index, respectively; α is the running of n_s; r is the tensor-to-scalar ratio; n_t is the tensor spectral index; Ω_{tot} is the critical density fraction; ρ_Λ is the vacuum energy in the potential basin where inflation ends.

parameters Θ to maximize the joint likelihood

$$\Theta \leftarrow \underset{\Theta}{\operatorname{argmax}}\, \mathcal{L}_m(\Theta \mid \{\mathbf{p}_i\}, \mathbf{d}) \qquad \mathcal{L}_m(\Theta \mid \{\mathbf{p}_i\}) \equiv \prod_i \ell_m(\Theta \mid \mathbf{p}_i, \mathbf{d}) p(\mathbf{p}_i)$$

where $\ell_m(\Theta \mid \mathbf{p}_i, \mathbf{d})$ is the likelihood of parameters Θ modeling $p_m(\mathbf{p} \mid \mathbf{d})$ and $p(\mathbf{p}_i)$ is the prior on $\mathbf{p}$. Since the choice of distribution to model $p_m(\mathbf{p} \mid \mathbf{d})$ is not obvious from expectations of the variability of some parameters in $\mathbf{p}$, a more plausible approach is to take the population of models as representing the distribution, without attempting the final likelihood-maximizing step.

Generic eternal inflation would mean that $p_m(\mathbf{p} \mid \mathbf{d})$ nearly vanishes outside of the region of parameter space spanned by $\mathbf{p}_{\text{eternal}}$ that corresponds to eternal inflation, invoking the concept of *almost everywhere* from measure theory – "the set for which the property holds takes up nearly all possibilities."

Frequentist (Less-Bayesian) Definitions Here our use of *frequentist* refers to more direct consideration of rates of eternal behaviors manifesting in populations of models sampled from the measure. From this point-of-view, we are concerned with estimating rates of incidence of a quantity characterizing eternal inflation meeting a predefined threshold, rather than the distribution over that quantity. Considered in these terms, generic could also mean that an estimate of the rate or probability of occurance of eternal inflation is close to 1. This has the advantage of not requiring one to presume a model for the distributions of parameters in

$\mathbf{p}_{\text{eternal}}$, but rather only of a rate parameter which can be taken to be binomial-distributed. Providing the means to do this (in a crude form, at least) is in large part the aim of this study. A disadvantage is that the output meshes less well with the inputs of the Measure Problem of Eternal Inflation, which is better informed by being fed representations of the distributions over $\mathbf{p}$ that are as complete as possible.

3.4 Candidate Measures

Which considerations have passed muster in the literature, in informing proposed measures over cosmological models? Are simpler measures always better? In order to avoid the impression of being finely-tuned *ab initio*, the measure should not encode too much *a priori* knowledge about the kinds of universes it is to produce. Here we briefly discuss three possible measures on the effective potential, initial conditions, or both; and

No-Boundary The No-Boundary proposal presented in [57] establishes criteria for spacetime to behave classically at late times – a prerequisite for the project of interpreting early universe cosmology in terms of an inflationary epoch. It attempts to assign a "wave function of the Universe" – the No-Boundary Wave Function (NBWF) – derived from simple arguments in such a way as to evade

specification of past boundary conditions. It yields a measure over the classical history of the inflaton given a pre-defined potential function.

The authors draw a distinction between *bottom-up* versus *top-down* probabilities – those prescribed by quantum theory and the NBWF versus those further conditioned on conditions needed to reproduce observational data, respectively. (We generally direct our attention to the top-down variety.) The No-Boundary Measure [58] assigns higher weight to models with very few e-folds of inflation beyond the minimum required to solve the horizon problem. Saddle points with sharp curvature are disfavored; broad saddle points can behave classically at late times. To evade the preference for few e-folds, the authors advocate a volume weighting of $\exp(3\mathcal{N}_E)$ in their calculation of top-down probabilities – after this adjustment, a large number of e-folds is slightly preferred in approximately quadratic models. The criterion for volume weighting to outpace suppression from the action in the NBWF is equivalent to that for stochastic eternal inflation to within a factor of order unity. The No-Boundary Measure ties the presence or absence of eternal inflation in our past with the Gaussianity of scalar density perturbations.

Refined de Sitter Swampland The "refined" de Sitter Swampland Conjecture [59] relaxes the requirements of the original somewhat, by allowing either the first derivative constraint in (3.3) or a new second derivative constraint (3.4) to satisfy the criterion. We can take the constraints as specifying a rudimentary

measure over potentials and initial conditions: the field is sampled from regions of a potential in which these conditions are satisfied, while potentials with any or more of such regions are favored by the measure. This can be viewed as using the landscape itself as a measure, keeping only the basins of attraction for which completion to quantum gravity is attainable.

The de Sitter swampland measure is too general, and does not give a natural prescription for probabilities apart from whether a small number of constraints on the potential are valid. It seems like an additional constraint to be administered to a broader measure, cutting away a large portion of parameter space.

QFT Plausibility/Complexity A possibility not discussed in the literature – though the motivation is often recognized as a value – is to weight effective potentials in terms of the complexity to reproduce them from allowed interaction terms in quantum field theory. In this measure, a quadratic potential – corresponding to a simple massive scalar field – would have high weight; a Higgs-like potential with quadratic and quartic contributions would not be far behind. Potentials with terms of a single field taken to a power greater than 4 are disallowed, etc. Unnatural potential shapes with wiggles and scaling discrepancies from one interval of field space to another would be heavily penalized.

A QFT complexity measure would require many priors assigned to the various parameters characterizing each term in the Lagrangian, and a mixture of

continuous (parameters) and discrete (terms present or not) outcome spaces.

Takeaways Each of the measures discussed above presents problems when it comes to sampling from the distribution to compute statistics of eternality and observables. How does one draw random samples from the No-Boundary Measure, for instance? We are limited to the most general statements about the behavior of late-time classical configurations, of which quick work has been made in the literature. We are in search of a measure that both prescribes well defined probabilities and can be easily sampled numerically; to accomplish this may mean to sacrifice on aesthetic qualities of realism or sophistication.

Chapter 4

Sampling the Measure-verse

Supposing a minimally coupled scalar field responsible for driving inflation is governed by an effective potential of whose origin we are ignorant, it would be worthwhile to discover with what probability (and what observational correlate) we encounter eternal behavior, subject to measures admitting variability in the potential that is not so simple as to be encapsulated in just a few model parameters. With a well behaved distribution over potentials, we could make some headway with a purely analytical approach, extending the results of works like [49]. But having a veritable trove of simulated data comes with the freedom to make arbitrary cuts on observables.

Since we are ultimately most interested in distributions for models that come close to producing observationally viable cosmologies – with parameters in $\mathbf{p}_{\text{obs}}$

landing in the ballpark of their measured values – we find a numerical statistical approach to be a useful tool for complementing and subverting our intuitions. In this chapter, we describe a collection of computationally feasible measures defined by draws of a potential and initial conditions, as well as a Monte Carlo methodology for simulating inflationary dynamics and recording observables and eternal inflation metrics.

4.1 Desperate Measures

The measures described in the previous chapter are well motivated, but would be difficult to sample in practice. If there is a "true" measure over inflaton potentials and initial conditions, it is of course unknown; nonetheless, we argue that just as observables inform inflation, even simple measure prescriptions can offer insight into what might be deemed "generic" versus "fine-tuned." From a stance of humility in light of the considerations discussed in § 3.3, we aim to travel a middle road of devising measures that are easily computable and provide adequate coverage of the space with a high degree of variability, while at least not flying in the face of possible physical justifications.

4.1.1 Sampling Potential Functions

Following the example of Tegmark [20], we draw effective potential functions as one-dimensional Gaussian random fields (GRFs). The GRF has several properties that make it suitable for this role: it is smooth and continuous, bounded from above and below, and its statistics are translation invariant. (The last stands in contrast to the one-parameter space of quadratic potentials, for example, which is guaranteed to have special behavior near $\varphi = 0$.) Furthermore, the GRF assigns "natural" versus "unnatural" potential shapes appropriate weights largely in agreement with commonly held notions of such.

We express the potential $V(\varphi)$ in terms of a dimensionless GRF

$$f(x) = \frac{a_0}{\sqrt{2}} + \sum_{k=1}^{k_{\max}} a_k \cos(kx) + \sum_{k=1}^{k_{\max}} a_{-k} \sin(kx) \tag{4.1}$$

and constants defining the mass scales of the potential (m_v) and the inflaton (m_h).

$$V(\varphi) = (m_v m_{\mathrm{P}})^4 f((m_h m_{\mathrm{P}})^{-1} \varphi) \tag{4.2}$$

Each coefficient a_k is sampled from a Gaussian distribution such that

$$\mathrm{Var}(a_k) = q^\gamma e^{-q^2/2}, \qquad q \equiv k/\sqrt{k_{\max}} \tag{4.3}$$

Tegmark found that varying the scale dependence of a_k through the parameter γ did not produce any interesting discrepancies in the resulting distributions, so we take $\gamma = 0$ for our analyses unless otherwise specified. We generally take

$k_{\max} = 30$.

The function $f(x)$ defines the shape of the potential, but we must also impose priors on the vertical and horizontal mass scales – m_v and m_h, respectively – to enact the full measure, and to compute statistics in subsamples aggregated from multiple mass pairings and binned with respect to the values of observables. For most results, we assume a prior that is uniform on a log-scale within the designated mass ranges; but we also consider a straight uniform prior, which of course gives greater weight to larger mass scales. Beyond this base prior, we adopt two schemes for constructing measures from arrays of mass scales:

- The *epektacratic* weighting scheme (rule by expansion) samples an equal number of potentials for each pairing of mass scales m_v and m_h, and lets them succeed or fail at producing sufficient e-folds of inflation. The total population is aggregated from successful inflation models at all mass scales, and that population is used to determine rates. Naturally this scheme will tend to give more representation to large field models.

- The *democratic* scheme gives every mass pairing within the specified range equal weight in informing $f_m(\mathbf{p}_{\rm eternal} \mid \mathbf{p}_{\rm obs})$ in (3.7), regardless of how common or rare it is for models comprising each to produce enough inflation. From each pairing, we sample as many potentials as it takes to get an equal number of successful models, or we give lower-expansion mass pairings extra

weight to the same effect. (We only want to simulate one set of batches, so to get the democratic estimates we effectively treat the uniform distribution over mass scales as an importance distribution, and weigh contributions from each by $1/P(\mathcal{N}_e > 70 \mid \{m_v, m_h\})$.)

In consideration of observational viability, we would ultimately condition on the smallness of the vacuum energy in the stable minimum where inflation ends. Rather than sampling the full distribution and then conditioning on ρ_Λ being many orders of magnitude smaller than the scale of the potential, we aim for a shortcut to approximate such a move without covering the vast regions of parameter space in which the vacuum energy is negative or significantly too large. Very simply, we first check whether any minimum in the search space has a vacuum energy within $\pm 0.01\, m_v^4 m_{\rm P}^4$; if so, then we shift the whole potential to bring the vacuum energy in that basin to zero. Inflation must end in that basin in order for that model to be counted.

To justify the above procedure, we need not assert that the properties of each model are unchanged, but only that we can identify populations of models with statistics corresponding to those in the original measure. When we shift the potential down to make the vacuum energy less positive, to first order the statistics of the starting point are comparable to that of unshifted potentials with a smaller vertical mass scale. So we must densely pack the starting mass scale

and then re-bin based on the effective m_v after the shift. If the shift is too large, then we start to see divergence from the effective-m_v approximation as the shape of $V(\varphi)$ appears noticeably stretched in the vertical.

We found a 1% shift in the potential to be an suitable compromise between distorting effects and sample size. For dynamics high on the potential, a shift is like a few percent scaling. Low on the potential, the effect is to make quadratic minima less convex, reducing the mean of $f''(x)$ by 2% and variance by 6% – increasing the effective horizontal mass scale.

4.1.2 Sampling Initial Conditions

Within the scope of our Monte Carlo analysis on the prevalence of eternal inflation, we are concerned with field configuration over one initial Hubble volume. Since this initial Hubble volume is situated in a larger inflating bulk, any measure must entail assumptions about nearest neighbor Hubble volumes; to address this, we assume nearly homogeneous initial conditions at the Hubble scale. Over homogeneous initial values of the inflaton φ, Tegmark adopted two measures:

A Sample field values maximizing $V(\varphi)$, weighted by the distance in field space between the two adjacent minima. (This is equivalent to sampling uniformly and then going uphill to the peak.) Discard instances in which $|\eta_V| > 1$ at φ_0.

B Sample field values uniformly. Discard instances in which $\epsilon_V > 1$ or $|\eta_V| > 1$ at φ_0.

We agree in broad strokes with the rationale for these measure choices in the context of a Monte Carlo analysis, and furthermore wish to compare our results with Tegmark's for repeatability and debugging purposes. Accordingly we adopt these two measures and add a third:

C Sample field values a distance in field space equal to $H/2\pi$ from local maxima of $V(\varphi)$, weighted by the distance in field space between the two adjacent local minima. Discard instances in which $\epsilon_V > 1$ or $|\eta_V| > 1$ at φ_0.

Measure C is equivalent to sampling from Measure A and then adding a standard deviation of the slow roll stochastic fluctuation of Hubble-scale modes to that sampled value.

All three measures as framed above require that both slow roll conditions are satisfied at the starting point, and then take

$$\ddot{\varphi} = 0 \qquad \dot{\varphi} = -M_{\rm P} V'(\varphi)/\sqrt{3V(\varphi)} \tag{4.4}$$

More properly, we would sample from a well-motivated distribution over $\dot{\varphi}$ and higher derivatives, and integrate the full equations of motion; φ could then barrel through a short enough interval where the potential slow roll conditions are met

without inflation taking place. As Tegmark pointed out, if

$$\dot{\varphi} \lesssim \sqrt{2V(\varphi)} \tag{4.5}$$

in an interval where $\epsilon_V, |\eta_V| < 1$, then the full equation of motion exhibits an attractor behavior leading quickly to the slow roll profile (4.4) [29]. Sampling $\dot{\varphi}$ from a distribution and then conditioning on slow roll, the population of surviving models would be those that approximate the above measures, with additional weighting like $m_v^2/\langle\dot{\varphi}^2\rangle^{1/2}$. Since we are drawing from an array of mass scales, we can model such effects without simulating the fully dynamics by adjusting the prior on m_v.

Inflation Below the Peak Stochastic inflation occurs in every model sampled to reflect Measure A that produces observables, since there is always an inflating interval contiguous with the maximum where $V'(\varphi)$ vanishes. If we waive the requirement that inflation continues through 70 e-folds *from the maximum*, and instead let inflation start lower on the potential if the potential slow roll conditions are met with φ varying slowly enough at the start of a slow roll interval, we allow for the possibility of non-stochastic inflation initialized at a non-inflating peak. We only require that $\dot{\varphi}$ is below the bound of the slow roll attractor when it reaches the top of an interval in which $\epsilon_V, |\eta_V| < 1$. With these considerations, we adopt the following modified version of Measure A:

A* Sample field values maximizing $V(\varphi)$, weighted by the distance in field space between the two adjacent minima. If $\eta_V > 1$ at the peak, then assume inflation starts where $\epsilon_V, |\eta_V| < 1$ first becomes valid ($\varphi_{\rm sr}$), if $\dot{\varphi}_{\rm sr} < \sqrt{2V(\varphi_{\rm sr})}$ along a trajectory approaching the peak as $t \to -\infty$.

To determine if $\dot{\varphi}$ comes in below the attractor bound, we integrate the coupled equations of motion for the homogeneous scalar field and the metric (only the scale factor $a(t)$)

$$\ddot{\varphi} = -3H(a, \dot{a})\dot{\varphi} - V'(\varphi) \tag{4.6}$$

$$\ddot{a} = 8\pi G a \left(\dot{\varphi}^2 - V(\varphi)\right) \tag{4.7}$$

backward in time, with initial conditions $\varphi = \varphi_{\rm sr}$, $\dot{\varphi} = \mathrm{sgn}(\varphi_{\rm sr} - \varphi_0) \times \sqrt{V(\varphi_{\rm sr})}$. If the solution overshoots the peak in the past, it would correspond to a velocity in the direction of $\varphi_{\rm sr}$ at some finite initial time. If the system were conservative, we could assume that as we dial that initial velocity at the peak to zero, $\dot{\varphi}$ approaches a value less than $\sqrt{V(\varphi)}$ at $\varphi_{\rm sr}$. The presence of Hubble friction complicates things somewhat, as it becomes possible that reducing this initial field velocity also reduces friction to the point that one gets a *greater* field velocity where slow roll begins. This can be tackled iteratively by a method of overshoot-undershoot, integrating backward in time trying to land with φ atop the peak at $t \to -\infty$. More expeditiously, in the case of an overshoot we can then initialize with a small

field velocity at the peak in the direction of the true-vacuum basin, and assume nothing changes as that small velocity vanishes.

4.2 Simulation Design

We characterize the evolution of the inflaton – including up to one Coleman-de Luccia or Hawking-Moss transition event – accurately enough to inform the distributions $f_m(\mathbf{p} \mid \mathbf{p}_{\rm obs})$ from Eq. (3.7), while exploiting what we argue are justifiable shortcuts in order to economize on computing time. For each instance toward building up the distribution, the steps are as follows:

1. **Initialization**

   (a) Sample a 1-D Gaussian random field $f(x)$ according to (4.1). From this and constants m_v, m_h construct the potential $V(\varphi)$ according to (4.2).

   (b) Initialize the inflaton at $\varphi_{\rm start}$ according to one of the Measures A, B, or C outlined above.

   (c) Determine the potential energy ρ_Λ of the minimum of the starting basin and in one neighboring basin in both directions. (For Measure A, the starting basin adjacent to the initial peak is chosen randomly weighted by width.) If $|\rho_\Lambda|$ in any basin in this search space is below a threshold,

shift the potential so that $\rho_\Lambda = 0$ in that basin. If ρ_Λ is negative and less than this threshold in the starting basin, abort.

2. **Instanton Pre-selection**

   Computing instanton profiles is time consuming, so we take the following steps to determine if a tunneling event is likely to be followed by sufficient inflation to produce a possibly observable universe in another basin of the potential.

   (a) If initialized in the true vacuum with $\rho_\Lambda = 0$, continue to (4).

   (b) If the thin-wall or Hawking-Moss approximations hold, continue to (3).

   (c) Taking the cutoff CDL instanton terminus on the true-vacuum side $\varphi_{\rm edge}$ to coincide with $V(\varphi_{\rm edge}) = 0.05\,V_T + 0.95\,V_{\rm bar}$, compute the maximum number of e-folds of inflation accrued over any field space interval in which the potential slow roll conditions are met between $\varphi_{\rm edge}$ and the true minimum. If the maximum e-fold count is less than 70, abort.

3. **Check for Quantum Tunneling**

   (a) If the thin-wall approximation is strongly valid or $m_h \gg m_{\rm P}$ (Hawking-Moss eminent), compute the transition rate, otherwise

   (b) Compute the Coleman-de Luccia tunneling profile; determine the instanton terminus on the true-vacuum side; compute the number of e-

folds of inflation, assuming inflation takes place anywhere below the terminus where the potential slow roll conditions are weakly met ($\epsilon_V, \eta_V < 1$).

4. **Characterize Slow Roll**

   (a) Look downhill from $\varphi_{\rm start}$ for breakdown of the slow roll approximation, $\varphi_{\rm end}$.

   (b) Compute the number of e-folds $\mathcal{N}_e$ in the current basin. If $\mathcal{N}_e < 70$, skip to (6).

   (c) Find $\varphi_{\rm exit}$, the field value at the horizon exit scale for CMB fluctuations, taken to be 55 e-folds before the end of inflation.[1]

5. **Check for Eternal Inflation**

   (a) Evaluate the stochastic inflation criterion (2.11) between $\varphi_{\rm start}$ and $\varphi_{\rm end}$ in each basin.

   (b) Check the second potential slow roll condition at all local maxima along the trajectory; compare to the upper bound for topological inflation (see 2.3).

[1] Our e-fold cutoffs (70 for successful inflation, 55 for imprinting of CMB fluctuations) of course depend on the fiducial reheating model. One could include those models in the input space, but we opt not to include that freedom in this analysis as doing so would likely obscure our conclusions.

(c) If a transition into the basin with $\rho_\Lambda = 0$ is followed by enough e-folds, compute the transition rate λ and compare to the upper bound in Eq. (2.15).

6. **Data Collection**

Record observables if inflation ends with $\mathcal{N}_e > 70$ in a vacuum with $\rho_\Lambda \ll 1$, along with indicators for eternal inflation:

$$\mathbf{p}_{\rm obs} = (Q_s, r, n_s, \alpha, n_t, \delta\rho/\rho, \log|\Omega - 1|) \tag{4.8}$$

$$\mathbf{p}_{\rm eternal} = (N_s, \langle\mathcal{N}_{e,\rm stoch}\rangle, b_t, \lambda_{\rm fv}, H_{\rm F}, b_{\rm HM}) \tag{4.9}$$

The parameters in Eq. (4.8) are the same as those defined in Footnote 4. In (4.9), $N_{\rm s}$ is the number of contiguous field space intervals in which the stochastic eternal inflation criterion is valid for at least one elapsed e-fold; $\langle\mathcal{N}_{e,\rm stoch}\rangle$ is the sum of the ratios of the widths of stochastic inflating intervals in field space to the amplitudes of quantum fluctuations characteristic to those intervals; $b_{\rm t}$ is a Boolean flag for topological eternal inflation; $\lambda_{\rm fv}$ is the rate of quantum diffusion from a meta-stable false vacuum; $H_{\rm F}$ is the Hubble parameter in that false vacuum; and $b_{\rm HM}$ is a Boolean flag indicating whether the transition is dominated by the

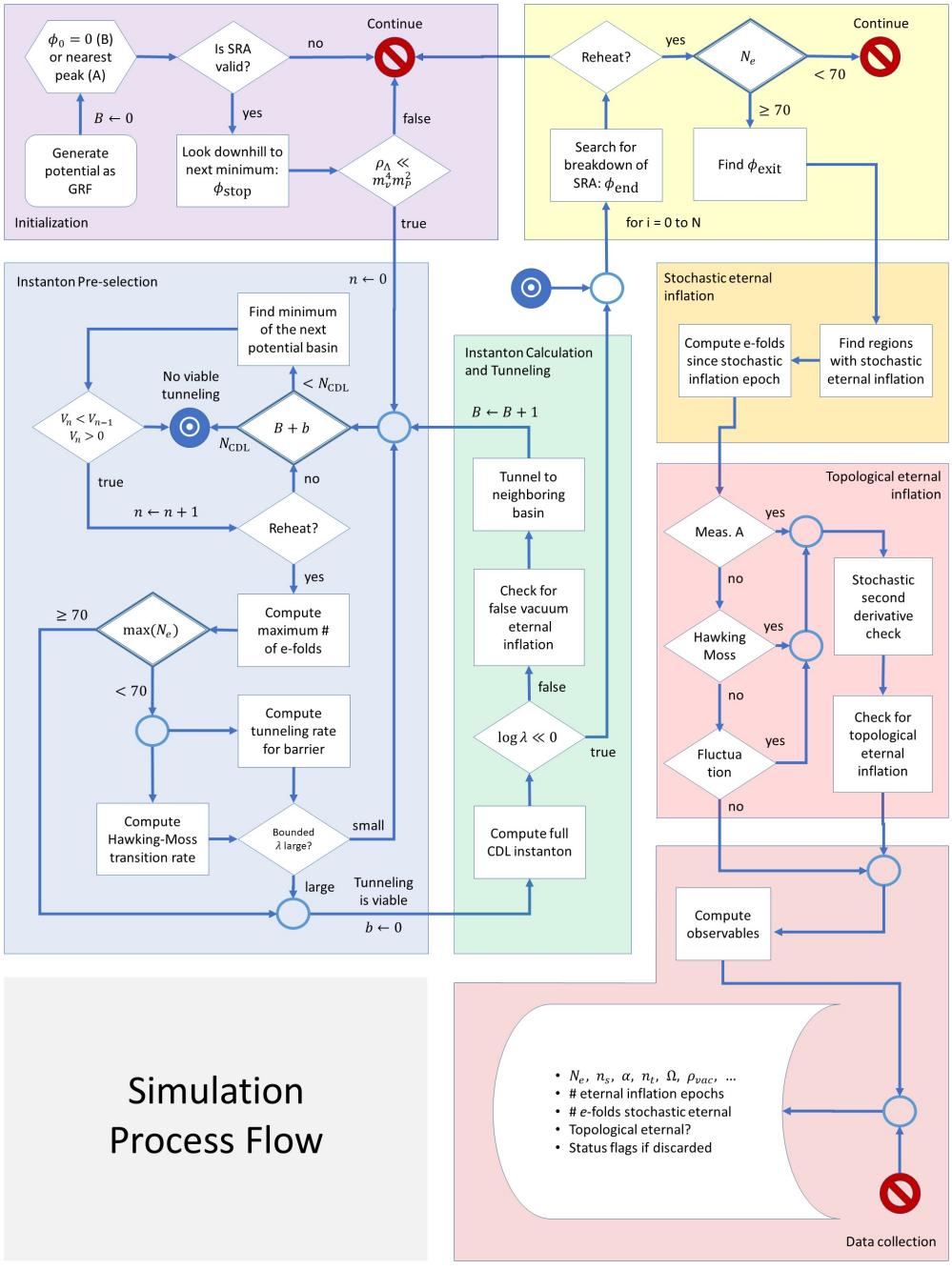

Figure 4.1: A flowchart illustrating our simulation process. Starts in the top left.

Hawking-Moss instanton.

$$Q_s^2 = V(\varphi_{\rm exit})/(150\pi^2\,\epsilon_V\,\kappa m_{\rm P}^2)$$

$$r = 16\epsilon_V$$

$$n_s = 1 - 6\epsilon_V + 2\eta_V$$

$$\alpha = 16\epsilon_V\eta_V - 24\epsilon_V^2 - 2\xi_V^2$$

$$n_t = -2\epsilon_V$$

$$\delta\rho/\rho = \log_{10}(V(\varphi_{\rm exit})/V(\varphi_{\rm end}))$$

$$\ln|\Omega - 1| = \ln(V(\varphi_{\rm start})/V(\varphi_{\rm exit})) - 2\mathcal{N}_{e,\rm before}$$

4.3 Algorithm for Instanton Solving

To treat transitions between de Sitter minima in our Monte Carlo simulations, we need the instanton profile $(\varphi(\xi), \rho(\xi))$ – to determine where the field is initialized on the true-vacuum side of the barrier. We also need the transition rate – to compare the rates of bubble nucleation or stochastic ascent of the peak with the expansion rate.

Instanton Pre-selection As discussed in § 2.2 and illustrated in Figure 4.2 from simulated data, the Hawking-Moss instanton dominates the transition be-

tween de Sitter minima if the top of the barrier is sufficiently flat [39]:

$$V(\varphi)/m_{\rm Pl}^2 \gg V''(\varphi) \implies m_h \gg (8\pi)^{-1/2} \tag{4.10}$$

Well above the scale $m_h = (8\pi)^{-1/2}$, it is safe to assume that the transition is Hawking-Moss; so the transition rate is closed-form and easy to compute. At field

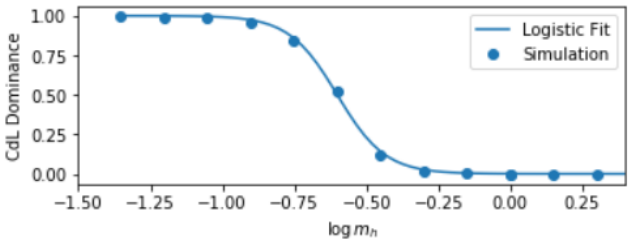

Figure 4.2: Fraction of models in which a Coleman-de Luccia instanton solution exists. At larger horizontal mass scales (flatter potential peaks), the Hawking-Moss instanton is dominant.

scales much smaller than M_P, we enter the thin-wall regime in which the CDL instanton dominates. The thin-wall instanton tends to terminate very near the true vacuum, traversing the barrier over a small interval in the Euclidean radial coordinate relative to $H_{\rm F}^{-1}$.

In the intermediate regime around $m_h = (8\pi)^{-1/2}$, it may not be an easy determination which instanton contributes most to the transition, and we must compute the profile to find out. In order to reduce program time allocated to computing transition rates in this regime, we first perform a check that inflation can start and end in the adjacent basin and that the maximum amount of inflation likely to occur is sufficient to produce $\mathcal{N}_e > 70$. If the effective mass is such that

$0.1 < (m^2_{h,\text{eff}} \equiv V/V_{,\varphi}) < 1$, we determine φ_{edge} such that

$$V(\varphi_{\text{edge}}) = 0.05\, V_T + 0.95\, V_{\text{bar}}$$

and take it as our trial starting point in the new basin. We search down the slope for the start (if the potential slow roll conditions are not already met at φ_{edge}) and end of slow roll ($\epsilon_V, |\eta_V| < 1$), and compute the number of e-folds that elapse in that interval assuming slow roll. If it is greater than the 70 e-folds needed to obscure any potentially observable relics of the transition, then we proceed with the full instanton calculation to determine where precisely the field is deposited. Otherwise, we assume that a transition does not result in a potentially observable universe, and so does not inform $f_m(\mathbf{p} \mid \mathbf{p}_{\text{obs}})$; we discard and continue to the next randomly drawn potential function.

Obtaining the Profile To determine the action-extremizing instanton profile for a given potential $V(\varphi)$, we use the algorithm employed in the CosmoTransitions package published with [60], modified to accommodate parallel processing in Matlab. The algorithm assumes initial conditions $\dot{\varphi}(0) = \rho(0) = 0$ with $\varphi(0)$ on the true-vacuum side, and takes the endpoint of the trajectory to occur at $(\varphi, \dot{\varphi}) = (\varphi_{\text{F}}, 0)$ (came to rest at the false vacuum) or $(\rho, \dot{\varphi}) = (0, 0)$ (geometry closed with no discontinuities). The former stopping criterion is only possible in the absence of gravity, though it can be approached in the thin-wall limit. If the

geometry closes ($\rho(\xi > 0) = 0$) with $\dot{\varphi}(\xi) \neq 0$, then that solution is singular and not admissible. The steps of the algorithm are as follows:

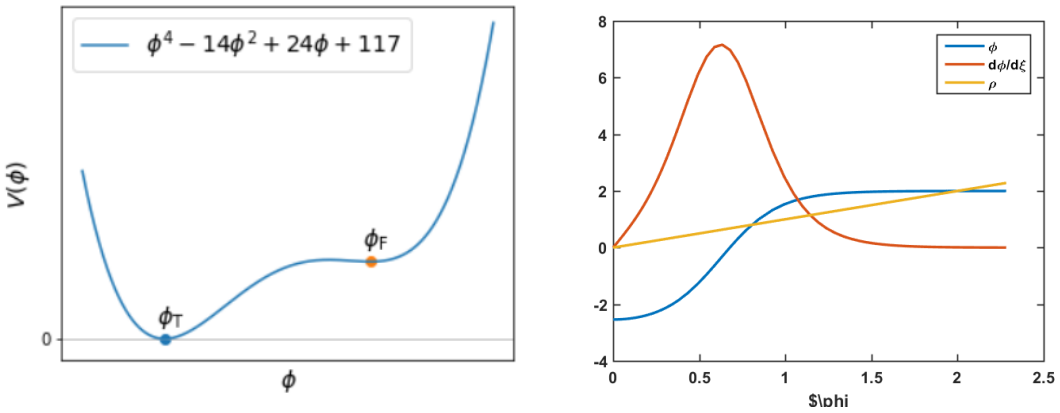

Figure 4.3: An example thick-wall instanton profile without gravity. (Left) The potential with stable and metastable minima. (Right) The instanton profile.

1. Guess a starting field value on the true-vacuum side of the barrier.

2. Integrate equations of motion (2.17) for the scalar field $\varphi(\xi)$ and Euclidean radius $\rho(\xi)$ of the bubble as a function of the radial coordinate ξ.

3. Stop integrating when one of the follow events occurs:

   (a) $\varphi(\xi)$ approaches φ_F with $\dot{\varphi}(\xi) \approx 0$ (Converge)

   (b) $\dot{\varphi}(\xi)$ approaches 0 with $\varphi \approx \varphi_F$ or $\dot{\rho}(\xi) \approx 0$ (Converge)

   (c) $\dot{\varphi}(\xi)$ changes sign with $\varphi \neq \varphi_F$ (Undershoot)

   (d) $\varphi(\xi)$ passes φ_F (Overshoot)

   (e) $\dot{\rho}(\xi)$ approaches -1 with $\dot{\varphi}(\xi) \approx 0$ (Converge) or $\dot{\varphi}(\xi) \not\approx 0$ (Overshoot)

(f) $\rho(\xi)$ changes sign (Converge)

4. If converged, we're done; return the profile.

5. If within a tolerance value of the top the barrier, report a single data point that fully characterizes the Hawking-Moss profile.

$$\{\varphi, \dot{\varphi}, \rho, \dot{\rho}, \ddot{\rho}\} \left(\tfrac{\pi}{2} w_{\rm top}^{-1}\right) = \left\{\varphi_{\rm top},\, 0,\, w_{\rm top}^{-1},\, 0,\, -w_{\rm top}\right\}$$

6. If the integration overshoots, move the guess closer to the maximum; if it undershoots, move the guess closer to the true minimum.

7. Go to Step 2.

Transition Rates with Gravity The tunneling rate in terms of the Euclidean action for the bubble and for the de Sitter background is computed as

$$\lambda H_{\rm F}^4 \approx (\tfrac{1}{2}\sigma \bar{R})^2 \exp(S_{E,\rm bkg} - S_{E,\rm bubble}) \tag{4.11}$$

where we take $\bar{R} = (R_0 + R_1)/2$ for the purpose of computing the prefactor, σ is the bubble tension, and $(\frac{1}{2}\sigma\bar{R})^2$ is the approximate (thin-wall) prefactor from Eq. (2.18). Beyond the outer radius R_1, the bubble and the de Sitter background have the same geometry and field configuration, so those contributions cancel out when computing the transition rate.

For thin-wall bubbles, the initial bubble radius R_0 defines the whole geometry;

for all bubbles, there is a finite radius inside of which $\dot{\varphi} = 0$. To compute the transition rate from the profile, we first compute the curvature of the bubble interior

$$w_{\text{int}} \equiv \sqrt{\tfrac{\kappa}{3} V(\varphi(R_0))}$$

When $w_{\text{int}} = 0$ the geometry of the interior is Minkowski. (The instanton profile typically terminates at a value $\rho > 0$, where the field velocity $\mathrm{d}\varphi/\mathrm{d}\xi$ effectively vanishes.) The vacuum in the tunneled-to basin is always Minkowski for the simulation settings chosen for this analysis; however, large-H de Sitter bubbles are also supported in the code, and may result when a sharply peaked barrier is adjacent to a flat interval on the potential in which the potential slow roll conditions are satisfied. When the vacuum energy in the interior is positive, the radius $\rho(\xi)$ of an anulus on the 4-sphere as a function of the distance from the pole goes like $\rho(\xi) = w_{\text{int}}^{-1} \sin(w_{\text{int}}\xi)$. The term contributing to the Euclidean action from the bubble interior are then

$$S_{E,\text{int},\varphi} = \int_0^{R_0} \mathrm{d}\xi \, 2\pi^2 \rho(\xi)^3 \, V(\varphi(0)) = \frac{3\mathcal{V}_{\text{int}}(R_0)\, w_{\text{int}}^2}{\kappa} \tag{4.12}$$

for the field, and in the de Sitter case

$$S_{E,\text{int},\rho} = \int_0^{R_0} \frac{2\pi^2 \, \mathrm{d}\xi}{\kappa w_{\text{int}}} \sin(w_{\text{int}}\xi) \left(-\sin(w_{\text{int}}\xi)^2 + \cos(w_{\text{int}}\xi)^2 - 1 \right) = -\frac{6\mathcal{V}_{\text{int}}(R_0)\, w_{\text{int}}^2}{\kappa}$$

for the background geometry. But this is twice the magnitude and opposite in sign

to the field contribution, so within the inner radius of the bubble the contribution is equal to $-S_{E,\text{int},\varphi}$. For Hawking-Moss instantons, the "bubble interior" covers the whole compact space, and we leave out the prefactor in (4.11) as there is no analogue to a bubble wall to be perturbed in the standard calculation. Likewise, the background de Sitter configuration consists entirely of the bubble "exterior."

With the interior and exterior covered, we add the contribution from the bubble wall where $V(\varphi)$ is not constant and $\rho(\xi)$ takes a different form. We integrate the full form of the Euclidean action (2.16) from the inner radius to the outer radius.

Chapter 5

Meta-statistics of Eternal Inflation

In Chapter 4, we described in detail a numerical methodology for assessing the prevalence of eternal inflation under measures with a programatically defined sampling procedure. It calls for computing inflationary dynamics across an ensemble of randomly generated potential functions, following the example of Tegmark's analysis of more general observable consequences of inflation in "What does inflation really predict?" [20]. Using a Gaussian random field to capture variability in the potential shape, we investigate simple measures over initial conditions and the characteristic scales of the single inflaton φ and its potential $V(\varphi)$, reporting rates of incidence of viable models that manifest eternal inflation, and their correlations

with observables.

5.1 Our Scope

Our goal is not to compute a single value for the likelihood of eternal inflation for each measure, but rather to investigate the prevalence of each mode of eternality in regions of the joint subspace of hyperparameters and of values for observables not yet ruled out by cosmological surveys. We have framed the mathematical formulation of genericity in Bayesian terms, but for our numerical approach adopt a mix of Bayesian and frequentist methods to analyze populations of simulated models. After binning models in the space of mass scales and/or observables, we take the number of models observed in each bin with or without eternal inflation to be a binomial-distributed random variable, with a deterministic but unknown probability of occurance λ for each bin. Our task is then to estimate the rate λ characterizing the bin population based on the number of observed events s in our sample of size n.

We would like to adopt something like a uniform prior on the rate of incidence of eternal inflation in each bin. However, it is not obvious whether we should work in terms of λ or $\log \lambda$. (Are we ambivalent with respect to the rate itself, or with respect to its order of magnitude?) As a middle road, we adopt the Jeffreys uninformative prior $p_J(\lambda) \propto \text{Beta}(\lambda; \frac{1}{2}, \frac{1}{2})$ for the rate parameter of the

binomial distribution, which is invariant under reparameterization of the rate parameter between the linear and log domains. We would then take the maximum likelihood value (using the uninformative prior) as our estimate of the incidence rate. However, for bins in which the number of models with or without a mode of eternal inflation is zero, the maximum likelihood rate is 0 or 1, and does not account for information we have from the sample size of that bin. For this reason, we often report a 95% confidence upper and/or lower bound on the incidence rate λ in our contour plots, which includes sample size information and makes for smooth contours in regions of parameter space in which positive events may be scarce. (Naturally, in the case of zero positive events the bound is determined entirely by the sample size.)

The hyperparameters defining the distribution functional over effective potentials are the masses identifying the scales of the field ($\varphi \sim m_h$) and the energy density ($V \sim m_v^4$), along with the shape parameter γ. We sample m_h from within a few orders of magnitude of the Planck mass, which of course limits the scope of applicability of our results to a small subspace of conceivable models. This choice was informed by noting for which field scales we are likely to get sufficient statistics to make meaningful statements about the prevalance of eternal inflation, in a subpopulation of successful inflation models ($\mathcal{N}_e > 70$) that are also observationally viable.

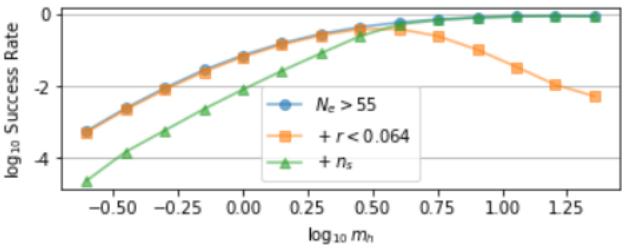

Figure 5.1: Success rates for matching model characteristics among the population of all simulated models in Measure B, binned by field scale $m_{\rm h}$. Lower bound on the total number of e-folds alone, and combined with constraints on the scalar index and tensor-to-scalar ratio. The low success rate for small field scales is reflected in the high upper bounds (assuming binomial statistics) in Figure 5.3.

Constraints on the scalar spectral index n_s and the running α pressure $m_{\rm h}$ from below this range in Measure A, and the upper bound on the tensor-to-scalar ratio r pressures $m_{\rm h}$ from above. This is also where we expect to encounter interesting behavior departing from the limiting cases where we are justified in extrapolating – e.g. in the large field limit.[1] Figure 5.1 shows rates of successful inflation (minimal e-fold count achieved) in Measure B, as well as success in conjunction with various CMB observables falling within *Planck* 68% confidence intervals; note that all rates drop precipitously in the small field regime. Taking the potential to vary on field scales within the range $\mathcal{O}(10^{-2}) \lesssim m_{\rm h} \lesssim \mathcal{O}(10)$, we sample m_v from a range in which the amplitude of scalar perturbations Q_s is most likely to be consistent with data from the *Planck* mission: $\mathcal{O}(10^{-5}) < m_v < \mathcal{O}(10^{-2})$.

[1]Furthermore, at scales much larger than $m_{\rm P}$ our confidence in accurately modeling inflation wavers in light of likely confounding effects from an as-yet unformulated theory of quantum gravity.

5.2 Matching Observables

Since we are most concerned with the subpopulation of observationally viable inflation models (for consideration of *top-down* probabilities), we should get acquainted with how those models are distributed within our mass-scale-shaped window onto model space. (These results have only to do with ordinary inflation with slight changes to Measures A, so they are roughly commensurate those presented in [20].) Figure 5.2 shows constraints on CMB observables as well as the potential slow roll parameters. We use these constraints to stand in for observational viability.

Measure A Figure 5.3 depicts the 95% confidence upper bounds on marginal rates of incidence for parameters describing the CMB power spectrum falling within *Planck 2018* 68% confidence intervals, calculated by the procedure described in 5.1. Comfortably in the super-Planckian regime: note the positive correlation of mass scales along tightly spaced contours defining equal rates of incidence for matching of the scalar amplitude Q_s. With Q_s going like $m_v^2 m_{\rm h} \times \mathcal{O}(10^{-2})$, one might expect that correlation to be negative – why the inversion? Since we select for potentials with a small vacuum energy in the final basin and then shift ρ_Λ to zero, inflation always ends. At this scale inflation almost always ends very close to the minimum, where the potential is approximately quadratic and perturbation

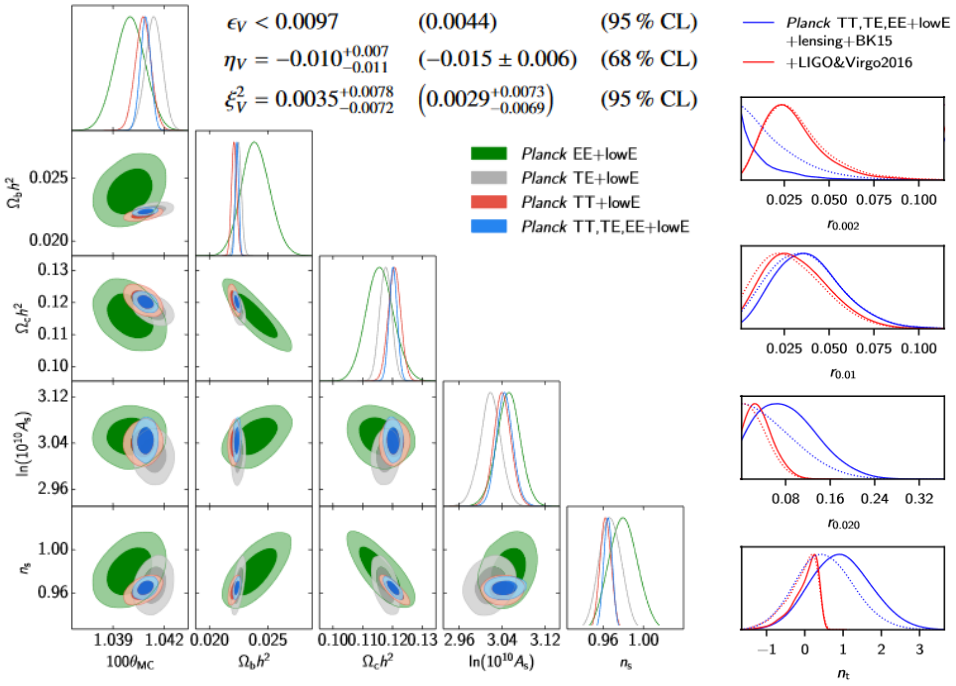

Figure 5.2: Table of confidence intervals for cosmological observables, reported in *Planck* 2018 *Constraints on Inflation*. θ_{MC}, angular size of the sound horizon at recombination; Ω_b, baryon density; Ω_c, cold dark matter density; A_s power of scalar perturbations at pivot scale; n_s, scalar spectral index; r, tensor-to-scalar ratio; n_t, tensor spectral index. Source: [3].

spectral parameters take their familiar forms for $V(\varphi) \sim \varphi^2$. In this regime, we more efficiently retain small fluctuations as m_v increases by delaying the end of inflation – drawing the horizon exit scale closer to the minimum where

$$f(x)^{3/2} \left| f'(x) \right|^{-1} \sim f(x)$$

is already very small – rather than reducing $m_{\rm h}$ to make small values of $Q_s \sim m_v^2 m_{\rm h}$ more likely far from the minimum where $V(\varphi) \sim m_v^4$. Furthermore, larger field scales are more likely to yield large inflating intervals contiguous with the maximum – bridging multiple smaller disjoint intervals, and giving a slow roll streak starting from the peak access to lower regions of $V(\varphi)$ where small Q_s can occur.

The constraints on n_s are easily satisfied for large $m_{\rm h}$ in Measure A, as they encompass the quadratic limit at 55 e-folds before inflation's end; but a sufficiently small tensor-to-scalar ratio is hard to come by in that regime.

$$\text{Quadratic limit } (\mathcal{N}_e = 55): \qquad n_s \approx 1 - 2\mathcal{N}_e^{-1} = 0.963 \qquad r \approx 8\mathcal{N}_e^{-1} \approx 0.15$$

At intermediate scales $0.1 \lesssim m_{\rm h} \lesssim 1$, it is no longer guaranteed that inflation continues all the way from the maximum to the quadratic neighborhood of the minimum; peaks must be low enough that horizon exit occurring high on the potential can still produce small curvature perturbations. For field scales more than an order of magnitude smaller than $m_{\rm P}$, we run into issues of sample size

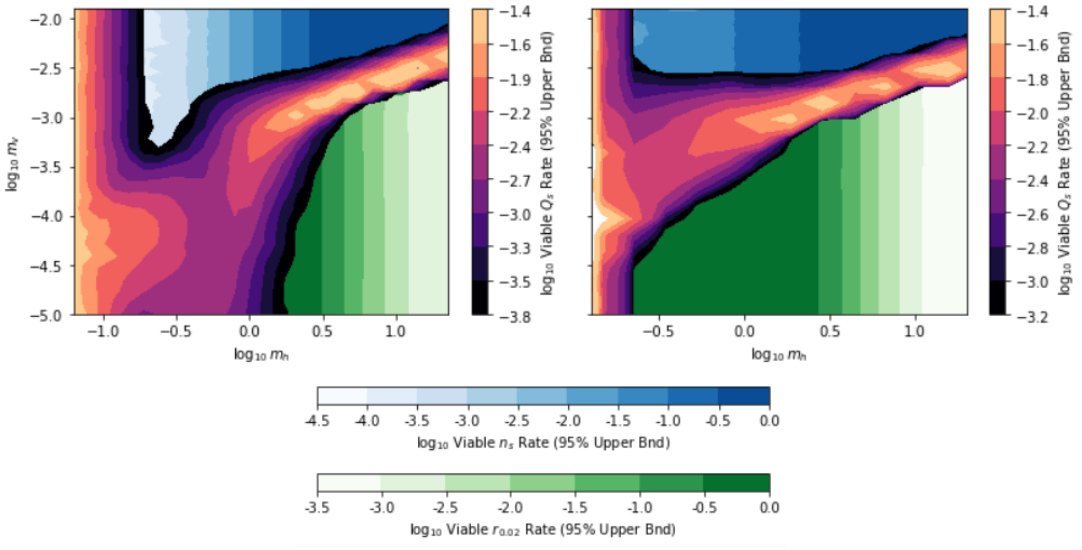

Figure 5.3: Marginal distributions of spectral parameters in Measures A (left) and B (right). Foreground (magma): 95% confidence upper bound on the rate of incidence of Q_s falling within *Planck 2018* 68% confidence interval. The vertical striation pattern emerging on the left-hand side reflects the shortage of samples with successful inflation at low $m_{\rm h}$ – due to slower accrual of e-folds and the second slow roll criterion not being met at the peak – resulting in a weaker bound. Background: rates of incidence of n_s (blue, upper) and r (green, lower) falling within *Planck*'s 68% confidence intervals, with higher color saturation (darker gray) indicating a higher rate.

that limit our ability to assign a small upper bound on the rate estimate, reflecting the difficulty of finding potentials varying on sub-Planckian scales that produce enough e-folds of inflation. This is acceptable for our purposes in Measure A, as only one in $\sim 10^4$ successful models at that scale fall in the confidence region for the spectral index, and so models from smaller field scales are unlikely to significantly affect results close to home in the space of observables.

Measure B Measure B produces similar distributions to Measure A in the large field regime, as whether or not inflation starts at a maximum makes no difference

if it persists along most of the potential slope to end close to the minimum. Approaching the Planck scale $m_h = 1$, we do not see a pronounced entry of models with smaller potential scales producing sufficiently small scalar perturbations as in Measure A. Inflation is highly concentrated around extremal points of the potential, and with no guarantee of starting in one of those intervals, we do not get much inflation with horizon exit occurring in the intervening part of the slope, where small m_v would give small Q_s.

Small sample size due to low rates of successful inflation becomes limiting at a larger field scale than in Measure A, since we are no longer initializing in a slow roll interval in every case. Among the successful models, the scalar tilt is significantly more likely to fall in the observed range at small field scales, as most Measure B models in that regime feature an extended slow roll plateau rather than merely a gently curved quadratic peak. (This is because the probability of sampling the initial field value within a slow roll interval is proportional to its width, and the number of e-fold counting toward the horizon problem threshold is not taken to be infinite as in Measure A.) Meanwhile, the small tensor amplitude becomes *slightly* harder to come by at large m_{h}, as there is some probability of large-field potentials eligible for inclusion in Measure A to be omitted from Measure B if the field value is sampled too close to the minimum.

Measure C When it comes to observables, Measure C departs from Measure A only in cases for which fewer than 55 e-folds elapse beyond a 1-σ deviation for Hubble-scale fluctuations in the direction of the Minkowski basin, so that horizon exit occurs in the excluded interval around the peak. Since the size of those fluctuations is typically much smaller than the field scale in this range, in those models inflation is almost entirely localized at the maximum. So we may expect a departure in the far end of the small-field regime, where inflation is localized at the peak and the scalar amplitude computed in that neighborhood can be sufficiently small (lower left corner of Figure 5.3).

5.3 Measure A: Summits

Many of the named classes of inflation models studied in the literature assume an inflaton initialized in a fairly homogeneous configuration atop a potential barrier or plateau; the most natural choice for codifying this trend is to initialize at the maximum with zero expected field velocity. (Another instantiation is examined with Measure C.)[2]

In Measure A, we sample half-basins of the potential with a nearly vanishing

[2]Other justifications for initializing at the top of a potential barrier – such as invoking a first order phase transition in the past, or Hawking-XXX's proposal based on arguments from Hawking-Moss instantons – have merit but rely on additional structure (extra fields and interactions, or dynamics in the past of our inflating volume) that goes beyond the scope of this study.

vacuum energy, weighted by the distance in field space from local maximum to minimum. Since this tends to be of order $m_{\rm h} m_{\rm P}$ in our space of Gaussian random fields, our draw of Minkowski half-basins does not differ appreciably from uniform sampling. We account for slow roll inflation that takes place in the true-vacuum basin contiguous with the local maximum. If slow roll is not sustainable at the peak (due to $\eta_V > 1$), we count inflation contiguous with a slow-roll interval lower on the potential, if at the top of the first such interval the attractor bound (4.5) is satisfied along a classical trajectory approaching the maximum as $t \to -\infty$ (as described in § 4.1.2).

Regarding the prevalance of eternal inflation, the first result (starting with row 1 in Table 5.1) can be obtained by inspection, at least valid within the scope of this analysis. If the second potential slow roll condition is met at the peak, then inflation will always thwart the collapse of any initially near-homogeneous field configuration into a quasi-static domain wall, and so continue in perpetuity. In those models, inflation is eternal by both stochastic and topological modes: quantum fluctuations dominate near the peak where $V'(\varphi)$ vanishes, and causally disconnected regions descending toward different minima of the potential are separated by an inflating domain wall.

If $M_P^2\, V''/V \lesssim -4/3$ in a suitably large neighborhood around the top of the potential barrier, then small inhomogeneities around the peak tend to grow with

	$\eta_V \lesssim 1$ @ Peak	SR Below Peak	Attractor Bound	Adjacent sgn(ρ_Λ)	Adj. SR Below Peak	Conditioned on	Result
1	✓						Stochastic and topological eternal
2	✗	✗					No successful inflation
3	✗	✓	✗				No successful inflation
4	✗	✓	✓				Stochastic eternal at all $m_{\rm h}$
5	✗	✓	✓			Q_s	Stochastic eternal at large $m_{\rm h}$, small m_v
6	✗	✓	✓			n_s, α	Successful inflation less often stochastically eternal than with no conditioning on CMB observables; generically eternal for $m_h \gtrsim 0.3$.
7				dS			False-vacuum and topological eternal
8	✗	✓	✓	M	✓		Always topological
9	✗	✓	✓	AdS	✓		Always topological
10	✗	✓	✓	M	✗		Maybe topological
11	✗	✓	✓	AdS	✗		Maybe topological

Table 5.1: Summary of Measure A results.

time in physical coordinates, as follows from the argument presented in § 2.3. The field's potential energy will not tend to dominate its kinetic energy for a sustained bout of inflation. Slow roll does not persist at the peak; but the model has a chance to accrue many e-folds lower on the slope of the Minkowski half-basin, if the field velocity is small enough in a field space interval in which $\epsilon_V, |\eta_V| < 1$, and go on to produce a viable cosmology. Absent these latter conditions, and if the scale of the domain wall around the sharp peak is sub-Hubble, the model lands in rows 2 and 3 in Table 5.1, with no thermalized regions preceded by enough e-folds of inflation to solve the horizon problem. For notational convenience, let us identify nested subsets of models belonging to a sample population from Measure A:

- Let A denote the set of all models in the sample from Measure A.
- Let $S \subset A$ denote the set of models in the sample that have *successful* inflation, meaning greater than 70 e-folds accrued in an interval in which the potential slow roll conditions are satisfied.
- Let $D \subset S$ denote the set of models that are successful AND in which the only sustained bout of inflation starts below the peak (delayed inflation).
- Let $D' \subset D$ denote the set of models with successful delayed inflation, in which the stochastic inflation criteria are never satisfied. (All models in S

but not in D' are stochastically eternal.)

5.3.1 Stochastic Eternality with Delayed Inflation

Rows 4-6 in Table 5.1 include models with both potential slow roll conditions met only below the potential maximum, and enough inflation in that interval to solve the horizon problem. (All such models belong to the sample subset D.) Only if Eq. (2.11) is satisfied on the slow roll interval lower on the potential do we get conventional stochastic eternal inflation; if not, then the model is a member of the subset D'. It is typical for classical trajectories initialized a 1-σ fluctuation away from the peak with zero field velocity to undergo slow roll for several e-folds along the descent, despite the potential slow roll conditions not being met. Avoiding stochastic eternal inflation near the peak relies on fluctuations superposing around the peak to produce inhomogeneities, which are amplified by the large second derivative of the potential and result in a terminal, short-lived bout of inflation within that interval of field space.

In Figure 5.5, we depict the rates of incidence of models with $\eta_V < -4/3$ at the initial peak, in which successful slow roll inflation could begin lower on the potential without meeting the stochastic inflation criterion. Considered as a frequentist ratio, the numerator and denominator for each data point in Figure 5.5 are the sizes of $D' \cap \{m_v, m_h\}$ and $S \cap \{m_v, m_h\}$, respectively, where $\{m_v, m_h\} \in A$

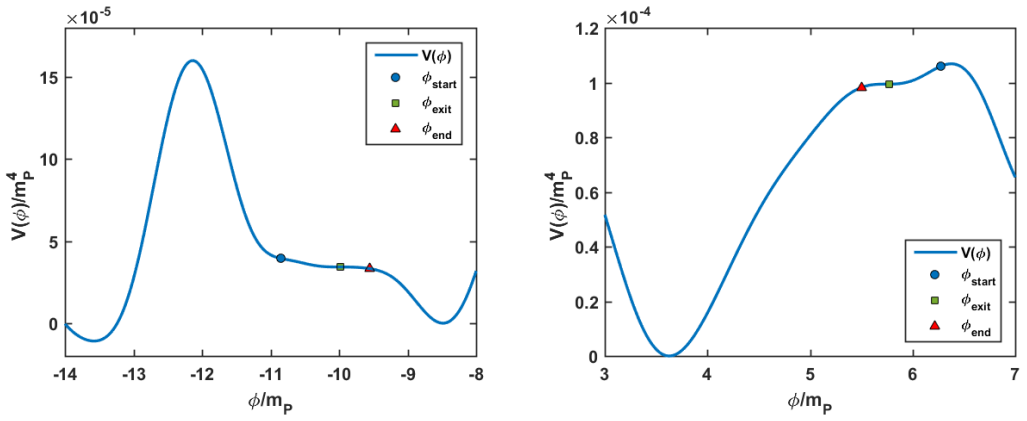

Figure 5.4: Examples of models drawn from Measure A that fall into subset D. The potential on the left represents the spirit of delayed inflation – a flat site for slow roll below a sharp peak. The potential on the right has $\eta_V < -4/3$ at the peak, but the curvature quickly shrinks to within the slow roll attractor; initialized with a small field velocity, inflation really continues uninterrupted between the peak and the interval in which the potential slow roll conditions are met, with the kinetic energy never rivaling $V(\phi)$.

is the subpopulation simulated with a particular pairing of mass scales. Stochastic eternal inflation is generic at large field scales $m_h > 1$, where $\eta_V \sim (m_{\rm h} m_{\rm P})^{-2}$ is easily within the bound of the slow roll approximation at the peak. This continues to low rates of possibly non-stochastic delayed inflation in Figure 5.5 for large $m_{\rm h}$.

The probability of ultimate interest is that of a model undergoing delayed inflation that is not stochastically eternal below the local maximum, given successful, viable inflation:

$$P(m \notin D' \mid m \in S \cap \{Q, n_s, \alpha, r, n_t, \dots\})$$

where the latter set contains models that satisfy constraints on observables. The probabilities represented by the purple data points in the left plot of Figure 5.5

are

$$P(m \in D' \mid m \in S \cap \{m_v, m_h\})$$

Below the Planck scale $m_{\mathrm{h}} \sim 1$, incidence of non-stochastically-eternal models among those with enough e-folds goes roughly as a power law with the scale of the inflaton, before conditioning on spectral features. The data points indicate 95% confidence upper bounds for those mass bins in which at least one non-stochastic model was observed. (Since this data is binned with respect to field scale, the epektacratic and democratic mass scale weightings do not come into play.)

Conditioning on Spectral Shape What is the effect of requiring that the angular scale dependence of the scalar CMB spectrum is consistent with *Planck* data, resulting in a scalar index n_s and running α within their respective 95% confidence intervals? At all field scales shown in Figure 5.5, the upper bound on rates of non-stochastic delayed inflation is greater by 1 to 2 orders of magnitude after conditioning on n_s and α; these data represent the conditional probabilities:

$$P(m \in D' \mid m \in S \cap \{m_v, m_h\} \cap \{n_s, \alpha\})$$

(The running α is generically within the bounds from measured data after conditioning on n_s.)

It looks as though varying m_v has no effect on the rate of stochastic eternal-

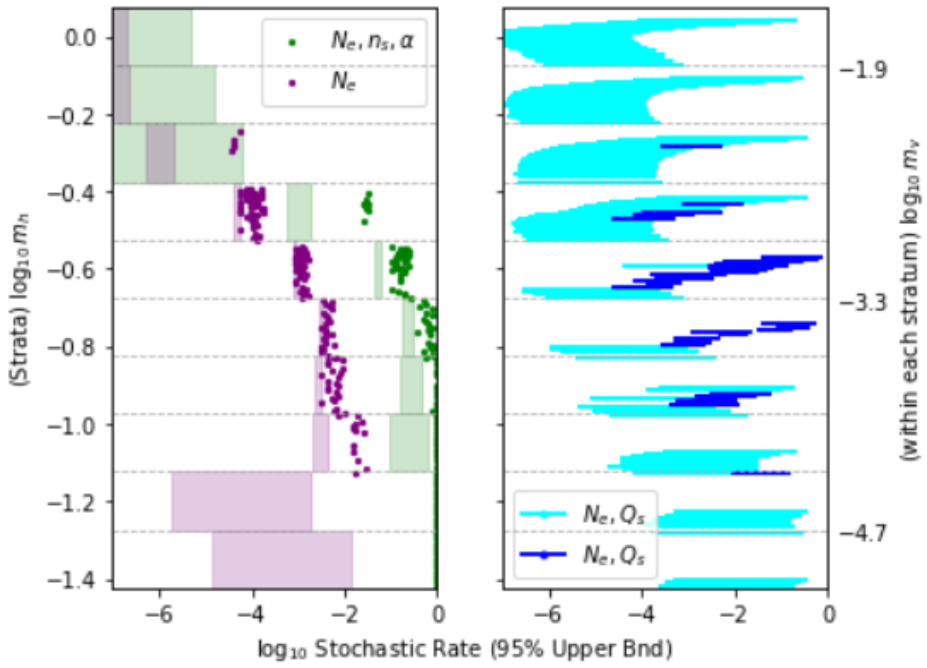

Figure 5.5: Incidence rate of models with slow roll starting below the peak with no stochastic inflation, among models in Measure A with 70+ e-folds. Each data point represents one batch of simulations with particular $m_v, m_{\rm h}$ (only showing batches with at least one positive event per sample). All models within a vertical stratum have the same value of m_h (the center of the stratum on the left axis); vertical position within the stratum reflects $\log_{10} m_v$ (range shown on the right axis). Data points reflect 95% confidence upper bounds. In the left plot, green data points are derived from samples conditioned on n_s and α; purple data points are conditioned only on minimal e-folds; the shaded bars indicate 90% confidence intervals taking models from all values of m_v as belonging to one sample. In the right plot, the blue lines show 90% confidence intervals derived from samples of successful models conditioned further on Q_s. Darker lines reflect samples that have at least one non-stochastic model in the sample, whereas lighter points are determined only by sample size.

ity among models with successful inflation and those further conditioned on n_s and α. This would mean that once we have the primary inflation epoch starting on a "shelf" below the peak, it is never borderline between stochastically eternal and non-eternal; if it were, then increasing m_v while holding m_h constant would have the effect of lowering the non-eternality rate represented in the left of Figure 5.5. We cannot infer independence of m_v without doing a statistical test; let our competing hypotheses be (H0) for given m_h, all batches conditioned on m_h with varying m_v have the same rate, with deviations owing to chance; and (H1) the rate parameter varies with m_v. We test this hypothesis using likelihood-ratios, with the numerater the likelihood maximized over a single rate parameter for all m_v, and the denominator maximized over separate rate parameters for each batch.[3] We found that generally we cannot reject the null hypothesis with an alpha of 0.01.

Since we cannot conclude that changing the scale of the potential in this range has an effect on the rate of stochastic inflation, we also depict combined results taking models from the full range of m_v (including mass bins with no positive

[3]If s_i events are observed in a sample of size n_i, with i indexing values of m_v, then we have for the log-likelihood ratio

$$\tau = 2\log\frac{\ell_0}{\ell_1} \qquad \ell_h = \begin{cases} \max\limits_{p} \prod_i \mathrm{Beta}(p, s_i+1, n_i-s_i+1), & h=0 \\ \max\limits_{\{p_i\}} \prod_i \mathrm{Beta}(p_i, s_i+1, n_i-s_i+1), & h=1 \end{cases} \tag{5.1}$$

We then compute the distribution over likelihood ratios in samples with the same sample sizes as the original batches, given the single rate that maximized likelihood in the null hypothesis.

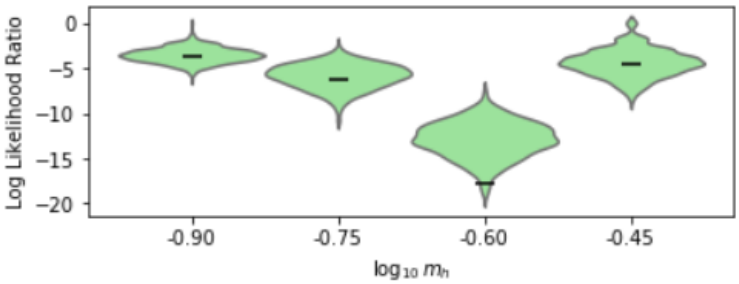

Figure 5.6: Distributions of log likelihood ratios, comparing maximizing over one rate parameter versus independent rate parameters for each m_v, from Monte Carlo simulation assuming the former null hypothesis. Ratios for the simulated data are indicated in black. Only for $m_h = 0.25$, with p-value 0.016, should we consider rejecting the hypothesis of a well defined rate of incidence of delayed non-stochastic inflation independent of m_v.

events) as belonging to one sample.

$$P(m \in D' \mid m \in S \cap \{m_h\} \cap \{n_s, \alpha\})$$

We report the resulting 90% confidence intervals represented by the shaded bars in the left of Figure 5.5. (We also show the same results for models conditioned only on number of e-folds, for which we also fail to reject the null hypothesis.) From this we can infer that delayed non-stochastic inflation falls short of being generic with high likelihood down to below $m_h = 0.1$, among models conditioned on n_s and α. For smaller field scales in this regime, what we have called non-stochastic-eternal inflation (which includes some generous assumptions that cannot be taken for granted) is neither generically present nor absent.

Conditioning on Spectral Amplitudes The sub-sample of S after conditioning on a viable complete spectrum – including $\{Q_s,\, n_s,\, \alpha,\, r,\, n_t\}$ – was too small to work with directly; but we can condition on the scalar and tensor amplitudes and 70+ e-folds alone, and use those results in conjunction with those conditioned on n_s and α above to make naive inferences from an assumption of statistical independence.

Turning attention to the righthand plot in Figure 5.5, we find that straightforwardly stochastic inflation is less prevalent at larger potential scales among models with viable spectral amplitudes, in comparison to all models in S. A larger scale for the potential correlates with a greater proportion of models with inflation below the peak among successful models satisfying constraints on the scalar amplitude Q_s. This may be somewhate suprising considering the stochastic inflation criterion is a lower bound on the amplitude of scalar curvature pertubations, which scales with m_v^4. But it makes sense when considered as an effect of selecting for a suitably small scalar amplitude born of a delayed inflationary epoch.

A larger Hubble parameter $\sim m_v^2$ means greater friction, allowing the potential to have a lot of curvature at the peak while tending toward somewhat smaller separation in field space between the peak and an interval of slow roll (greater allowance for $V'(\varphi)$), as well as a smaller field velocity at the top of that inter-

val. When the potential is large, the requirement of a small amplitude for scalar perturbations means inflation must end low on the potential slope, which is more likely in models with inflation starting below the peak. With greater potential energy the upper bound on $\dot{\varphi}$ for the slow roll attractor is greater, allowing more models to accrue many e-folds below the peak.

5.3.2 Topological Eternality with Delayed Inflation

The above analysis considers the incidence rate of stochastic eternal inflation if we erect a reflecting boundary at the maximum, to the effect that fluctuations always send Hubble volumes toward the Minkowski side of the barrier. This treatment of course eliminates the possibility of topological inflation, with the intent to isolate the occurence of eternal inflation owing to stochastic fluctuations. Without such an unphysical boundary, quantum fluctuations of the inflaton always dominate the effects of the potential gradient in a sufficiently small neighborhood around the potential peak, and so are overwhelmingly likely to result in an inhomogeneous field configuration descending toward the minima of both conjoining half-basins.[4]

For models in the sample subset D, so long as φ somewhere obtains the peak value, there is always a Hubble-sized region at the top of the slow roll interval

[4]Diffusion also implies that the number of e-folds in the past of any thermalized region is finite even if we start with a homogeneous and stationary expectation value at the maximum.

below the peak that must pass through an inflationary epoch, as the field therein descends the slope toward the Minkowski vacuum. This is the case in which the characteristic scale of domain wall thickness is greater than the characteristic Hubble scale in the wall's core; even as small inhomogeneities around the peak are initially magnified, the wall is supported against collapse to sub-Hubble scales by the shape of the potential, and we still end up with inflating defects interpolating between the two vacua. Does this imply that all successful delayed inflation in Measure A is always topologically eternal, since the intervening space separating regions occupying the vacua is inflating?

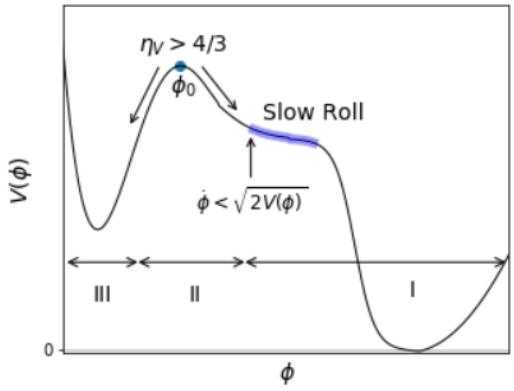

Our hypothesis: almost (but not quite) certainly. Suppose that in Regions I, II, and III, the field occupies the Minkowski true-vacuum basin (including an interval of slow roll), the neighborhood of the sharp peak, and the adjacent basin, respectively. Only if Region III grows to a size larger than the Hubble scale in that basin – effectively "pinning" the de Sitter horizon surrounding that region to

a value in the adjacent basin – do we get a *topological* defect. So long as the defect is contained within a single de Sitter horizon, one can entertain the possibility of a nonperturbative fluctuation that could in principle put the field in Regions I-III in the true-vacuum basin, and make possible an end to inflation.

The question of topological eternality then comes down to whether the inhomogeneous configuration becomes a topological defect or can be excised via quantum tunneling, and how the rate of that process compares with the rate of production of new defects in the late-time limit. There are three scenarios for the basin adjacent to the Minkowski vacuum:

7. The adjacent minimum is largely positive. Inflation takes place in the false vacuum, and the defect grows to a size of many Hubble volumes. The barrier above the slow roll interval is sharply peaked, meaning that a Coleman-de Luccia instanton dominates if the false vacuum has a vacuum energy greater than the potential energy during inflation. Since the barrier includes an interval in which the potential is very flat, a CDL instanton deposits the field at the top of the slow roll shelf. However, one can assume that the tunneling rate is generically too small to avoid false-vacuum eternal inflation.

8-9. The adjacent minimum is Minkowski or anti-de Sitter, and there is a period of inflation between the peak and that minimum. Again we get an inflating defect spanning many Hubble volumes that cannot be excised.

10-11. The adjacent minimum is Minkowski or anti-de Sitter, and there is no slow roll inflation on that half-basin. The zero or positive pressure region expands outward, displacing the negative pressure inflating bulk with a spherical boundary approaching the speed of light.

In Scenarios 10-11, the volume in Regions II and III is contained within a de Sitter horizon. The field interpolates between the negative-energy minimum and the start of the inflating region on the $\rho_\Lambda = 0$ side; the nearest de Sitter horizon is associated with the inflating volume that surrounds the defect. A homogeneous anti-de Sitter space cannot tunnel to a Minkowski or de Sitter one [30]; since the Wick rotated geometry is not compact, when we subtract the background Euclidean action we get an infinite negative contribution to the exponent in the tunneling rate. But perhaps such an interpolating configuration can tunnel to one with the field everywhere at the top of the inflating interval, or otherwise to the right of the barrier.

Unlike the $O(3,1)$-symmetric solutions studied in Coleman-de Luccia, such transitions cannot be treated in terms of φ and ρ as functions only of a single radial coordinate ξ. To determine rates of such transitions, one would have to simulate Euclidean evolution of configurations with at most $O(3)$ symmetry, in terms of $\varphi(\xi, \chi)$ and $\rho(\xi, \chi)$. Eventually the distribution $\rho(\varphi, t)$ will assign most of the comoving volume to one or the other basin, and the rate of production of new

topological defects – regions of negative $V(\varphi)$ surrounded by inflating background – approaches a late-time limit. If transitions that destroy defects exist, then the rate of tunneling out of the negative or Minkowski false vacuum need not be much faster than the rate of production of new defects. Once all of the existing topological defects have tunneled away in a macroscopic region, all volume is on the Minkowski side of the barrier, and the remaining inflating regions are no longer topologically eternal toward the future. If such special tunneling solutions do not exist, which seems likely, then Scenarios 10-11 also result in topological eternal inflation.

5.4 Measure B: Uniform

Measure B draws initial field values uniformly; because the statistical behavior of GRFs is translation-invariant, this is equivalent to simply choosing $\varphi_0 = 0$ for each newly sampled potential function.Many of the small field models from Measure B that produce enough inflation will be initialized very near the maximum, and stochastic fluctuations may send Hubble volumes into both conjoining half-basins. Despite this caveat, we consider draws of the potential and initial conditions as belonging to one of two classes for the purpose of the analysis below: those initialized in either the true- (Minkowski) or false-vacuum (de Sitter)

basins of attraction.[5]

For Measure B we do not account for inflation in a slow roll interval that is not contiguous with the initial field value, as in the delayed inflation scenario in Measure A. This is because those inflating intervals are already included in the domain of Measure B, and a history in which slow roll starts higher on the potential and begins to inflate at the top of that region does not differ observationally from a history in which the field is initialized in that interval. Furthermore, it is less clear cut than in Measure A how we should sample the initial field velocity to make the determination of whether the dynamics quickly reduce to slow roll at a lower site on the potential.

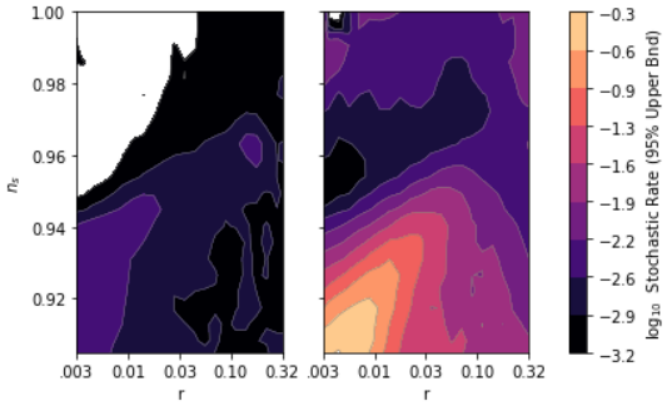

Figure 5.7: 95% confidence upper bound on the rate of incidence of stochastic inflation in Measure B, binned with respect to scalar tilt and tensor-to-scalar ratio, with at least 70 e-folds (left) and 200 e-folds (right), subject to epektacratic field scale weighting.

[5]Recall that the true vacuum basin is the one in which we have artificially shifted an already-low vacuum energy to precisely $\rho_\Lambda = 0$; a false-vacuum basin is one of the two adjacent to the true-vacuum basin, in which the vacuum energy is positive. We only consider one transition event.

5.4.1 Initialized in a True-Vacuum Basin

Stochastic Eternality Unlike in Measure A, not every downhill trajectory for models in Measure B passes through an extremal point on the potential. In the left plot in Figure 5.7, we depict rates of incidence of stochastic eternal inflation among models with greater than 70 e-folds, using epektacratic field scale wighting and binning with respect to the scalar spectral index and tensor-to-scalar ratio. Stochastic inflation is most prevalent in the vicinity of $n_s \approx 0.963$ and $r \approx 0.15$; this corresponds to the quadratic limiting behavior in large field models, where the field excursion during a Hubble time goes like $m_{\rm h}^{-1}$ making stochastic inflation more likely. Even then, fewer than 1% of models from all mass scales in the population are stochastically eternal.

Rates of stochastic eternal inflation presented here may be suppressed because we require merely that $\epsilon_V, |\eta_V| < 1$ to assume slow roll takes place in the full dynamical evolution, rather than the strong versions of those inequalities. Although the attractor behavior of the full equations of motion leads to authentic slow roll being met, this choice could be letting through models that accrue e-folds in intervals with larger $V'(\varphi)$ or $V''(\varphi)$ than would be admissible if the strong inequalities were enforced at the initial field value. If we turn our attention to regions of parameters space in which the scalar index $n_s \approx 1 - 6\epsilon_V + 2\eta_V$ is close to 1, it suggests that the potential slow roll parameters are small enough to sat-

isfy the strong inequality at least near the horizon exit scale in those models. To compensate for this possible bias and to showcase dependence of the results on e-fold count, we also show rates conditioned on at least 200 e-folds in the plot on the right of Figure 5.7.

In our region of parameter space around $n_s = 0.96$ and small r, the effect of requiring more e-folds is to only slightly increase the likelihood of stochastic inflation. All of the dramatic effects of conditioning on more inflation occur for redder scalar spectra than are viable based on *Planck* data. Observables n_s and r are highly correlated along contours of equal probability of eternal inflation in the lower left region of both plots, corresponding to red spectra and small tensor perturbations, which makes sense as the commonality lies in both quantities' dependence on ϵ_V, which can be made to appear in the stochastic inflation criterion. It seems that before conditioning on the amplitude of the scalar spectrum, our region of this parameter space represents a local *minimum* for probability of eternal inflation in this range.

Figure 5.8 depicts the rates of incidence of stochastic eternal inflation among successful models with small scalar amplitude $Q_s \leqslant 10^{-3}$ (our maximum likelihood value is close to $10^{-4.3}$), as well as the number of models aggregated in each bin – to inform where sample size is determining the estimate. Eternal inflation is suppressed considerably for scalar-dominated spectra after conditioning on small

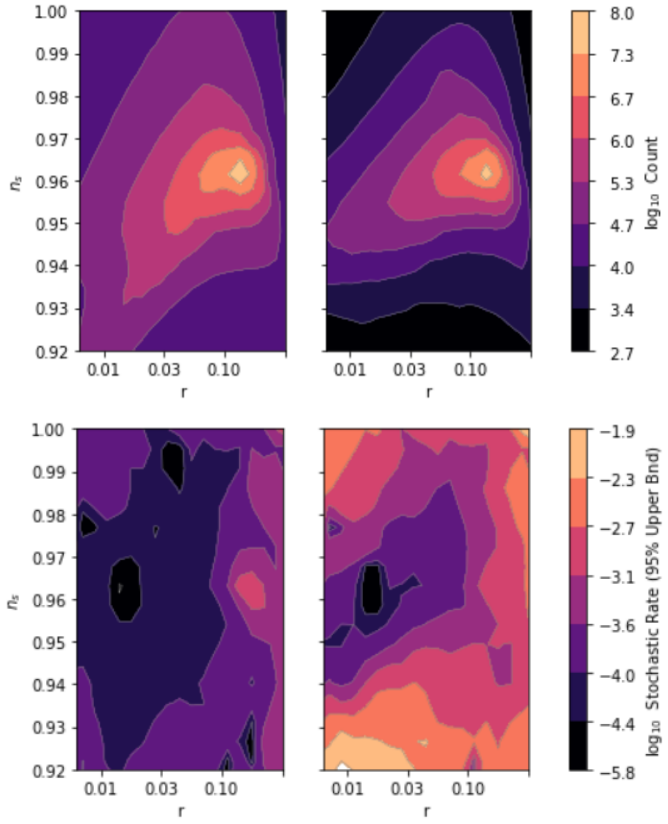

Figure 5.8: (Top) Total number of successful models with $Q_s < 10^{-3}$ in each bin. (Bottom) 95% confidence upper bound on the rate of incidence of stochastic inflation in Measure B, binned with respect to scalar tilt and tensor-to-scalar ratio, with at least 55 e-folds (left) and 200 e-folds (right), for $Q_s < 10^{-3}$ and subject to epektacratic field scale weighting.

scalar perturbations, with rates smaller by up to 3 orders of magnitude compared to the sample of successful models. Our region of parameter space continues to appear as near a local minimum for the probability of stochastic eternal inflation.

Topological Eternality Topological eternal inflation can come about in Measure B, if the field value is initialized close enough to the maximum that fluc-

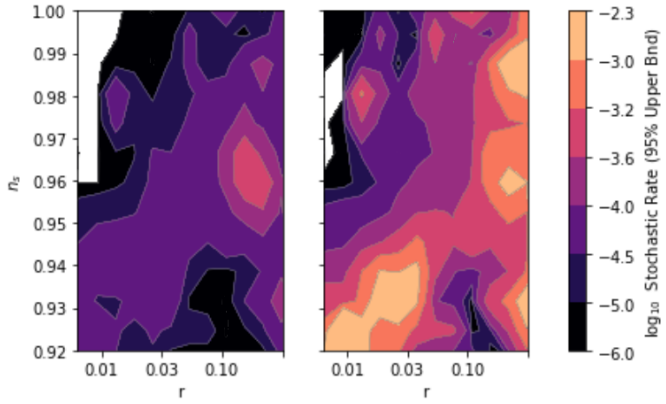

Figure 5.9: Same as the bottom plots in Figure 5.8, but subject to democratic field scale weighting. The jagged apperance reflcts the small sample size of bins remaining after one conditions on a small amplitude of scalar perturbations.

tuations are likely to result in at least one Hubble volume with a field value on the other side of the barrier. (This can only happen if the stochastic inflation criterion (2.11) is satisfied in an interval containing the starting point.) In Figure 5.10, we depict bounds on the incidence rate, among successful models and those conditioned further on spectral features, of those in which the uniformly sampled initial field value lands close enough to the maximum that fluctuations are likely to result in at least one Hubble volume on the other side of the barrier after a Hubble time. This is the case when

$$\operatorname{erfc}\left|\phi_{\text{start}} - V'(\phi_{\text{start}})/3H^2 - \phi_{\text{peak}}\right| > 2e^{-3} \tag{5.2}$$

In fewer than 1 in 10^4 models with a small scalar amplitude do we find this condition to hold. The only sample in which we get positive events is that of all models with succesful inflation; in that sample, the incidence of topological eternal

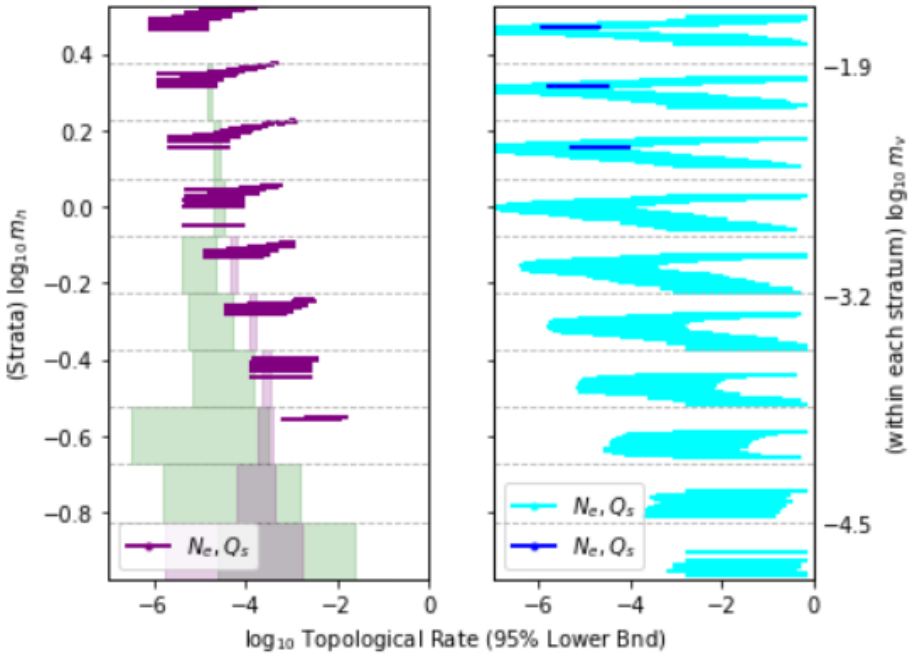

Figure 5.10: 95% confidence lower bound on incidence rate of models with high probability of topological inflation, among models in Measure A with 70+ e-folds. In these models, quantum fluctuations are comparable in size to $|\varphi_0 - \varphi_{\max}|$, allowing $\gtrsim 1$ Hubble volume to descend toward the opposite local minimum after a Hubble time with high probability, and produce a persisting topological defect. Each line represents one batch of simulations with particular $m_v, m_{\rm h}$ (only showing batches with at least one positive event per sample or a sample size of 100). All models within a vertical stratum have the same value of m_h (the center of the stratum on the left axis); vertical position within the stratum reflects $\log_{10} m_v$ (range shown on the right axis). In the left plot, green data points are derived from samples conditioned on n_s and α; the purple 90% confidence intervals are conditioned only on minimal e-folds; and the shaded bars indicate 90% confidence intervals taking models from all values of m_v as belonging to one sample. In the right plot, the blue data points are derived from samples of successful models conditioned further on Q_s. Darker points have at least one non-stochastic model in the sample, whereas lighter points are determined only by sample size.

inflation does exhibit a dependence on m_v, with higher potential scales yielding higher rates of topological inflation. This follows simply from the fact the the size of fluctuations goes like m_v^2, making it easier to atain large fluctuations that carry the field over the peak. No events were observed in the population conditioned on a viable scalar spectral index, and so the bounds in that sample are determined entirely by sample size.

This is a rather high bar, indicating that the conditions for topological inflation to proceed are highly probable to come about within a few Hubble times. Figure 5.10 does not account for models that are initialized in a stochastic inflation interval contiguous with the maximum, but in which fluctuations from the initial field value are not likely to reach all the way to the maximum. In such models, the field would gradually climb the potential as it undergoes stochastic eternal inflation, eventually to reach the peak and descend down the other side – becoming also topologically eternal.

5.4.2 Initialized in a False-Vacuum Basin

When φ lands in a basin with a positive vacuum energy adjacent to the Minkowski basin, we assume that large regions come to occupy the false vacuum. We compute the Coleman-de Luccia instanton profile interpolating between

the starting basin and "true" vacuum[6], or determine that a CDL solution does not exist. When accounting for gravity, the CDL instanton terminates on the slopes of the barrier rather than precisely at the local minima; so if a solution exists we then initialize φ with a new starting position at its terminus on the slope on the true-vacuum side of the barrier, and tally e-folds below that point. If a CDL instanton does not exist, then the Hawking-Moss instanton gives the largest contribution to the transition amplitude between de Sitter and Minkowski basins. This happens when the top of the barrier is sufficiently flat [39]

$$V(\varphi_{\rm top}) \gtrsim m_{\rm P}^2\, V''(\varphi_{\rm top}) \tag{5.3}$$

in which case φ following a Euclidean classical trajectory either cannot build up enough kinetic energy to close the bubble on the false-vacuum side or loses it to friction. Well above the Planck scale $m_{\rm h} = 1$, it is therefore safe to assume that the transition is Hawking-Moss. In that case, φ is re-initialized at the top of the barrier, as in Measure A.

Having landed in the false vacuum basin, *generically eternal* would mean that among models that produce observables consistent with *Planck* spectral fit and $\rho_\Lambda = 0$ after tunneling, the transition rate is generically below the threshold given in (2.15) or generically Hawking-Moss (leading to stochastic and topological

[6]Since the domain of the Gaussian random field is infinite, one can always find a lower energy vacuum. We limit consideration to the vacua to either side of the Minkowski basin.

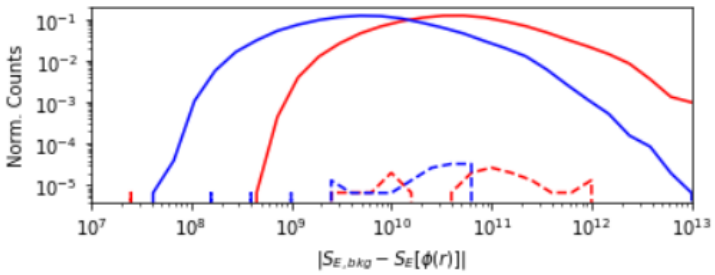

Figure 5.11: The bimodal distribution of $S_{\rm E,bkg} - S_{\rm E}[\phi(r)]$ for Coleman-de Luccia transitions in models initialized in the false vacuum, for $m_v = 0.0025$ (red) and 0.0042 (blue). The normalized counts for values of the tunneling suppression are plotted with respect to its absolute value; the solid lines correspond to slow tunneling, for which inflation is eternal, while the dashed lines are fast tunneling.

inflation irrespective of the tunneling rate; there is always inflation at the peak when HM dominates).

Coleman-de Luccia When CDL instantons exist, transition rates generically fall below the eternal inflation upper bound, as shown in Figure 5.11. The distributions for different energy scales of inflation differ by a translation in the log domain, scaling with m_v^4. Vertical mass scales on the order $m_v^4 = \mathcal{O}(10^{-5})$ would correspond to a point where the distribution has support in the vicinity of $9/4\pi$ and the determination of genericity becomes more nuanced, but that is far above the range where small scalar and much smaller tensor curvature perturbations are likely to be found at horizon exit. So models with a CDL transition are generically eternal within the scope of this analysis. The challenge is to get enough e-folds on the other side of the barrier, and to characterize statistical behavior of the

tunneling rate among those very rare events.

The distributions of the number of e-folds after Coleman-de Luccia tunneling for $\gamma = 0$ and $\gamma = 4$ (referring to the shape parameter in (4.3)), accounting for all field scales with epektacratic weighting, are shown in Figure 5.12. Among models aggregated from all field scales $m_{\rm h}$ and for which the field value after tunneling satisfies slow roll, the distribution resembles log-normal for $\gamma = 0$ in (4.3), with an expectation value of less than one e-fold (in effect, no inflation). Also shown are the expectation values and 2-σ ranges (assuming log-normal) for populations sampled with a single field scale and $\gamma = 0$, along with the number of standard deviations between the mean and 55 e-folds where horizon exit of CMB modes could occur. For $\gamma = 4$, practically the entire distribution is localized below 1 e-fold – yielding no inflation post-transition.

Determining the rate of non-eternal inflation comes down to the distribution of the tunneling rate among models with CDL instanton solutions that are just on the threshold of not existing – with the field landing very close to the maximum, but outside the stochastic inflation regime around the peak. For this reason, we consider models in which the CDL solutions dominate as effectively not contributing to the population of observationally viable models, for the purpose of determining whether eternality is generic under Measure B. For a similarly defined measure in which initial field values in the true vacuum basin are excluded, one

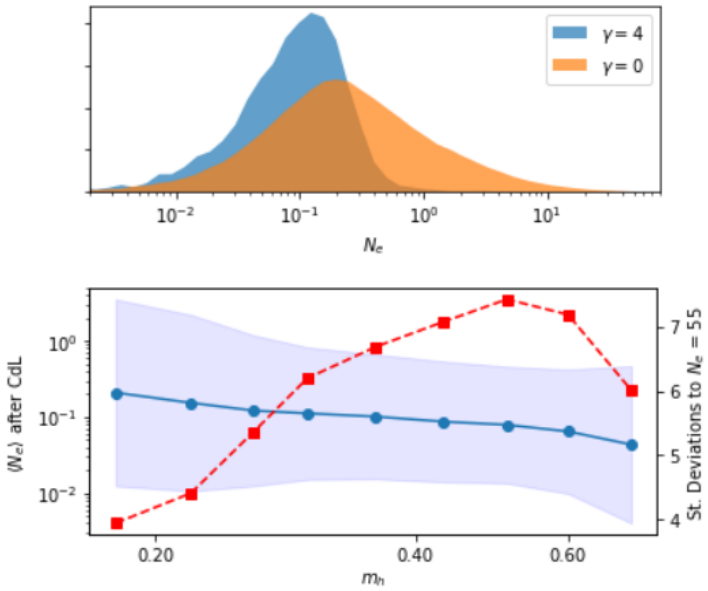

Figure 5.12: (Top) Distributions of the number of slow roll e-folds in the true vacuum basin after CDL tunneling, for two values of the shape parameter γ characterizing the potential in (4.3). (Bottom) Moments of the distribution of number of e-folds after CDL tunneling when inflation ends in the tunneled-to basin, as a function of $m_{\rm h}$. The blue plot (solid line with circular markers, left axis) shows the mean of $\log_{10} N_e$ and the shaded 2-σ confidence interval. The red (dashed line with square markers, right axis) is the number of standard deviations between the mean and $\log_{10} 55$.

would need a way of sampling such very rare potential shapes that give sufficient inflation after a CDL tunneling event, in order to characterize the prevalence of eternal inflation among small field models.

Hawking-Moss An interpretation of the Hawking-Moss [35] instanton as a limiting behavior in the CDL formalism paints a picture of the entire Hubble duration of the field configuration within a Hubble volume sitting on top of the barrier. Rather, we take the Hawking-Moss calculation to give the rate at which Hub-

ble volumes occupying the false vacuum basin *thermally* fluctuate into the true-vacuum basin, with energy comparable to the height of the barrier [39].

Since the potential is only sampled at the false vacuum and at the top of the barrier, the Hawking-Moss transition rate is independent of $m_{\rm h}$; so we can expect this same distribution at higher field scales as well, in regions where Q_s is likely to match observation. Tunneling rates only begin to approach the fast-tunneling regime when the potential approaches the Planck scale. This corresponds to an enormous scale for the inflaton $m_{\rm h} \sim 10^6$ in order to get a small enough scalar amplitude. It then comes down to how we interpret the fast-tunneling Hawking-Moss instanton. It is not eternal on the usual false-vacuum grounds, but supposedly ends with the field everywhere in a Hubble sized region sitting atop the maximum, where we would expect that it would fluctuate away from the peak into the true vacuum basin and give topological inflation.

5.5 Measure C: Hilltops

If the inflaton starts with zero expected field velocity at the maximum and is nudged off the peak by quantum fluctuations, then $\mathcal{N}_e$ is not infinite; the number of e-folds to elapse before exiting the regime where quantum fluctuations dominate is described by a Gaussian random walk. The total number of e-folds expected

along the worldline of an observer born in the initial Hubble volume is

$$\langle \mathcal{N}_{e,\text{total}} \rangle = \langle \mathcal{N}_{e,\text{stoch}} \rangle + \mathcal{N}_{e,\text{since}}, \tag{5.4}$$

where $\langle \mathcal{N}_{e,\text{stoch}} \rangle$ is the expected number of Hubble times taken to traverse the interval of stochastic eternal inflation, and $\mathcal{N}_{e,\text{since}}$ are elapsed between the breakdown of the stochastic inflation criterion (2.11) and the end of inflation. This expected e-fold count characterizes the rate of production of terminally inflating regions, and might play a role in some candidate volume-weighting measures for predictions within a single model that undergoes eternal inflation.

If we neglect the classical field excursion when the stochastic criterion is met (evolution is fluctuation-dominated), the random walk is unbiased with standard deviation $\sigma = H/2\pi$ at each step, for which the mean distance traveled after N steps goes like $\sigma\sqrt{N}$. Taking a population of future-directed world-lines uniformly sampled within the initial Hubble volume, the expected number of Hubble times (and hence e-folds) to reach the edge of the fluctuation-dominated interval of width $\Delta\varphi$ (and exit stochastic eternal inflation) along a worldline uniformly sampled from that set is then

$$\langle \mathcal{N}_{e,\text{stoch}} \rangle = (2\pi H^{-1} \Delta\varphi)^2$$

So large fluctuations near the maximum in fact *reduce* the *a priori expected* number of e-folds for a comoving volume measure, by nudging φ away from the high-$\mathcal{N}_e$-

density maximum. (At later times, the volume measure changes to weigh higher $\mathcal{N}_e$ world-lines more strongly.) After (2.11) breaks down, evolution is dominated by slow roll, and we tally e-folds as usual based on the background trajectory.

Suppose the inflaton field value in an initial Hubble volume is drawn at some characteristic distance in field space – say $H/2\pi$, or one standard deviation for Hubble-scale fluctuations – away from the local maxima of potential barriers randomly sampled by the procedure defining Measure A. If the field space interval around the maximum in which fluctuations dominate is narrower than this gap, then the model has a chance to avoid stochastic and topological inflation. How often is stochastic eternal inflation localized entirely within that neighborhood of the peak, with enough inflation lower on the potential to solve the horizon problem? In other words, how often is $\langle \mathcal{N}_{e,\mathrm{stoch}} \rangle < 1$? In principle, some Measure A models with inflation at the peak can be excluded from Measure C, if fluctuations are larger than the inflating interval around the maximum that includes the would-be horizon exit scale.

A large field widens the fluctuation-dominated interval near the peak, but also correlates with tall peaks in regions of model space in which scalar curvature perturbations reflected in the CMB are the right size; the latter leads to larger fluctuations around the peak. Approximating as quadratic the neighborhood of the potential around the maximum in which fluctuations dominate, we can get a

sense for when quantum fluctuations are larger than the width of that stochastic inflating interval. Evaluating Eq. (2.11) at a field value separated from the maximum by the width of Gaussian fluctuations $\delta\varphi$, we have

$$(V(\varphi_{\rm peak}) + \tfrac{1}{2}V''(\varphi_{\rm peak})\,\delta\varphi^2)^{3/2} > 6.6\ |V''(\varphi_{\rm peak})\,\delta\varphi|\,M_{\rm P}^3$$

Taking quantum fluctuations of size $\delta\varphi^2 = H^2/4\pi^2 = \frac{2}{3\pi}m_v^4 m_{\rm P}^2 f(x)$, where x is the dimensionless field value at the peak,

$$m_v^6\left(f(x) - \frac{1}{3\pi}\frac{m_v^4}{m_{\rm h}^2}f(x)f''(x)\right)^{3/2} \gtrsim \frac{6.6}{16\pi^2\sqrt{3}}\frac{m_v^6}{m_{\rm h}^2}f''(x)\sqrt{f(x)}$$

and assuming typical values for the shape function of order unity, $f(x) = f''(x) = 1$, we obtain in terms of the mass scales characterizing the potential:

$$\left(1 - \frac{1}{3\pi}\frac{m_v^4}{m_{\rm h}^2}\right)^{3/2} \gtrsim \frac{6.6\,m_{\rm h}^{-2}}{16\pi^2\sqrt{3}}$$

Considering the large field regime, we set $m_{\rm h} \sim 10^6\,m_v^2$ to delineate the region in Figure 5.3 where the scalar amplitude Q_s most often takes its value modeled from measured data. We find that 1-σ fluctuations deposit the field beyond the breakdown of the stochastic inflation criterion when $m_v \lesssim 10^{-3.4}$ or $m_h \lesssim 1$ – just about where the highly localized linear trend begins in Figure 5.3.

So granted the above assumptions we should expect a comfortably wide site of stochastic inflation at the peak among large field models that are most likely to give the observed amplitude of scalar curvature perturbations. Then, what

explains the hook-shaped incursion of the contours of relatively low incidence of peaky stochastic inflation in Figure 5.13, approaching $n_s \sim 0.96$ from below in the large-m_v and large-m_h regions? These plots show the rate of incidence of stochastic inflation among Measure C models respecting *Planck 2018* constraints on the scalar and tensor amplitudes, binned with respect to the scalar index and the vertical or horizontal mass scale.

Large-field models producing a tensor-to-scalar ratio less than 0.07 are those in which horizon exit occurs far from the quadratic minimum where ϵ_V is small; for the scalar spectral index to also be more red than the quadratic limit of 0.96, the second potential slow roll parameter η_V must be larger at horizon exit, correlating with a narrow stochastic inflating interval around the peak. Inflation yielding a redder spectrum with small scalar and tensor perturbations thus typically breaks the approximations used in the above calculation, with $f''(x)$ atypically large. Entry of higher order terms that would break the quadratic approximation coincides with breakdown of (2.11). (Taking into account that the field excursion is in fact greater than (2.11) assumes when $V''(\varphi)$ is significant, the stochastic eternal interval is actually smaller; so the above estimate of the lower bound on m_v is conservative – more cheritable to stochastic inflation.)

In the intermediate zone $-3.5 < \log_{10} m_v < -3$, inflation no longer necessarily ends in the quadratic regime, but peaks that are atypically high in energy can,

and they have a better chance of scoring a selection boost. As the energy scale shrinks further, without much new selection pressure on $m_{\rm h}$ coming from the Q_s constraint, fluctuations once again become smaller than the eternal inflation interval, and stochastic inflation becomes more prevalent below $\log_{10} m_v \sim -3.5$. Below $m_v \sim 10^{-4}$ or $m_{\rm h} \sim 0.2$, most models with small Q_s are far too red to be consistent with observation, and we lack sufficient samples in the range of Figure 5.13 to place bounds. When binning with respect to field scale, incidence rates for stochastic inflation are consistently low below $m_h \sim 1$ – in the realm of common but not generic.

So for the range $0.955 < n_s < 0.975$, eternal inflation peeks into the realm of genericity (at $> 95\%$ incidence) by the stochastic mode for vertical mass scales in the middle of our range. Figure 5.14 shows rates of stochastic inflation conditioned on $-4.5 < \log_{10} Q < -4.1$, and binned with respect to scalar spectral index and tensor-to-scalar ratio, including models from all mass ranges represented in Figure 5.3 with epektacratic weighting. Stochastic inflation is generic for all spectral index values when $r > 0.1$, including all mass scales or just those less than $m_{\rm P}$. For small tensor-to-scalar ratio, eternal inflation is suppressed.

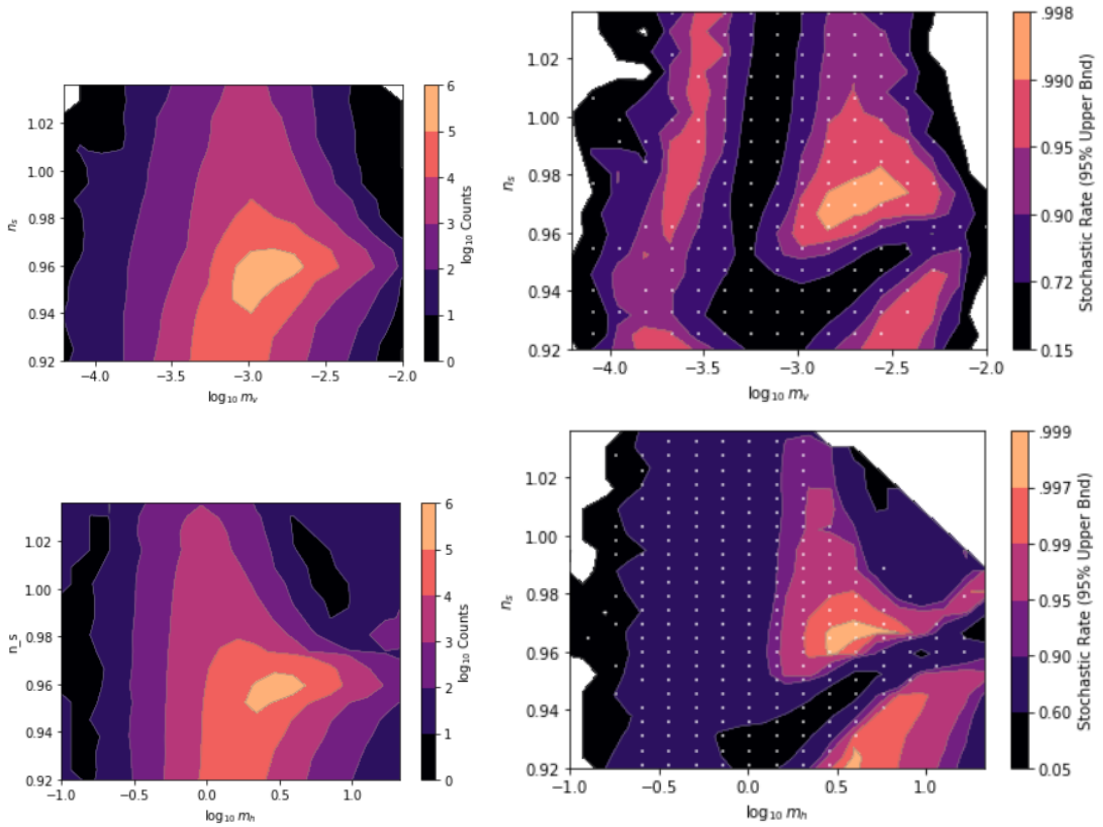

Figure 5.13: (Left) Bin counts. (Right) 95% confidence lower bound on the rate of incidence of models with fluctuations smaller than the width of the stochastic inflation interval around the maximum, under epektacratic weighting in Measure C, binned with respect to scalar tilt and (top) vertical or (bottom) horizontal mass scale, and conditioned on $r < 0.064$, and $-4.5 < \log_{10} Q < -4.1$. The grid points indicate the centers of bins with a non-zero number of *non*-eternal models. Where grid points are absent, the reported bound is determined only by sample size; a small, uninformative lower bound in regions with few samples.

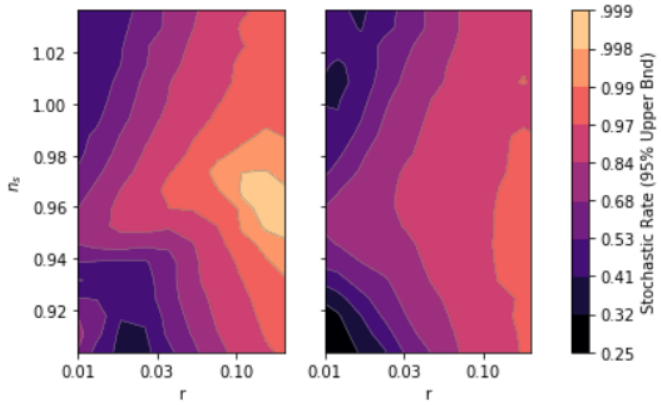

Figure 5.14: 95% confidence lower bound on the rate of incidence of stochastic inflation in Measure A, binned with respect to scalar tilt and tensor-to-scalar ratio, and conditioned on $-4.5 < \log_{10} Q_s < -4.1$. The left plot includes all mass scales with epektacratic weighting. The right includes only $m_{\mathrm{h}} \leqslant 1$.

Chapter 6

Discussion

6.1 Executive Summary

Among Hubble volumes initialized at the local maxima of Gaussian random potentials, we considered separately questions of genericity of stochastic and topological modes of eternal inflation. Among large field models, and intermediate models with acharacterstically broad barriers, a sustained bout of inflation begins at the peak leading generically to both stochastic and topological modes of eternal inflation. In intermediate field-scale models, initializing at the peak does not necessarily entail *stochastic* eternal inflation; we can avoid sustained slow roll near the peak if it has a large second derivative, while accruing enough inflationary e-folds for a viable cosmology at a lower site on the potential in which (2.11) is

not satisfied. At small enough field scales, successful inflation conditioned on the scalar index and running does not generically take place in intervals in which both the potential slow roll conditions and stochastic eternal criteria are satisfied. For some models that meet this description, it is clear that a homogeneous configuration initialized with a small field velocity at the maximum never exits slow roll, despite $\eta_V < -1$ – as in the potential on the righthand side of Figure 5.4. Counting these models as non-stochastically eternal suppresses the rates of eternality presented in Figure 5.5, which should be taken as fairly generous to the prospect of terminal inflation.

Even models with "delayed inflation" are likely always topologically eternal, even though the peak itself does not satisfy the potential slow roll conditions. It is conceivable but not settled from arguments presented here that inflation can be considered non-eternal in some of these models if the adjacent basin has a small or negative vacuum energy, and interpolating field configurations can quickly tunnel to the side of the barrier containing our observable universe. We have had to focus on edge cases in which eternal inflation might *conceivably* be avoided, as the straightfoward cases are generically eternal when initialized at a summit. We suspect most readers will interpret these labored and at times speculative mental gymnastics as suggesting eternal inflation is indeed difficult to avoid in Measure A at all field scales explored in this study.

Stochastic and topological modes of eternal inflation are not generic in Measure B below $m_{\rm h} \sim \mathcal{O}(100)$, with the initial value of the field sampled uniformly from intervals satisfying the potential slow roll conditions. After conditioning on Q_s, models that give observables consistent with an approximately quadratic potential at horizon crossing are those most likely to be stochastically eternal. Binning with respect to the scalar index and tensor-to-scalar ratio, parameter values that best model observation correspond to a local minimum in the rate of stochastically eternal models within the range examined. Strongly topological eternal inflation, taken to occur when quantum fluctuations are likely to produce at least one Hubble volume descending toward the adjacent minimum, is naturally rare due to needing luck to land so near to the peak. Models with stochastic eternality tend to be initialized in a stochastic inflating interval contiguous with the local maximum, and are therefore *de facto* topologically eternal – stochastic fluctuations will carry the field in some regions over the top of the barrier to produce an inflating topological defect.

For small field scales, Coleman-de Luccia instantons exist, but they tend to be thin-walled with the field landing very close to the true minimum and not producing an observationally viable cosmology with sufficient e-folds of inflation. Among the models that do result, the transition rate is generically small enough to yield false vacuum eternal inflation. At scales larger than m_P, the Hawking-Moss

instanton dominates, giving generic eternal inflation.

Measure C offers a variant of Measure A, initializing the field value *near* the local maxima of the potential but with the possibility of non-topological inflation if fluctuations are subdominant at the starting point. At small field scales, inflation falls short of being generically eternal, neither satisfying the stochastic inflation criterion (2.11) nor leading inevitably to an inhomogeneous inflating configurtion straddling the potential barrier. Above the Planck scale $m_h \sim 1$, inflation is also less-than-generic among models with redder spectra satisfying *Planck* constraints on the scalar and tensor amplitudes.

6.2 Conclusions from Monte Carlo Analyses

Our first research question was "Is eternal inflation a generic consequence of inflation conditioned on observations?" Embarking on this investigation, it was clear that this question could not have a single answer given the ambiguity in the measure over inflationary models. Furthermore, it was unclear whether it is even sensible to seek a single verdict for any particular measure, akin to the *top-down* probabilities discussed in [57]. Our second research question offers greater latitude for exposition: "By what modes and to what extent is inflation generically eternal?" Topological eternal inflation is only clearly generic when initializing at the top of the barrier, an initial state from which it is nearly inevitable that

an inhomogeneous configuration interpolating across the barrier will come about. Stochastic inflation is generic at large field scales in Measures A, and in pockets of the space of mass scale parameters in Measure C; it is generically absent in all regions of the space of CMB spectral parameters examined conditioned on minimal inflation. The data suggest that transitions between de Sitter minima in viable cosmological histories – whether Coleman-de Luccia or Hawking-Moss – generically entail eternal inflation.

Our third question "How is genericity to be defined?" is treated to a preliminary discussion and mathematical formulation in § 3.3. In formulating our numerical methodology and converging on appropriate statistical methods for analysis, our criteria for genericity changed. We adapted from a rather starkly formal definition in terms of joint estimation of many metrics parameterizing eternal inflation, to a more practically minded approach of estimating frequentist rates of incidence of eternal behaviors in populations of models sampled from the measure.

Our final research question was "How much freedom do we have in affecting genericity of eternality in choosing a probability measure?" The data suggests that genericity differs wildly among the three measures adopted in this numerical study, and within submeasures obtained by adopting different weights on the mass scales in the measure over potentials.

6.3 Implications for Landscapism

Results of consideration of the form of the string landscape suggest that sampling the potential as a Gaussian random field is not an absurd proposition. If the one-dimensional reduction of field trajectories within a multifield landscape can be characterized as a Gaussian random field in 1D, then results of the above analysis weigh on what we might expect from a string landscape. Since this setup involves considering an ensemble of trajectories through a higher-dimensional potential, our scope of considering the future 4-volume coincident with an initial Hubble volume does not characterize the occurance of eternal inflation generally within the landscape, but rather whether that initial Hubble volume with conditions sampled according to the measure is more or less likely to lead to eternality.

The results most subject to change in such a framework are those concerning topological inflation, as the structure of formation of topological defects varies with the dimension of the field space (and the dimension of spacetime). False-vacuum eternal inflation results are also subject to revision, as transitions between de Sitter minima are dominated by instantons that take curving paths through the higher-dimensional field space.

6.4 Further Research

There are many avenues open for future work toward elucidating representation of eternal inflation in the space of inflation models. We outline some of these possible directions below.

While the "Is it generic?" research question has been suitably addressed within our intended scope, we were limited in our ability to answer the "How generic?" questions in some regions of hyperparameter- and observable-space. We would like to know about genericity of eternal inflation at small field scales, less than an order of magnitude below the Planck mass (or an $\mathcal{O}(1)$ fraction of the reduced Planck mass). The variance of the standard Monte Carlo estimates based on sampling from the distribution of Gaussian random fields was too great to be very informative, due to the limited size of the sample containing models with successful inflation; and the sample shrinks further when conditioning on or binning with respect to observables. Furthermore, the sample sizes for the analysis of successful inflation following a Coleman de Luccia transition were far too small to say much of meaning using this methodology. To take the analysis further, we could use importance sampling to probe the measure over small field scales and very rare false vacuum transitions, without sampling the measure's native distribution and waiting for them to happen. We could generate potentials using a genetic algorithm or some other means to sample these regions containing low-frequency

events; compute the likelihood that that potential would be sampled from a Gaussian random distribution or another sort; and weigh accordingly when estimating rates.

One could apply the same numerical methodology to simulations that include the full dynamics, to eliminate some of the guesswork inherent in the economical approach adopted here. As a middle road, one could use machine learning techniques to identify deviations between smaller data sets computed with full dynamics and those computed using simplifying assumptions, and correct deviations in much larger data sets including the latter.

The string landscape is populated by low energy effective theories generally featuring multiple interacting fields, so these results are interesting largely to the extent that they can be generalized to multifield cases. In higher dimensional potentials spanned by multiple scalar fields, there is a reduction in the effective dimension experienced by a field space trajectory as it approaches a minimum. For particular multfield models with a lot of extra symmetry (e.g. Higgs inflation with $\mathcal{O}(4)$ gauge symmetry, addressed with non-minimal coupling in [61]), multifield dynamics reduce to effectively single-field well before the era of inflation that influences what we observe. Does a measure on initial conditions naturally emerge given statistical characteristics of the landscape, identifying where on the slope the potential becomes effectively one-dimensional? The CosmoTransitions

package includes code for computing Euclidean action-minimizing trajectories in multifield potentials, and could be used to investigate false vacuum inflation in N-D Gaussian random fields. Stochastic inflation must account for possibly non-Gaussian fluctuations in the context of interacting fields.

One could perform a similar analysis in the single- and multifield cases, while accounting for non-minimal coupling [62] or "warm inflation" – modifications to the treatment that can be applied given any potential. Warm inflation considers the effect of adding a thermal friction term atop the usual Hubble friction – typically by coupling to a light radiation field. The addition of thermal fluctuations amplifies the scalar spectrum, lowering the threshold criterion for stochastic eternal inflation and making a small tensor-to-scalar ratio less dependent on fine-tuning of the potential. One could also replace the amplitude of inflaton fluctuations in (2.11) with the adiabatic regularized version proposed in [42].

Finally, one could explore the possibility of field configurations lacking $O(3,1)$ symmetry – interpolating from a Minkowski or anti-de Sitter minimum, over a sharp peak, and into an interval of slow roll – tunneling to a configuration in which the field is entirely on the Minkowski side of the barrier. A confirmation of our hunch that these transitions are not possible – or generically have slow tunneling rates or lead to curvature singularities – would close the prospects of non-eternal inflation occuring in Measure A.

Chapter 7

Conclusion

Inflation has been demonstrated to be highly successful as a paradigm for early universe cosmology, addressing naturalness problems lingering in the Big Bang picture while offering a coherent explanation for the origin of primordial curvature perturbations implied by observations of the Cosmic Microwave Background. Its grandest prediction of all may be that we live in an eternally inflating multiverse, producing an unbounded number of causally disconnected regions with wildly varying cosmological histories.

For research culminating in this dissertation, we investigated whether and to what extent eternality can or must be considered a genuine prediction of inflation – in the sense of following generically from conditions giving rise to the latter in the context of more-or-less physically-justifiable measures on the space of infla-

tionary cosmologies. We shed light on how one would go about evaluating claims that features of a model are generic or fine-tuned. Using a computational methodology developed to assess the typicality of eternal inflation with applied statistics, we found that genericity is highly dependent on the measure, and that its determination inevitably involves some nuance. In Appendix A, we go on to explore the toy landscape of Gaussian random potential functions in conjunction with computable measures over initial conditions, probing characteristics of eternal inflation like the fractal dimension. We demonstrate the absence of an informative relationship between the running of the spectral index and presence of stochastic eternal inflation in models with a uniform sampling of initial field values.

This work adds to an ongoing conversation pertaining to the credibility of the anthropic view of the cosmos that has gained traction in recent decades. Whether or not eternal proliferation and a "multiverse" generically follow from inflation has profound implications for this picture, as anthropic arguments require a large population of trial sites where apparently fine-tuned quantities can vary. In addition to direct scholarly contribution, we intend to publish a code package for simulating inflation across an ensemble of randomly generated inflaton potentials using modern programming tools; others may build upon this package in furtherance of related research objectives.

There may be no way of assigning probabilities to partitions of the space of

cosmological models that is not contaminated by human prejudice. If that were the case, should any weight be assigned to the intuitions and conceptual biases of scientists and philosophers in judging the credibility of proposals that elude falsification by evidence? Or should we be content with remaining agnostic when apparent naturalness problems crop up in our scientific theories?

The answer to this question depends largely on the dispositon of the answerer with respect to the role of science. If the objective in science is limited to illucidating the reproducible, experimental facts of the natural world, then the scientist should pay little attention to naturalness problems, which by their nature evade unambiguous framing and definitive closure (except perhaps by the supersession of the paradigm that is the context for the problem). If, on the other hand, one views science as in some respects a form of elite art – to be appreciated in detail by a highly trained community of experts and in likeness by the general public – then aesthetic and philosophical questions are fair game, and perhaps the whole point of the enterprise.

Bibliography

[1] Sean M. Carroll. In What Sense Is the Early Universe Fine-Tuned? 2014. arXiv:astro-ph.CO/1406.3057.

[2] Anna Ijjas, Paul J. Steinhardt, and Abraham Loeb. Inflationary paradigm in trouble after *Planck* 2013. *Physics Letters B*, 723(4):261 – 266, 2013.

[3] Y. Akrami et al. Planck 2018 results. X. Constraints on inflation. *Astronomy and Astrophysics*. Accepted Aug 2019.

[4] Michael R. Douglas. The Statistics of string / M theory vacua. *JHEP*, 05:046, 2003.

[5] Leonard Susskind. The anthropic landscape of string theory. *Universe or multiverse*, pages 247–266, 2007.

[6] Tom Banks, Michael Dine, and Elie Gorbatov. Is there a string theory landscape? *Journal of High Energy Physics*, 2004(08):058–058, sep 2004.

[7] Lawrence J. Hall and Yasunori Nomura. Evidence for the multiverse in the standard model and beyond. *Phys. Rev. D*, 78:035001, Aug 2008.

[8] Alan H. Guth and Erick J. Weinberg. Could the universe have recovered from a slow first-order phase transition? *Nuclear Physics B*, 212(2):321 – 364, 1983.

[9] A.D. LINDE. Eternal chaotic inflation. *Modern Physics Letters A*, 01(02):81–85, 1986.

[10] Alexander Vilenkin. Birth of inflationary universes. *Phys. Rev. D*, 27:2848–2855, Jun 1983.

[11] Anthony Aguirre. Eternal inflation, past and future. In Rudy Vaas, editor, *Beyond the Big Bang*, chapter 3. Springer-Verlag Berlin and Heidelberg GmbH & Co. KG, 2014.

[12] A.D. Linde. Chaotic inflation. *Physics Letters B*, 129(3):177 – 181, 1983.

[13] Alan H. Guth. Eternal inflation and its implications. Feb 2007. arXiv:hep-th/0702178.

[14] Alexander Vilenkin. The Birth of Inflationary Universes. *Phys. Rev.*, page 2848, 1983.

[15] Ken D. Olum. Is there any coherent measure for eternal inflation? *Phys. Rev. D*, 86(6):1–10, Feb 2012.

[16] Andreas Albrecht and Daniel Phillips. Origin of probabilities and their application to the multiverse. *Phys. Rev.*, D90(12):123514, 2014.

[17] Anthony Aguirre, Max Tegmark, and David Layzer. Born in an Infinite Universe: A Cosmological Interpretation of Quantum Mechanics. *Phys. Rev.*, D84:105002, 2011.

[18] Yasunori Nomura. Physical Theories, Eternal Inflation, and Quantum Universe. *JHEP*, 11:063, 2011.

[19] Raphael Bousso and Leonard Susskind. The Multiverse Interpretation of Quantum Mechanics. *Phys. Rev.*, D85:045007, 2012.

[20] Max Tegmark. What does inflation really predict? *Journal of Cosmology and Astroparticle Physics*, 04, 2005.

[21] Alan H. Guth. The Inflationary Universe: A Possible Solution to the Horizon and Flatness Problems. *Phys. Rev.*, D23:347–356, 1981.

[22] A. D. Linde. A new inflationary universe scenario: A possible solution of the horizon, flatness, homogeneity, isotropy and primordial monopole problems. *Physics Letters B*, 108:389–393, February 1982.

[23] Andreas Albrecht and Paul J. Steinhardt. Cosmology for grand unified theories with radiatively induced symmetry breaking. *Phys. Rev. Lett.*, 48:1220–1223, Apr 1982.

[24] C. B. Netterfield et al. A measurement by Boomerang of multiple peaks in the angular power spectrum of the cosmic microwave background. *Astrophys. J.*, 571:604–614, 2002.

[25] David Kaiser. Primordial perturbations from inflation: An informal primer. Unpublished notes, Dec 2011.

[26] Chris Pattison, Vincent Vennin, Hooshyar Assadullahi, and David Wands. Stochastic inflation beyond slow roll. *Journal of Cosmology and Astroparticle Physics*, 2019(07):031–031, Jul 2019.

[27] Jerome Martin and Vincent Vennin. Quantum Discord of Cosmic Inflation: Can we Show that CMB Anisotropies are of Quantum-Mechanical Origin? *Phys. Rev.*, D93(2):023505, 2016.

[28] David Polarski and Alexei A. Starobinsky. Semiclassicality and decoherence of cosmological perturbations. *Class. Quant. Grav.*, 13:377–392, 1996.

[29] A.R. Liddle and D.H. Lyth. *Cosmological Inflation and Large-Scale Structure*. Cosmological Inflation and Large-scale Structure. Cambridge University Press, 2000.

[30] Sidney R. Coleman and Frank De Luccia. Gravitational Effects on and of Vacuum Decay. *Phys. Rev.*, D21:3305, 1980.

[31] Matthew C. Johnson. *Vacuum Transitions and Eternal Inflation*. PhD thesis, University of California Santa Cruz, 2007.

[32] Jaume Garriga. Nucleation rates in flat and curved space. *Physical Review D*, 49(12):6327–6342, 1994.

[33] Martin Bucher, Alfred S. Goldhaber, and Neil Turok. Open universe from inflation. *Phys. Rev. D*, 52:3314–3337, Sep 1995.

[34] A. Aguirre, T. Banks, and M. Johnson. Regulating eternal inflation. II. The Great divide. *JHEP*, 08:065, 2006.

[35] S.W. Hawking and I.G. Moss. Fluctuations in the inflationary universe. *Nuclear Physics B*, 224:180–192, 08 1983.

[36] Andrei D. Linde and Dmitri A. Linde. Topological defects as seeds for eternal inflation. *Phys. Rev.*, D50:2456–2468, 1994.

[37] Alan H. Guth and Vitaly Vanchurin. Eternal Inflation, Global Time Cutoff Measures, and a Probability Paradox. 2011. arxiv:hep-th/1108.0665.

[38] Arjun Berera. Warm inflation. *Phys. Rev. Lett.*, 75:3218–3221, 1995.

[39] Puneet Batra and Matthew Kleban. Transitions between de sitter minima. *Phys. Rev. D*, 76:103510, Nov 2007.

[40] Viatcheslav F. Mukhanov, L. Raul W. Abramo, and Robert H. Brandenberger. On the Back reaction problem for gravitational perturbations. *Phys. Rev. Lett.*, 78:1624–1627, 1997.

[41] L. Mersini-Houghton and L. Parker. Eternal inflation is "expensive". 2007. arXiv:hep-th/0705.0267.

[42] Leonard Parker. Amplitude of Perturbations from Inflation. 2007. arXiv:hep-th/0702216.

[43] Elliot Nelson. Quantum Decoherence During Inflation from Gravitational Nonlinearities. *JCAP*, 1603:022, 2016.

[44] Kimberly K. Boddy, Sean M. Carroll, and Jason Pollack. How Decoherence Affects the Probability of Slow-Roll Eternal Inflation. *Phys. Rev.*, D96(2):023539, 2017.

[45] William H. Kinney and Katherine Freese. Negative running can prevent eternal inflation. *Journal of Cosmology and Astroparticle Physics*, 2015.

[46] Cumrun Vafa. The String landscape and the swampland. 2005. arXiv:hep-th/0509212.

[47] T. Daniel Brennan, Federico Carta, and Cumrun Vafa. The String Landscape, the Swampland, and the Missing Corner. *PoS*, TASI2017:015, 2017.

[48] Hiroki Matsui and Fuminobu Takahashi. Eternal Inflation and Swampland Conjectures. *Phys. Rev.*, D99(2):023533, 2019.

[49] Tom Rudelius. Conditions for (no) eternal inflation. *Journal of Cosmology and Astroparticle Physics*, 2019(08):009–009, Aug 2019.

[50] Konstantinos Dimopoulos. Steep Eternal Inflation and the Swampland. *Phys. Rev.*, D98(12):123516, 2018.

[51] Suddhasattwa Brahma and Sarah Shandera. Stochastic eternal inflation is in the swampland. *Journal of High Energy Physics*, 2019(11):16, Nov 2019.

[52] William H. Kinney. Eternal Inflation and the Refined Swampland Conjecture. *Phys. Rev. Lett.*, 122(8):081302, 2019.

[53] Ben Freivogel, Matthew Kleban, Maria Rodriguez Martinez, and Leonard Susskind. Observational consequences of a landscape. *JHEP*, 03:039, 2006.

[54] Alan H. Guth and Yasunori Nomura. What can the observation of nonzero curvature tell us? *Phys. Rev.*, D86:023534, 2012.

[55] Melchiorri A. Di Valentino, E. and J. Silk. Planck evidence for a closed universe and a possible crisis for cosmology. *Nature Astronomy*, 2019.

[56] G. W. Gibbons and Neil Turok. The Measure Problem in Cosmology. *Phys. Rev.*, D77:063516, 2008.

[57] J. B. Hartle and S. W. Hawking. Wave function of the universe. *Phys. Rev. D*, 28:2960–2975, Dec 1983.

[58] James Hartle, S. W. Hawking, and Thomas Hertog. No-boundary measure in the regime of eternal inflation. *Phys. Rev. D*, 82:063510, Sep 2010.

[59] Sumit K. Garg and Chethan Krishnan. Bounds on Slow Roll and the de Sitter Swampland. *JHEP*, 11:075, 2019.

[60] Carroll L. Wainwright. Cosmotransitions: Computing cosmological phase transition temperatures and bubble profiles with multiple fields. *Comput. Phys. Commun.*, 183:2006–2013, 2012.

[61] Ross N. Greenwood, David I. Kaiser, and Evangelos I. Sfakianakis. Multifield Dynamics of Higgs Inflation. *Phys. Rev.*, D87:064021, 2013.

[62] Chao-Jun Feng and Xin-Zhou Li. Is non-minimal inflation eternal? *Nuclear Physics B*, 841(1):178 – 187, 2010.

[63] Mukunda Aryal and Alexander Vilenkin. The fractal dimension of the inflationary universe. *Physics Letters B*, 199(3):351 – 357, 1987.

[64] Nobuyuki Sakai. Generality of topological inflation. *Class. Quant. Grav.*, 21:281–288, 2004.

Appendix A

Explorations in a Toy Landscape

In the above chapters, we focused on characterizing the prevalence of eternal behavior among observationally viable inflation models, by simulating inflation on Gaussian random potentials. In this appendix, we explore what other insights can be gleaned from the simulated data obtained from that numerical methodology.

A.1 Does Negative Running Prevent Eternal Inflation?

In [45], it is argued that a value of the running of the spectral index α below a small negative threshold (-4×10^{-5} for a pair of viable values of the scalar amplitude and spectral index) is a sufficient condition for no stochastic eternal inflation in the past of horizon exit of CMB perturbations, given assumptions about higher-order runnings; an outline of the argument is reproduced in § 3.2.

(The running indicates how the scale-dependence of power in spherical harmonic modes of the CMB in turn depends on wavelength.) The bound claimed for non-eternal inflation is

$$\alpha \equiv \frac{\mathrm{d}^2(\ln \mathcal{P}_\mathcal{R})}{\mathrm{d}(\ln k)^2} < \frac{(1-n_s)^2}{4 \ln Q_s^2} \tag{A.1}$$

This assumes that higher runnings-of-the-running (higher derivatives given by $\mathrm{d}^n(\ln \mathcal{P}_\mathcal{R})/\mathrm{d}(\ln k)^n$) are non-positive for odd n and non-negative for even n. (Since $\ln k/k_*$ is negative in the past of CMB horizon exit, this ensures that higher-order runnings do not compensate for the negative first running to raise the maximum amplitude of curvature perturbations.)

To test this proposed bound in our toy landscape of Gaussian random potentials, we compare the running of the spectral index computed at horizon exit to the quantity on the RHS of Eq. (A.1) for models simulated in Measure B (uniform sampling of initial field values within slow-roll intervals on the potential). To obtain a test most relevance to our cosmological history, we would first condition on the scalar amplitude Q_s and spectral index n_s falling within *Planck* constraints; but the residual sample size after that selection is too small in Measure B. Since the underlying argument presented in [45] is not conditioned on particular values of Q_s and n_s, we instead do a more limited conditioning step – requiring $Q_s < 10^{-3}$ and $0.9 < n_s < 1.02$.

We find that given our assumptions for the simulation in Measure B, the bound

(A.1) is not consistent with the simulated data. Under all choices for the measure over mass scales that we analyzed, the distribution of the running among stochastically eternal models is localized below the negative lower bound (A.1) (in one case: entirely below). In the top left of Figure A.1, the population is all

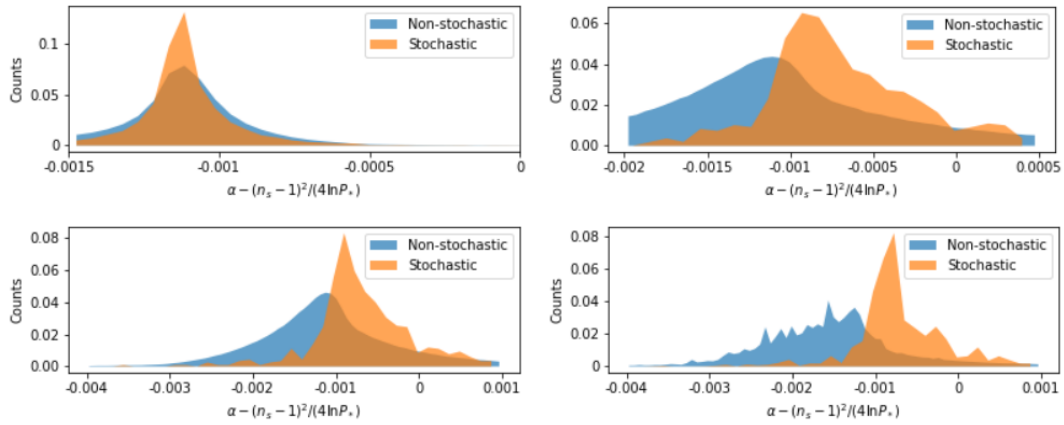

Figure A.1: Histograms of values of the running α among stochastic eternal and non-eternal models sampled from Measure B. (Top Left) All field scales, epektracratic weighting; (Bottom Left) all field scales, $Q_s \leqslant 10^{-3}$, epektracratic weighting; (Top Right) $m_h \leqslant 1$, epektacratic weighting; (Bottom Right) $m_h \leqslant 1$, $Q_s \leqslant 10^{-3}$, democratic weighting

Measure B models with successful inflation, using epektaratic weighting (simulate the same number of models at each log-sampled field scale m_h, then aggregate all models with enough e-folds). The distributions for eternal and non-eternal models are almost identical, with slightly greater excess kurtosis in the eternally inflating population. This is because large field models dominate the epektacratic measure; the running is calculated at horizon exit near the minimum, where behavior is pretty much the same whether or not there was eternal inflation higher on the

potential slope. With other cuts on field scale (considering only $m_h \leqslant 1$) and weighting schemes, we see some separation between the two distributions. However, the stochastically eternal distribution remains localized below the proposed lower bound.

This suggests at least one of several factors at play. The higher order runnings play a significant role and are generically not obeying the constraints assumed in deriving the bound. It is also possible that our weak criteria for slow roll (requiring only $\epsilon_V < 1$ and $|\eta_V| < 1$), are admitting models in which the bound derived in [45] is not effective, and were we to substitute strong inequalities the situation would be different. In any case, we can feel comfortable in concluding that the behavior of the potential at horizon exit is in many cases not well correlated with that higher on the potential where stochastic inflation tends to occur – at least in Measure B where eternal inflation is generically absent.

Although the lower bound (A.1) is not supported, one could go further to ask under what conditions the running serves as an effective classifier, providing good separation between models with and without eternal inflation. Figure A.2 plots Receiving Operator Characteric (ROC) curves for various measures on mass scales in Measure B. The ROC plot compares the rates of correct classification of eternal models agains the rate of false positives (Type I errors). Maximizing the area under the ROC curve is equivalent to optimizing detector performance;

in a two-class system, a diagonal line performs as well as random assignment of class labels. We can see that the running performs the best as a classifier among small field models ($m_h < 1$) with democratic field scale weighting (a prior on logarithmically-spaced mass bins that is the inverse of the success rate).

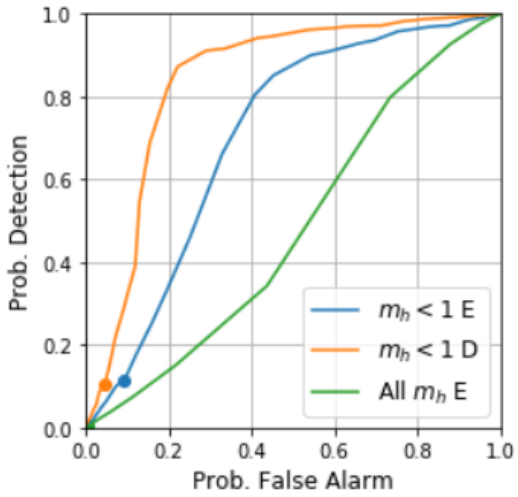

Figure A.2: Receiver operating characteristic (ROC) curve obtained by treating the running of the spectral index α as a detection statistic for stochastic eternal inflation. The points indicate where the negative upper bound on the running lies. In the legend, 'E' and 'D' refer to epektacratic and democratic field scale weightings, respectively.

A.2 Fractal Dimension of Topological Defects

As argued in § 5.3, inflation driven by a single scalar field φ starting near the maximum of its potential $V(\varphi)$ is generically eternal. Quantum fluctuations dominate the slow classical evolution of $\langle\varphi\rangle$ near the peak, resulting in an inhomogeneous field configuration with φ descending toward the minima of both

conjoining half-basins, separated in space by an inflating topological defect that can never be excised. When the size of Hubble-scale fluctuations, given by $H/2\pi$, is much smaller than the width of the field space interval around the maximum in which fluctuations dominate, these defects take on a fractal character after many Hubble times, as suggested in the early days of inflation and first tackled in depth in [63]. It is fractal both in the sense of measuring volume in inflating versus post-inflationary regions, and volume descending toward one or the other adjacent minimum.

What can be said about typical values for the fractal dimension of the fluctuation-dominated cores of such defects, in the context of measures on the space of inflation models and initial conditions? In other words, if we sample the space at different distance scales to determine the volume of space in the eternally inflating phase, how does the measure of volume scale with the spatial frequency of the sampling? Furthermore: what happens when the stochastic inflating interval is smaller than the width of typical fluctuations around the peak, or when topological considerations are the sole enforcer of eternal inflation?

In this appendix, we compute statistics of the fractal dimension for volume in thermalized regions, and for volume that has exited eternal inflation, descended from inflating topological defects in single-field models, given a simple measure over potentials standing in for an inflationary landscape. We go on to discuss

how one should go about computing the fractal dimension of topological defects in models in which a sustained bout of inflation starts only below the maximum (due to $\eta_V \gtrsim 1$ at the peak), and in which fluctuations are larger than the fluctuation-dominated inflation interval around the maximum.

A.2.1 Random Walks and Fractal Dimension

Accounting for stochastic fluctuations of the inflaton atop the classically behaved field excursion, we must describe the trajectory of the inflaton in a given Hubble volume as a biased Gaussian random walk, where the size of the bias varies depending on the distance from the peak as $V'(\varphi)/3H^2 \approx M(\varphi - \varphi_{\rm peak})/3H^2$ where $M \equiv -V''(\varphi_{\rm peak})$.

$$\varphi(t_0 + H^{-1}) \leftarrow \varphi(t_0) + \mathcal{N}(M(\varphi - \varphi_{\rm peak})/3H^2, H/2\pi)$$

Because the whole space is inflating, there are correlations between *when* asynchronous, enduring deviations from the bulk occurred and the scale of those deviations – older deviations manifest at larger distance scales. This is a natural recipe for fractal structure.

Fractal dimension indicates how the measure of volume depends on the scale of coarse graining when probing a particular function of space – e.g. a binary evaluation of inflating vs. non-inflating. What does coarse-graining mean in the

context of nested inflating and non-inflating regions? If we imagine sampling space at intervals separated by a distance ξ, and take the number of those points that are thermalized multiplied by the volume ξ^3 as a measure of the volume of thermalized regions, then the volume measured will scale with the coarse-graining as

$$V \sim \xi^3 (R/\xi)^d$$

If across a significant range of the coarse-graining scale ξ the exponent d takes a nearly constant non-integer value, then the space is a fractal with respect to that function.

Aryal and Vilenkin [63] computed the fractal dimension of an eternally inflating universe for potentials approximated around the maximum as $V(\varphi) \approx V_0 - \delta V(\varphi)$ in three cases:

$$d = 3 - \begin{cases} H^2/32\varphi_c^2, & \delta V = V_0 \Theta(|\varphi| - \varphi_c) \\ M^2/3H^2, & \delta V = \frac{1}{2} M^2 \varphi^2 \\ C\lambda^{1/2}, & \delta V = \frac{1}{4!} \lambda \varphi^4 \end{cases} \tag{A.2}$$

where Θ is the Heaviside step function, H is the Hubble parameter at the peak, and $C \approx 0.28$ is a constant independent of the potential.

The distribution of field values in a comoving volume as a function of time, $\rho(\varphi, t)$, obeys the Fokker-Planck equation (2.12). For an inverted quadratic potential centered at $\varphi = 0$ with initial conditions $\rho(\varphi, 0) = \delta(\varphi)$, the solution is

Gaussian with a time-dependent variance

$$\rho(\varphi, t) = \frac{1}{\sqrt{\pi\sigma(t)^2}} \exp\left(-\frac{\varphi^2}{2\sigma(t)^2}\right) \qquad \sigma(t)^2 \equiv \frac{3H^4}{4\pi^2 M^2}\left[\exp\left(\frac{2M^2 t}{3H^2}\right) - 1\right]$$

With the rationale that the end of inflation comes far away from the peak at $\varphi \gg H^2/M$ – where the field is not likely to climb back up the potential slope by chance – they invoke an effective absorbing boundary at $\varphi_{\rm end} \gtrsim H^2/M$. In the late-time limit, the distribution $\rho(\varphi, t)$ is nearly uniform for $\varphi \lesssim H^2/M$, giving an inflating fraction $\sim \exp(-M^2 t/3H)$ and fractal dimension given in (A.2).

When the amplitude of quantum fluctuations is considerably smaller than the width of the fluctuation-dominated interval where stochastic eternal inflation occurs, we can use Aryal and Vilenkin's expression for the fractal dimension in the vicinity of a peak dominated by quadratic or quartic terms. In Figure A.3, we depict the (geometric) mean deviation of fractal dimension from 3, among models from Measure A with inflation starting at the peak, for which the amplitude of fluctuations at the peak is smaller than the size of the stochastically inflating interval; the data is binned with respect to n_s and either m_v or m_h. To calculate the fractal dimension, we determine whether the dominant contribution around the peak in the interval in which stochastic eternal inflation occurs is the quadratic or quartic term, and then apply the formulas in (A.2). (Of course the vast majority of potentials are dominated by the quadratic term.)

For all mass scales, fractal dimension departs from 3 by only a tiny amount,

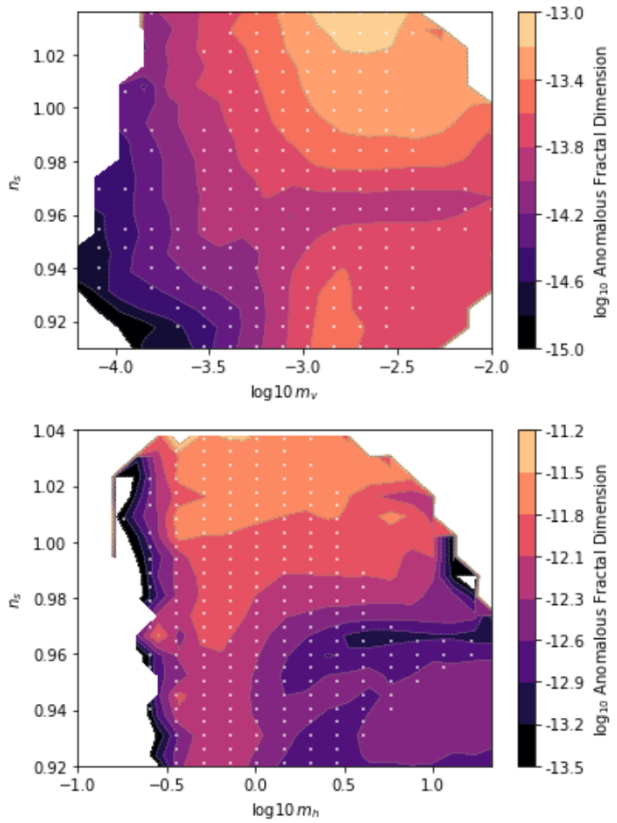

Figure A.3: Mean deviation of fractal dimension from 3 among models with fluctuations of size smaller than $H/2\pi$, binned with respect to scalar tilt and vertical mass scale, and conditioned on $-4.5 < \log_{10} Q_s < -4.1$. The left plot includes all mass scales with epektacratic weighting. The right includes only $m_h \leqslant 1$.

with the variation among scales much smaller than the discrepancy between values of $d - 3$ and $\mathcal{O}(1)$. Binning with respect to field scale increases the size of deviations. A fairly regular diagonal striation is interrupted by another signal centered around $n_s = 0.96$ in the m_v plot. Even though n_s is determined by m_h, the m_h plot shows some interesting non-correlation.

When binning with respect to n_s and r, the range deviation in fractal di-

mension is shifted toward larger scales by 2-3 orders of magnitude. Small tensor perturbations correlate with small fractal dimension, suggesting that if our observable universe descends from such a defect, the fractal effect is orders of magnitude smaller than it could have been given a higher upper bound on the amplitude of tensor perturbations.

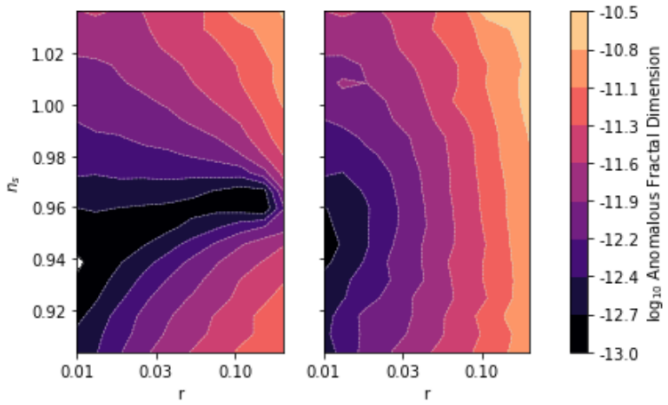

Figure A.4: Mean deviation of fractal dimension from 3 among models with fluctuations of size smaller than $H/2\pi$, binned with respect to scalar tilt and tensor-to-scalar ratio, and conditioned on $-4.5 < \log_{10} Q_s < -4.1$. The left plot includes all mass scales with epektacratic weighting. The right includes only $m_h \leqslant 1$.

A.2.2 Beyond Aryal-Vilenkin Assumptions

Aryal and Vilenkin's calculations assume that the field space interval in which fluctuations dominate is much larger than the size of fluctuations, that inflation within a topological defect occurs near the top of a potential barrier, and that the part of the potential where inflation ends does not affect behavior of $\rho(\varphi, t)$ in the fluctuation-dominated interval. In this section, we identify a few scenarios in

which one or more of these assumptions is violated, and discuss whether and how the prescription for computing fractal dimension must be altered in those cases.

A.2.2.1 Large Fluctuations

When inflation starts at the initial maximum, the stochastic eternal inflation criterion is always satisfied in some neighborhood of the peak, and we can only compare the size of fluctuations to the width of that fluctuation-dominated interval in field space. If fluctuations are much larger than that interval's width, then they cannot *continue* to dominate the classical descent away from the peak in the space threaded by a congruence of future-directed worldlines emanating from any given Hubble volume for much more than a Hubble time, as both directions are "downhill" and volume will continually fluctuate out of the small neighborhood of the peak and into field space where $V'(\varphi)$ dominates.

Instead these models undergo topological inflation, with the field quickly fluctuating away from the flattest part of the peak and thenceforth evolving classically. Even if the probability of landing within the stochastic interval after a Hubble time is less than $1/e^3$ – so that the inflating volume right around the maximum tends to shrink over time – the topological nature of the defect prevents it from ever being fully excised. With an infinite number of Hubble times to wait, improbable fluctuations will eventually be realized, replenishing inflating volume at the peak. Topological inflation always wins out in such a scenario, even amidst large

inhomogeneities [64].

In the case of large fluctuations, it is rare for Hubble volumes with fluctuations drawn from the tails of the distribution to find their way back into the fluctuation-dominated interval. The Measure C results on the prevalance of stochastic eternal inflation expounded in § 5 reflect the rate of incidence of this condition. For such models, Aryal and Vilenkin's assumption that the boundary of the fluctuation dominated interval occurs far away from the peak is not satisfied, and so the prescription for the fractal dimension of such defects must be reconsidered. When delayed inflation takes place on an inflationary shelf lower on the potential, there is a region of fast evolution as the field descends the sharply peaked barrier out of slow roll – potentially adding further complexity to the calculation.

A.2.2.2 Delayed Decoherence

Perturbation modes are taken in the standard treatment to decohere (and so start behaving classically) either instantaneously after exiting the horizon or an elapsed Hubble time then-after. In [43], a calculation of explicit decoherence due to interaction with metric perturbations suggests that it takes more like $\mathcal{O}(10)$ Hubble times for super-Hubble modes to decohere and behave as contributions to the classical background. Taking 10 to be a representative figure, let us define the

retarded e-fold count $\mathcal{N}_{e,\mathrm{ret}}$ as

$$\mathcal{N}_{e,\mathrm{ret}} = \mathcal{N}_e - 10$$

Then the amplitude of fluctuations is determined by conditions at a retarded field value given by

$$\varphi(\mathcal{N}_{e,\mathrm{ret}}) = \varphi(\mathcal{N}_e) + M_{\mathrm{P}}^2 \int_0^{10} \frac{V'(\varphi)}{V(\varphi)}\, \mathrm{d}\mathcal{N}_e$$

During slow roll, the Hubble parameter is nearly constant, so we can take the amplitude of modes that decohere presently to be the same as of those that crossed the horizon several Hubble times in the past. The implications for stochastic inflation in this simple case (found to be minimal), are discussed in [44].

But suppose there is a period of non-slow-roll evolution between the peak and ϕ_{sr}, followed by a period of adjustment subject to the slow roll attractor, followed by slow roll. If we account for a long decoherence time for modes that have crossed the horizon, then the fluctuations "put into effect" when slow-roll inflation starts below the peak actually correspond to conditions ten or more Hubble times in the past. At this retarded "time," the inflaton was evolving out of slow-roll higher on the slope (if we assume the analysis of decoherence is not substantially changed in this regime). Does this have any non-transient effects on the prospects of stochastic eternal inflation taking place on an inflationary shelf?

If fluctuations are not likely to drive the inflaton back into this non-slow-roll

regime – so that regions in which the field has started slow roll continue to inflate until preheating – then this long decoherence effect is a one-time occurrence, and should not significantly alter the fractal structure. If we introduce dependence on a retarded e-fold count, the Focker-Planck equation then becomes path-dependent and non-Markov. In terms of the retarded log-scale-factor $\mathcal{N}_{e,\mathrm{ret}}$ and the present $\mathcal{N}_e$, the Fokker-Planck equation becomes

$$\frac{\partial \rho}{\partial t} = \frac{H(\varphi)H(\varphi_{\mathrm{ret}})^2}{8\pi^2}\frac{\partial^2 \rho}{\partial \varphi^2} + \frac{1}{3H(\varphi)}\frac{\partial}{\partial \varphi}\left(\rho \frac{\mathrm{d}V}{\mathrm{d}\varphi}\right) \tag{A.3}$$

Can we find an approximation in which it is Markov? The answer to this question is key to characterizing the fractal behavior of topological defects if decoherence of quantum fluctuations must really be considered to occur much later than horizon exit.